WLH 50: How Australia Informs the Worldwide Pattern of Pleistocene Human Evolution

MILFORD H. WOLPOFF
Department of Anthropology, University of Michigan, Ann Arbor, MI 48109-1092, USA; wolpoff@umich.edu

SANG-HEE LEE
Department of Anthropology, University of California at Riverside, Riverside, CA 92521-0418, USA; shlee@ucr.edu

submitted: 15 July 2013; accepted 9 September 2014

MONOGRAPH CONTENTS

PaleoAnthropology **2014: 505–564.** **ISSN 1545-0031**
doi:10.4207/PA.2014.ART88

MONOGRAPH CONTENTS (CONTINUED)

MONOGRAPH ABSTRACT

WLH 50 is the ~26,000 kyr (16.5–37.4 kyr) year-old calotte of a large (1540cc) young-to-middle-aged male found in dune deposits near Lake Garnpung, one of the Willandra lakes in New South Wales, Australia. Its importance stems from the significant similarities it appears to have with the nearby and most probably earlier human sample from Ngandong, Indonesia. Two implications of these similarities are important—the implications for Australian ancestry and the implications for the place of Ngandong in human evolution. We discuss the historic context for issues of indigenous Australian ancestry and show how WLH 50 informs these issues. We provide both a systematic and comprehensive description of the WLH 50 fossil in a comparative context, and an interpretation of its place in human evolution. A comparative analysis of the WLH 50 cranium is important for understanding its morphological pattern and addressing its ancestry; in particular, whether there are multiple ancestors for WLH 50 and other Australians that include Late Pleistocene Indonesians from Ngandong. Besides these anatomical considerations, the issues of indigenous Australian ancestry also are framed by genetic analysis including both paleogenetics and observations of mitochondrial and nuclear DNA from modern populations, and we discuss their implications as well. We conclude that WLH 50 is a normal specimen without evidence of pathology or deformation, and that elements of its anatomy are found throughout the Australian fossil record, as it is known today. Our comparisons reveal WLH 50 has substantial similarities to the Ngandong hominids (but not identity with them) and a demonstrable pattern of multiple ancestors that includes Ngandong, as part of the network of human evolution in Australasia.

> "WLH 50, an opalised cranium and partial skeleton, found on a lakeshore to the north of Mungo, is much more robust and archaic than any Australian hominid found previously. It makes the Kow Swamp remains look gracile by comparison. This new specimen greatly reinforces the regional continuity linking Indonesia and Australia. The morphological sequence found in Australia shows clearly that regional features must be separated from grade features seen worldwide in order to understand the differing patterns of Late Pleistocene human evolutionary change." Alan G. Thorne [1939–2012] (1984).

INTRODUCTION

Discussions of the details of Australian prehistory have continued for more than a century, and play a key role in the ongoing understanding of Late Pleistocene and Holocene human evolution across the world. Questions concern how Australians relate to other human populations. Do Australians have one or several ancestral sources, and how can the complex pattern of migrations to Australia be untangled? In this monograph we turn to WLH 50, a previously undescribed specimen that informs these and other related issues. WLH 50 is a ~26,000 kyr (16.5–37.4 kyr) calotte of a large (1540cc) young-to-middle-aged male found in dune deposits near one of the Willandra lakes in New South Wales, Australia. The overarching issue this specimen has raised is about its anatomy and the question of whether and how its anatomy reflects its ancestry. More than any other Australian fossil, WLH 50 addresses some of the more general issues prominent in studies of Late Pleistocene and Holocene human evolution. One of these is the prevalence of evidence for mixture between seemingly different hominids, now recognized in studies of human genetics (Pääbo 2014). Another is the recognition that these mixing groups had more genetic variation between populations than is now evident in *Homo sapiens* (Hawks 2013). The consequences of these two facts should be evident in anatomical studies as well as genetic ones, and WLH 50 has the potential to address them. In this regard Australian prehistory may be seen to resemble European prehistory, in that the modern Europeans have a complex ancestry in which different human subspecies (Wolpoff 2009) mixed in the Pleistocene (Wolpoff et al. 2001).

Australia is one of the most recent regions of the Old World to be inhabited. It is widely, perhaps universally, accepted that the human migration or migrations to Australia

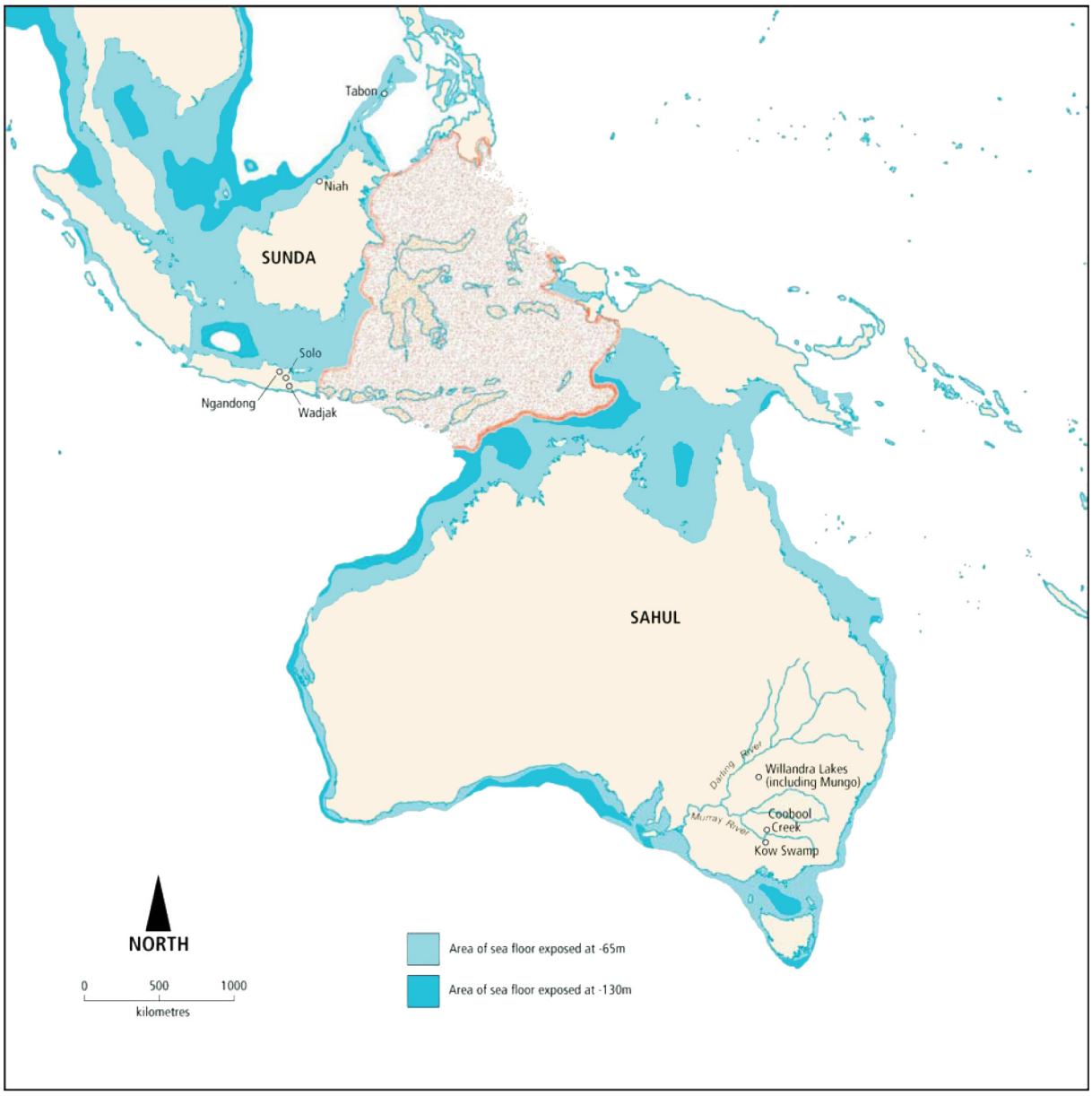

Figure 1. The Pleistocene extent of Sahul and Sunda, with the locations of Late Pleistocene fossil sites. Pleistocene Australia, the major part of Sahul, shows the locations of most of the fossils discussed here. At no time during the Pleistocene was it possible to reach Australia without crossing water (from Pardoe (2006, Figure 1), with permission).

were of modern humans with an established, sophisticated seafaring technology (O'Connell et al. 2010) based on bamboo (Birdsell 1977). Once purposeful, albeit sporadic, movement to the continent began, there is no reason to expect that it was interrupted for long. Beginning some 50 kyr ago, the ancestors of recent indigenous Australians began to cross a biogeographic divide (Wallacea) over gaps, some of which were as much as (depending on the sea level at the time) 70km of water, a distance far enough beyond the horizon that it was not possible to see across to land. The prevailing currents and the absence of suitable, bamboo-like building materials in Australia assured that the direction of travel was most likely one-way (Allen and O'Connell 2008; Westaway and Lambert 2014). Because it was uninhabited, many consider this Australian colonization as migration rather than dispersal (Balme 2013).

The deep prehistory of Australian ancestors cannot be found in Australia. It is in this context that comparisons of the Late Pleistocene/Holocene fossil record of Australia and the nearby lands are significant. With its peripheral location, isolation by sea (Figure 1), and the likelihood that gene flow to the continent was limited to the later Pleistocene and mostly one-way as noted above, Australia has come to play a unique role in understanding the worldwide pattern of Pleistocene human evolution, and WLH 50 addresses key issues of recent indigenous Australian ancestry. Anatomical comparisons and genetic evidence, discussed below, clearly reflect what has long been obvious; Australians

came from East and Southeast Asia. But what parts of Asia, and when, have been researched and discussed for more than a century.

Throughout the 20th century there was a succession of scientists who contended the source population of Australian ancestors was Indonesian. The putative Indonesian ancestors were first thought to be the *Pithecanthropus* remains known from Trinil (later including the Sangiran crania), and finally settled to be their descendants, represented by the more recent Ngandong crania. Ngandong is the sample of potential ancestors nearest to Australia in space, and closest to WLH 50 in time. Yet, it would be fair to say that the contention that some of the ancestors of Australians were from Ngandong, or from Ngandong-like populations, has been and continues to be controversial. The problem created by a Ngandong ancestry is that the Ngandong crania are variously classified as *Javanthropous soloensis*, *Pithecanthropus soloensis*, *Homo soloensis*, or as a late-surviving *Homo erectus*, but only rarely as *Homo sapiens*. The implications assessed for the contention that Ngandong was one of the ancestors of recent indigenous Australians reflect issues of race that have plagued paleoanthropology from its beginnings (Wolpoff and Caspari 1997).

By virtue of its age and anatomy, we believe WLH 50 is very well positioned to address these and other related issues of Australian ancestry. We present here the full and complete details of the anatomical observations and measurements possible on the WLH 50 calotte, and systematically compare these to the adult crania from Ngandong, following the pattern of other monographs and long papers on fossil hominid crania that are both descriptive and comparative (e.g., Condemi 1992; Frayer et al. 2006; Heim 1976; Sergi 1948; Suzuki 1970; Weidenreich 1943). In doing so we rely both on the measurements and observations for WLH 50, the crania from Ngandong and Kow Swamp, and observations made of the Coobool Creek crania by one of us (MHW), Weidenreich's (1951) Ngandong descriptions and observations, and Holloway's (1980) cranial capacity assessments for Ngandong, as well as the sources cited below. It is our intent to systematically examine the possibility that Ngandong or a Ngandong-like population is among the ancestors of WLH 50; we treat this as our null hypothesis.

We also compare WLH 50 to a selected sample of Australian fossils to address the issue of whether its anatomy reflects pathology, and to what extent its features fall within the range of anatomical variation in Late Pleistocene and Holocene Australia. With a variety of tests and approaches, we also compare metric and non-metric aspects of WLH 50 to the sample of earlier African Pleistocene crania, to examine whether there is a credible case for a unique African ancestry without Ngandong input.

Finally, we discuss the importance of population genetics and paleogenetics in understanding the sources and pattern of migrations to Australia. Even though mitochondrial and nuclear DNA have not been obtained from WLH 50 or Ngandong, and it unlikely that this will ever be possible for WLH 50, much is known about the recent and deep history of the region from genetic analyses and these help frame the possibilities for WLH 50, Ngandong, and their relationship.

Paraphrasing the words of Silvana Condemi in introducing her monograph on the Saccopastore Neandertal crania (1992), the goal of this monograph is to provide both a description and an interpretation of the WLH 50 fossil. In this monograph we ask about the place of WLH 50 in human evolution, and what the pattern of human evolution has been that creates such a place for this specimen?

BACKGROUND

Hermann Klaatsch [1863–1916] addressed the pattern of ancestry in Australia early in the 20th century, proposing a single lineage interpretation of indigenous Australian origins (1908a). He linked the recent/living populations of Australia to the "*Pithecanthropus*" remains from Trinil, Indonesia. Of equal importance, Klaatsch stood apart from most of his colleagues in recognizing that the recent indigenous Australian populations were not especially related to European Neandertals (1908b). Huxley (1863) thought that Australians were related to Neandertals, and this was accepted by many of Klaatsch's contemporaries (Burkitt and Hunter 1922; Cunningham 1907; and later Jones 1934), although not by Klaatsch himself. Somewhat later, cognizant of the 1922 publication of additional discoveries by Eugene Dubois [1858–1955], Sir Arthur Keith [1866–1955] proposed an interpretation of Australian ancestry similar to Klaatsch's earlier position, but adding other key specimens such as Ngandong. He imbedded the interpretation in a broader scheme of human evolution (1936).

By 1946, Earnest A. Hooton [1887–1954] was depicting recent indigenous Australian ancestry in a similar but even more complex manner in his influential textbook *Up from the Ape* (1946: 413, Figure 71). He showed a line of descent from "*Pithecanthropus*" to "*soloensis*," extending it to include the later crania from Wadjak and the "Australoids." Hooton's view of Australian ancestry was complex because it included a reticulating branch from Melanesians, whose origin in turn was from the branch leading to African "Negroids."

In fact, many early and mid-century researchers, like Hooton, hypothesized multiple Australian origins (from Smith 1918 to Wunderly 1943). In more recent times there has been a diversity of interpretations, many of which came from Hooton's students. Carleton Coon [1904–1981] alone restated Klaatsch's proposal, in positing a singular and unique ancestry for Australians, evidenced by his (1962) chapter-title description: "*Pithecanthropus* and the Australoids". Coon considered the Australoids as one of the five major human races, each with its own, mostly independent, evolutionary pathway, and each becoming modern (crossing what he called the "sapiens threshold") independently, at different times. William W. Howells [1908–2005] once favored "Coon's view, at least in distinguishing recent indigenous Australians from people everywhere while allying them closely with Tasmanians and Melanesians" (1976: 142) and suggesting that (as he put it): "Solo man may have

had an influence on *Homo sapiens*, and one or two of the apparently old Australian skulls (not Keilor) are exceedingly heavy-browed" (1967: 338). At that time Howells found no special relationship with East and other Southeast Asians (1967: 159), although his opinion changed on this issue and he later suggested ancestral roles for other Asians. But the Hooton student with the most sophisticated understanding of Australian prehistory was Joseph Birdsell [1908–1994], discussed below.

WEIDENREICH

Franz Weidenreich [1873–1948] provided a complex interpretation of Australian origins that combined the suggestions of (1) ancestry in the Middle and Late Pleistocene hominids of Indonesia with (2) other ancestral Asian populations. This was part of his polycentric interpretation of human evolution. Weidenreich's interpretation set the stage for virtually all subsequent discussions of ancestry. Like some earlier writers, he noted many specific resemblances of some recent indigenous Australians to the earlier Indonesian remains (Figures 2 and 3), stating:

> "When … [the skulls] of modern Australian natives are compared with *Homo soloensis* the likeness is surprising, after due allowance is made for the fact that the Australian is further developed phylogenetically than is *Homo soloensis*. In Figure 264C [reproduced here as Figure 2] the skull of an Australian (No. 792) is depicted. … When this specimen is compared with the Ngandong Skull 5, the latter being reduced to the same length, the only difference is the greater height of the modern skull and the more pronounced vaulting of the vertex region. There is, however, no great divergence of the cranial capacity, which amounts to 1255 cc in the Ngandong and 1211 cc in the Australian. But there is considerable difference in the maximum length: the Ngandong skull measures 219.5 mm while the Australian has a length of 203 mm. In spite of its modern form the Australian skull shows well-developed superciliary ridges; a flat, far-receding forehead; a prelambda depression; a torus-like demarcation line between occipital and nuchal plane and, finally, a sharp bend between the upper and lower scales of the occipital bone. In addition the pterion region reveals a short sphenoparietal articulation measuring only 5 to 8 mm. The infraglabellar notch is deep and narrow as it was, apparently, in the Ngandong Skull 5" (Weidenreich 1943: 248–249).

These resemblances were not found in all Australians. Cognizant of the range of normal variation in the full Australian sample, Weidenreich considered the Ngandong-Australian relationship as *only part of Australian ancestry*, as one of many links in the polycentric pattern of human evolution that he recognized. Moreover, the same resemblances are not found in all of the Ngandong specimens, as the comparison of Figure 2 (the specimens Weidenreich compared) and Figure 3 (our substitution of a different Ngandong cranium) shows. Comparisons of the Australian Weidenreich illustrated with different Ngandong specimens[1] reveal different patterns of similarities and differences. This is one reason why our comparisons of WLH 50 (below) are with each of the Ngandong male specimens, and not with their average.

The complex relationship of recent indigenous Australians with nearby ancestral populations is a small part of the network of ancestry for all human evolution that Weidenreich described through the Pleistocene (1946: Figure 30, reproduced here as Figure 4). In this interpretation past populations had many descendants and recent/living populations had many ancestors. The specific implications for Australian ancestry were[2]:

> "At least one line leads from *Pithecanthropus* and *Homo soloensis* to the Australian Aborigines of today. This does not mean, of course, that I believe all the Australians of today can be traced back to *Pithecanthropus* or that they are the sole descendents of the *Pithecanthropus*-*Homo soloensis* line." (Weidenreich 1943: 248–250).

Weidenreich thusly posited multiple ancestors for Australians. He was unusual in choosing a network to illustrate this and other relationships between Pleistocene and recent/living populations, rather than the more commonly used tree of relationships, but he chose a network for good reasons:

> "If the Hominidae are one species in the genetical sense and an exchange of genes was possible in phases I to IX [the prehistoric phases shown in Figure 4] as it is possible in phase X (modern man), the commonly used form to represent their lineage gives an entirely wrong idea. The tree with a common stem and more or less abundant ramifications leaves no possibility to indicate graphically an exchange of genes. The branches and sub-branches appear to evolve completely independent of each other once they have deviated. In reality, there must have been inter-communications between the branches. The graph which best fits this perception is a network. Its interconnections indicate the lines along which the exchange of genes could be effectuated." (Weidenreich, cited from his unpublished book manuscript on human evolution, stored in the Anthropology Department of the the AMNH).

Using a network to depict the relationships and pattern of human evolution was a break with Klaatsch, with the highly influential evolutionary polygenist Ernst Haeckel [1834–1913], and even with Weidenreich's mentor Gustav Schwalbe [1844–1917]. Weidenreich would not arrange human fossils on a genealogical tree because a tree cannot depict reticulation. Weidenreich's insight was to understand that the population structure within the human species was important for understanding human evolution, and that in the overall pattern of human evolution, older populations that did not become extinct had multiple descendants, while recent/living populations had multiple ancestors[3]. The network approach to understanding human population structure has withstood the test of time and plays a key role in the modern genomic era. Thus, Templeton (2005, 2007) regularly uses it in depicting the pattern of Pleistocene human evolution. Hammer and colleagues recently

Figure 2. Comparison of a recent indigenous Australian (above, after Weidenreich 1943: Figure 364C) and Ngandong 5 (below, after Weidenreich 1951: Plate 23). This figure replicates the comparison from the Zhoukoudian cranial monograph (Weidenreich 1943), substituting a clearer view of Ngandong 5 from Weidenreich (1951). The face of the Australian was obscured by Weidenreich to present the same regions as the Ngandong cranium preserves. The specimens are scaled to the same size and shown facing in the same direction. In this comparison the contour (angulation and flatness) of the frontal, projection of the supraorbital region, the tall vertical occipital plane and angular torus development are quite similar. We recognize that Weidenreich picked this Australian cranium for purposes of showing similarity, and, that not all Australian crania share these characteristics. But the specimen is not at all unique in these aspects and we have been careful to test hypotheses that address issues of variation, not similarity alone (see Figure 3).

Figure 3. Comparison of the same Australian as in Figure 2 (above, after Weidenreich 1943: Figure 364C) and a different Ngandong cranium: Ngandong 1 (below, after Weidenreich 1951: Plate 23). The face of the Australian was obscured by Weidenreich to present the same regions as the Ngandong cranium preserves. The specimens are scaled to the same size and shown facing in the same direction. In this comparison as in Figure 2, the details of the forehead are also similar. There are additional similarities in the shape and orientation of the mastoid process, the more posterior position of the greatest cranial height, and the contours and other details of the cranial posteriors such as the rearward projection of the entire occipital plane and its straight, vertical posterior surface.

wrote (2011: 15123):

> "The observation that populations from many parts of the world, including Africa, show evidence of introgression of archaic variants suggests that genetic exchange between morphologically divergent forms may be a common feature of human evolution. If so, hybridization may have played a key role in the *de novo* origin of some our uniquely human traits."

Networks are widely accepted as a valid way to depict the Pleistocene pattern of human evolution (Lordkipanidze et al. 2013; Templeton 2005). We discuss the human evolutionary network here because this approach informs our own.

NEW FOSSILS, NEW DETAILS

In the almost 70 years since Weidenreich wrote, the Australian fossil record has considerably increased in size[4], and new dates and archaeological associations for the human remains make them valuable in establishing the details of Late Pleistocene evolution in the region, and beyond. One specific implication of Weidenreich's reticulating network was in its reflection of a multiple migration model for Australia. In fact, he was the first to do so while designating one of the sources as Ngandong and earlier Indonesian homi-

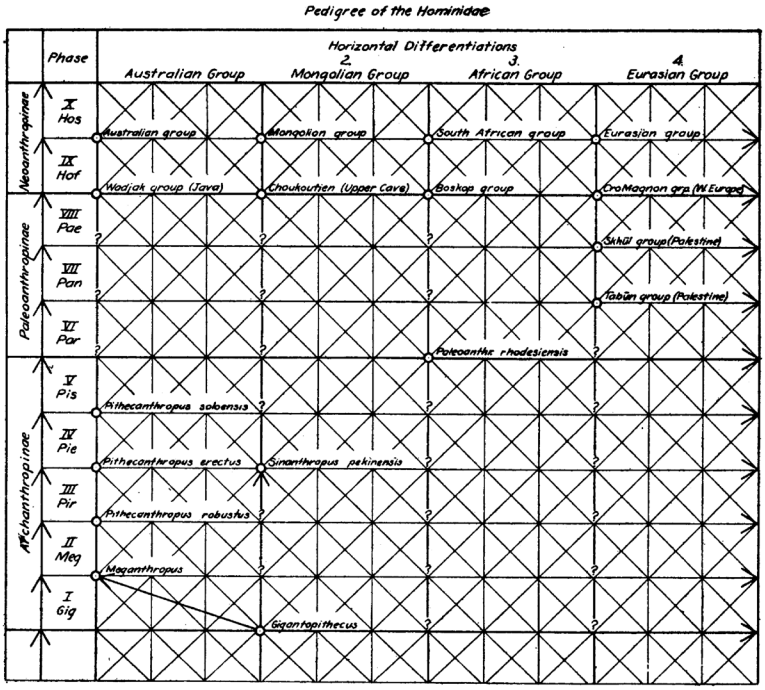

Figure 4. Weidenreich's network of human evolution, as illustrated in his book Apes, Giants, and Man (Weidenreich 1946: 30, Figure 30).

nids. Apart from the evolutionary link with Ngandong, he provided few details for this model. Weidenreich died before his Ngandong monograph was finished and the 1951 publication did not have sections on interpretations and discussion. But his publications on other Australian fossils (e.g., 1945) made it clear that Ngandong was not the only ancestral source he considered—Ngandong was not the sole ancestor of recent indigenous Australians.

Many multiple migration interpretations of Australian ancestry were subsequently proposed—Birdsell (1967a, b); Bräuer (1989); Freedman and Lofgren (1979); Howells (1976); Macintosh (1965, 1967); Pietrusewsky (1984); Thorne (1976, 1977, 1980, 1984); and, Thorne and Wilson (1977). Birdsell (1967a, b) presented the most complex scheme of multiple migrations in his trihybrid hypothesis, with an archaic "white" ancestral group somehow allied to the Ainu, a "Negrito" group that was part of an ancient dispersal from the Congo Pygmies to the Andamanese, and a "Carpentarian" group from India. He speculated that some of the features found in the "Murrayian and Carpentarian types" of Australian ancestral groups could have been the result of mixture with *H. soloensis*, a contention (as noted above) with which Howells agreed.

Webb (2006) thought that the first migrants to Australia were *H. soloensis* populations from Indonesia. According to Webb, these were followed by "modern human" groups that evolved outside of Australia, with "African roots" and "Negrito or Negrito-like" anatomy, including small stature. Encountering the earlier migrants led to mixing and because the constituent populations were subspecies in this interpretation, this could be described as hybridization that was dominated by the "modern" group because of continued migrations to the continent from Southeast Asia (Brown 2013), which resulted in recent and modern indigenous Australians. Curnoe (2009: 981) summarized the current formulation of this two-migration model[5] incorporating the new fossils and most recent dates (reviewed by Thorne and Curnoe 2000):

> "The first group of people with a 'gracile' cranial morphology, represented by WLH 1 and WLH 3 (and probably later by Keilor [Figures 5,6]), colonized Australia at perhaps 50-70 kyr. These remains are characterized by steeply walled and relatively thin boned vaults, which lack postorbital constriction, exhibit absence or a marked reduction in ectocranial structures (crests, ridges and tori), a relatively narrow facial skeleton, reduced prognathism, and a small to moderate dental size. A second group of morphologically 'robust' people, first represented by WLH 50, and later by some Kow Swamp and the Cohuna and Nacurrie individuals, is posited to have arrived perhaps about 20 kyr. These remains are characterized by thickly boned vaults, with marked frontal recession, strong postorbital constriction, well-developed ectocranial structures, relatively broad facial skeletons, high prognathism, and moderate to large dental size." (Curnoe 2009: 981)

Migrations versus Sources

The issue of how many sources contributed to the colonization of Australia has been debated for a long time (Kirk and Thorne (eds.) 1976; O'Connell and Allen 2004). The question was originally framed in terms of migrations, as discussed above. While the migration interpretations have never disappeared (Reyes-Centeno et al. 2014), focus shifted from numbers of **migrations** to numbers of **sources**

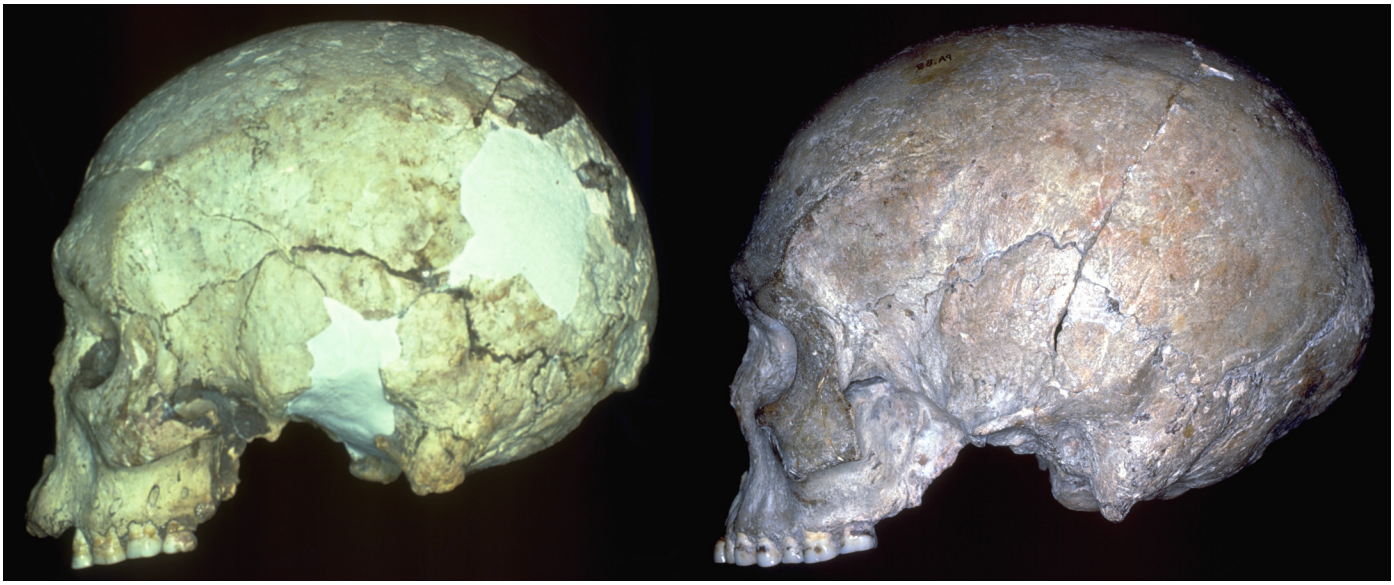

Figure 5. The many similarities of Keilor (from Australia, left) and Liujiang (from South China) may reflect an Asian migration to Australia (as reviewed by Curnoe and Thorne 2006a) and help establish its origin. These crania, shown to the same size and facing in the same direction, share a transversely flattened, vertical face with slight alveolar prognathism (greater in Keilor), anterior-facing cheeks, and a low, flattened nasal profile with a weak nasal root. The superciliary and other tori are weakly developed and the forehead is high and rounded. Supporting this interpretation, Matsumura (2006: Figure 2.3a) shows a dendrogram of Q-mode correlation coefficients based on seven cranial measurements with a cluster with Keilor including Liujiang, Wajak, and Minatogawa, contrasting with a second cluster that includes Tasmanians and Australians. Features shared by Keilor and Liujiang contrast with the characters of (what Curnoe (2009) describes as) "robust cranial anatomy," represented earliest by WLH 50, and later by some Kow Swamp folk and the Cohuna and Nacurrie crania. These observations and analyses, and the fact that Keilor is from Australia and Liujiang is from South China, combine to suggest the possibility that some Australians descend from immigrants who were directly or indirectly of Chinese origin.

when Thorne first stated his two migration interpretation in terms of "robust and gracile" groups, using robustness in the sense of ruggedness, and gracility as its opposite (1976, 1977). Robustness and gracility replaced descriptions of *H. soloensis* and Negrito-like cranial anatomy, respectively, but these have become misleading and inaccurate terms[6] that could reflect many things besides ancestry, including environmental adaptation (Bulbeck 2001) and economic-related activities (Collier 1989). Thorne (1984) was specific in defining them as anatomical contrasts he perceived did not come from distinct migrations, but rather reflected two distinct geographical sources. This opened the possibility that colonization could have involved many migrants at varying times throughout Australian prehistory, in particular, from Indonesia, and East Asia (China). As he often put it, once migrants began to arrive by sea, why not expect they did so continuously throughout Australian prehistory and history? Accepting that the question was about sources, "robustness" and "gracility" descriptions of cranial anatomy became the wrong contrast to apply to this comparison (*contra* Curnoe and Thorne 2006a), just as primitive and modern was the wrong contrast to apply in earlier formulations. We agree that the valid contrast is in features that relate to geographic origin.

The recognition of several different geographic sources for Australians creates the potential for models of a complex population history, because there is no mechanism that could have kept hunter-gatherer populations from different geographic sources separated or distinct. "It is not conceivable that groups of widely differing morphologies could coexist at the same place for tens of thousands of years" (Pardoe 2006: 14). Supporting this notion, Adcock and colleagues (2001) analyzed ancient mtDNA from fossil crania regarded as "gracile" and "robust," finding that most[7] belong to a single mtDNA clade that also includes the sequences found in living indigenous Australians. Different cranial morphologies were not associated with different mtDNA lines. The mixture of migrants from different regions was thorough, and evidently happened long before these fossils lived. Supporting this interpretation, in the two large fossil samples (Kow Swamp and Coobool Creek) the features of some specimens suggest some Indonesian ancestry while other specimens not only lack these features, but in some cases they have other anatomies suggesting some East Asian ancestry. Different crania combine different sets of features and the most reasonable interpretation is that their ancestry is mixed[8]:

> "In Kow Swamp 15, the browridge is continuously developed, dipping only slightly over the nose, and its thickness is close to the Solo average. The frontal of Kow Swamp 1 retains a sagittal keel[9] that runs almost to the

Figure 6. Keilor (left) and Liujiang (right) are shown to the same size and facing in the same direction. Similarities visible in this view include the low rectangular orbits, broad interorbital area, and thickening at the zygofrontal suture (but without a trigone at this position on the frontal). That Keilor is from Australia and Liujiang is from South China suggests some Australians descend from immigrants who were directly or indirectly of Chinese origin.

> browridge and eliminates the groove between the browridge and the forehead. The outer part of the browridge in Kow Swamp 9 follows the temporal line backwards, forming a backward-pointing triangle at the upper corner of the orbit [frontal trigone]." (Wolpoff 1980: 327–330)

But at the same time the resemblances of Keilor are with Liujiang (see Figure 5; Figure 6) and with Zhoukoudian Upper Cave (Thorne 1980; Curnoe 2007). Other specimens such as Mungo 1 and 3, two of the earliest dated Australian remains, also show similarities with East Asians. Yet:

> "Mungo 1 closely resembles Kow Swamp 4 and 16 while Mungo 3 (male) resembles Kow Swamp 14 in browridge development and Kow Swamp 14 and 15 in frontal curvature. In other words, the range at this site encompasses most of the known [Australian] fossil material." (Wolpoff 1980: 330)

Variations in the anatomy of indigenous Australian populations such as those described above may suggest multiple geographic sources for Australians, for instance, from Indonesia or East Asia, but picking through fossil and recent specimens in the hope of finding specific individuals of Indonesian, African, or East Asian ancestry is misleading and an invalid use of the data, because all skeletal samples are mixed. Current evidence places the migration or migrations to the continent as beginning some 50,000 years ago (Hiscock 2008; O'Connell and Allen 2008, 2012), with dispersals throughout the continent by 40,000 years ago (O'Connell and Allen 2004; Pardoe 2006). No fossil or archaeological evidence suggests the isolation or segregation of Australian populations from the rest of the world once migration to the continent began, and every indication suggests significant gene flow throughout the continent (Habgood and Franklin 2008).

Was There a Single Source Population?

The alternative to multiple sources for indigenous Australians is a single source. Ultimately, of course, the ancestors of all Pleistocene human populations originated in Africa. The question is about proximal sources of Australians. This proved to be a more complicated discussion for Australia than it had been for most other regions.

During the same period that multiple sources of Australian ancestry were under discussion, a number of workers promoted the hypothesis that there need not have been more than a single geographic source region, and that subsequent variation among Australians evolved *in situ* from it (Abbie 1968; Brown 1987; Bulbeck 2001; Cameron and Groves 2004; Habgood 1986; Howells 1977; Pardoe 1991, 2006; Pietrusewsky 1990; Stone and Cupper 2003; Wright 1976). It is not simple to disprove this contention, since the adaptive changes in Australia parallel changes in other parts of eastern Asia (Brown 1992; Brown and Maeda 2004), and more broadly in other parts of the Old World. Whatever the number of sources, the likelihood of adaptive changes in Late Pleistocene and Holocene Australians, as these authors described, is quite high, and provides an alternative explanation for the pattern and details of Australian variability (Pardoe 2006) that has been difficult to disprove. Moreover, there was limited consensus on where the single source region might have been.

One specific possibility that can be addressed is whether as they migrated to the continent, the early Australian

immigrants were directly descended from an African population whose ancestors had left Africa not very long before (Mellars et al. 2013; Oppenheimer 2009). Archaeological evidence for a direct migration from Africa is lacking (Habgood and Franklin 2008), and unambiguous evidence of diagnostic African anatomy in the Australian fossil record is yet to be demonstrated. Evidence rejecting a direct African origin for Australians also comes from our demonstration, below, that systematic comparisons of WLH 50 to earlier African crania fail to demonstrate unique descent from these Africans. These comparisons, however, cannot exclude the possibility that some Australian ancestry was African.

The Simplest Origins Hypothesis

Considering geography and the Pleistocene pattern of ocean currents, the most likely possibility is that the proximate geographic origin for Australians was in the regions closest to Australia—in eastern Asia and island Southeast Asia. As discussed above, some of the earlier scientists contended that one of these islands was Indonesia, and in one way or another an Indonesian origin, or more precisely the idea that one of the source populations for Australians was Indonesian, has remained an important intellectual thread throughout the history of Australian prehistory. We accept this contention as our null hypothesis, that one of the ancestors of Australians is Ngandong or a sample similar to it.

Archaeologically, demographically, and anatomically, the populations of Australia evolved throughout the part of the Pleistocene that the continent was inhabited. Our second hypothesis is that the pattern and direction of their evolution was similar to other regions of the world; specifically, that WLH 50 differs from Ngandong in ways that reflect the pattern of evolution from the Late Pleistocene in other parts of the world. This is not parallelism. It would imply significant archaeological and biological connections between Australia and its neighbors; the continent could not be considered an isolated *cul-de-sac*.

WLH 50

Of the new Australian fossils found in the latter part of the 20th century, WLH 50 (Figure 7) is not the most complete, but is by far the most provocative discovery. On the basis of its size and the development of cranial superstructures, WLH 50 is a male calotte (see Figure 7), found with some associated fragmentary facial bones in 1980 on the surface of a lunette near Lake Garnpung in the Willandra Lakes area of New South Wales, Australia (see Figure 1). While in the 21st century, Australian ancestry is usually assessed as (mostly Southeast) Asian (Dennell and Porr 2014), date assessments for the Pleistocene Australian fossil record are recent enough for the expectation that evidence of additional ancestry in either (or both) Indonesian (Ngandong) or Late Pleistocene African populations could potentially be found.

A number of age estimations have been published for the WLH 50 site and the fossil itself (Caddie et al. 1987; Simpson and Grün 1998); in our view, the most recent determination of its age (Grün et al. 2011) is the best grounded and supplants earlier age assessments:

> "If reworking or burial is considered, the age of the WLH 50 human remains lies between 12.2 ± 1.8 and 32.8 ± 4.6 ka. The remains most likely date to around 26 ka but realistically will fall into an age range of 16.5 - 37.4 ka" (Grün et al. 2011: 604).

We believe WLH 50 is an adult, probably a young to middle age male on the basis of cranial suture closures. The sutures preserved for WLH 50 present a mosaic of closures and fusions, as commonly is the case. All endocranial sutures are closed, although visible to different extents. Meindl and Lovejoy (1985) show ectocranial closure is superior to endocranial suture closure as an age indicator. They divided the ectocranium into two regions for analysis of suture closure at specific points, the vault system and the lateral-anterior system (comprised of pterion, the mid-coronal point, sphenofrontal point, inferior sphenotemporal point, and superior sphenotemporal point, all illustrated in their Figure 1). The lateral-anterior system was found to be superior to the vault system for age assessment. Unfortunately, only the mid-coronal suture remains of the lateral-anterior suture system in WLH 50. The WLH 50 coronal suture is minimally closed and easily visible ectocranially, at least across the top of the vault to the position of the temporal lines (stephanion). In the mid-coronal position it matches the "minimum closure" illustrated by Buikstra and Ubelaker (1994: Figure 22b). The lambdoidal suture is only slightly more closed, not as closed as the examples of "significant closure." The lambda and bregma positions are not closed on the lambdoidal and coronal sutures, respectively, and the condition of the other preserved sutures support a younger rather than an older age assessment. In contrast the sagittal suture is fully fused and obliterated externally, though somewhat visible internally. The advanced closure stage of the sagittal suture is unusual for a younger adult, according to Meindl and Lovejoy (1985), as is its combination with the minimum closure of the coronal suture, but ectocranial closure of the sagittal suture is age-independent (Hershkovitz et al. 1997) and thereby unreliable for estimating age.

As described below, WLH 50 is arguably the largest and most rugged of the Late Pleistocene Australians. But neither its size nor its anatomical features are anomalous or unique for a Late Pleistocene hominid, and the observation that most of its characteristics appear in other, more recent crania from the Australian fossil record, and persist in some historic individuals, suggests that WLH 50 can validly inform the contention that indigenous Australians descend from more than one geographic source, and the hypothesis that one of those sources is Late Pleistocene Indonesians.

GOAL OF THE DESCRIPTION AND ANALYSIS

The goal of this monograph is to provide both a description of the WLH 50 fossil and an interpretation of its place

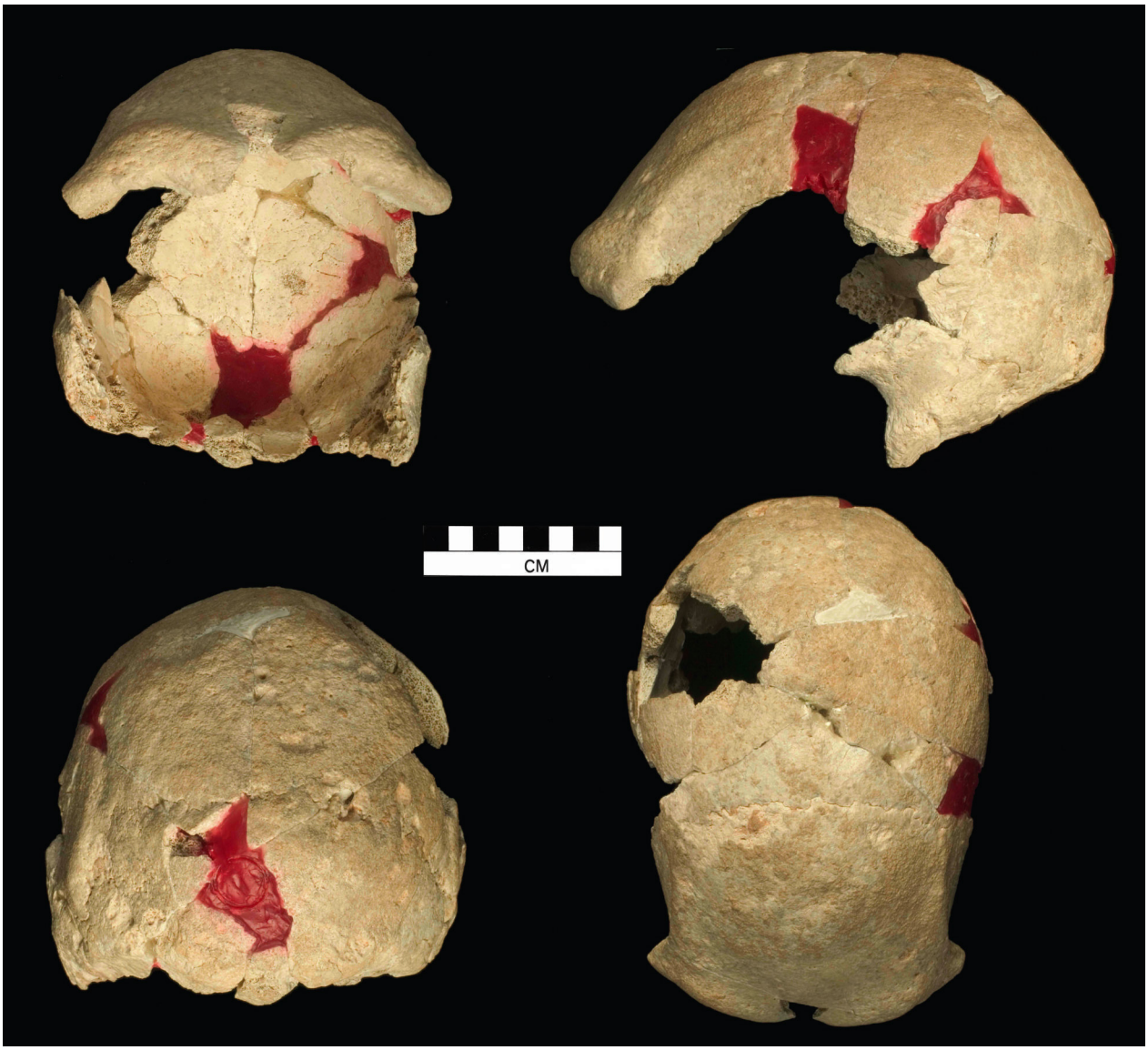

Figure 7. WLH 50 as reconstructed by Thorne, modified after Curnoe (2011: Figure 2). Upper left is the frontal view, upper right is the lateral view, lower left is the posterior view, and lower right is the superior view.

in human evolution. Because of its anatomy and geologic age, WLH 50 provides a unique opportunity to address issues of indigenous Australian ancestry, and we approach this in a comparative context. A detailed description and comparison of the WLH 50 cranium is important for examining many of the relationships that have been proposed for Australian fossils, discussed above, and for addressing issues of multiple sources for Australians, including Late Pleistocene Indonesians from Ngandong. The Ngandong remains comprise the closest hominid cranial sample in both space and time, from outside the Australian continent (see Figure 1).

The age of the WLH 50 cranium is between the dates estimated for Ngandong and for the Kow Swamp/Coobool Creek Australian samples. Ngandong[10] is unquestionably earlier (Antón et al. 2007; Indriati et al. 2011; Huffman et al. 2010, who thoroughly discuss all issues of provenience). Other Terminal Pleistocene-early Holocene aged Australian samples that have been described as retaining some Indonesian-like features may overlap with the latest portion of the WLH 50 age estimate, but most probably are later. The largest of these are Coobool Creek (n=126), where there are uranium/thorium dates of 12,500 ±400 (Brown 1987) and 14,300±1000 (Brown 1989) for Coobool 50.65, and Kow Swamp (n=22), with a reported date of 22–19 kyr (Stone and Cupper 2003).

Systematic comparison of WLH 50 with the Ngandong crania specifically addresses questions of whether Ngandong could be one of his ancestors. The issue is *not* about whether WLH 50 is part of the Ngandong sample; anatomy, geography, and date estimations show it most certainly is not.

Nor is the issue discussed here whether WLH 50 should be considered an anatomical link or intermediary between Ngandong and recent or living Australians, or whether it shows continuity between Ngandong and recent or living

Australians. History shows us that these interpretations could sound as though there was a single, unique line of descent from Ngandong to WLH 50 and this is not a hypothesis that we either consider or believe could be valid. If there had been a unique line of evolution from Ngandong to WLH 50 to later Australians, the interpretation of WLH 50 as an anatomical link might be possible, but our contention is that these relationships are more complex than linear evolution because they involve mixture with other populations at each point. Our interest is in whether Ngandong *is one of* WLH 50's ancestors. This would provide evidence that some indigenous Australian ancestors were Pleistocene Indonesians.

Nor is this issue whether WLH 50 can be described as "archaic," "modern," or "intermediate," or is part of the same taxon Ngandong belongs to if that taxon is different from *Homo sapiens*. We will return to this point.

We focus here on a question of ancestry, one that we believe can be systematically addressed as a testable hypothesis (illustrated in the pattern of evolution shown in Figures 4 and 8): **does WLH 50 indicate that Ngandong-like populations are among the ancestors of indigenous Australians**? There may be significant ways in which WLH 50 differs from the Ngandong crania; the question is whether these are ways in which other recent Australian crania also do not resemble Ngandong.

We address this hypothesis of ancestry phenetically, on the basis of similarities (or their absence) because in this case a hypothesis of ancestry cannot be addressed cladistically. Whatever the correct taxonomy is, the putative ancestors of WLH 50 are too closely related to WLH 50 for any formal cladistic assessment to be accurate (Curnoe 2003; Hawks 2004; Westaway and Groves 2009), if for no other reason than for so close a relationship, many times more data than actually exist would be required for reasonable accuracy. To do so, we undertake below a detailed comparative study of the data we collected for WLH 50[11], and the anatomical and statistical comparisons that address hypotheses of ancestry and normality for WLH 50.

Many of these comparisons were quantified with measurements. The grand measurement set from which measurements of WLH 50 were defined is comprised of standardized measurements from R. Martin (1928), the Biometrika school, the W.W. Howells data set, and other normally used sources. Added to these were measurements developed to allow comparisons of fragmentary cranial remains too incomplete for standard measurements to be possible. This provides a measurement set of many more measurements than has ever been used before in comparisons with WLH 50, and *one particularly designed to maximize comparisons of crania that are not complete*.

The descriptions following also include systematic anatomical comparisons[12] with the Ngandong crania. We report Weidenreich's (1951) allocations of sex, but with some skepticism. While Weidenreich's estimation is that 4 of the 6 complete calottes are male, we recognize the tendency to over-estimate the number of males in fossil hominid populations (Weiss 1971), and while accepting Weidenreich's assessments for Ngandong, in our view, sex determination within this sample of faceless calottes lacking associated postcranial remains will always be problematic. For this reason our comparisons are with the individual crania and not with the sample means, or with the means for the putative males.

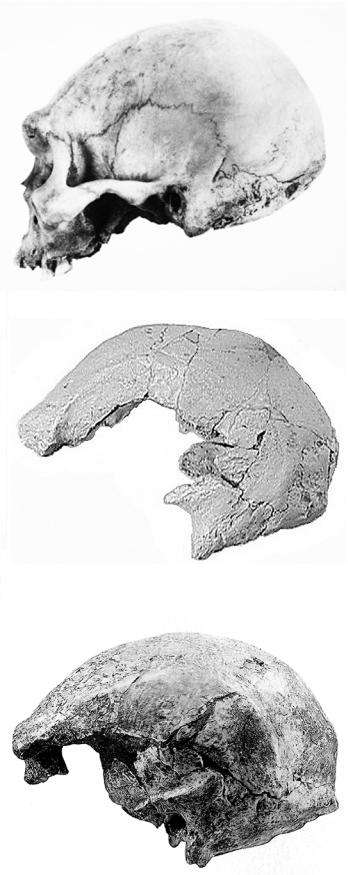

Figure 8. Comparison of an Australian (top) from Western Arnhem (from Jelínek (1979), after Curnoe and Thorne 2006b: Figure 9), a cast of WLH 50 (middle), and Ngandong 1 (below) from Weidenreich (1951: Plate 19). The specimens are scaled to the same size and shown facing in the same direction to facilitate comparisons of cranial shape. While each differs from the others, the figure illustrates some of the similarities the three crania share. But this is not meant to illustrate a simple relationship of linear evolution. For instance, in some ways the greater similarities are between the Australian and Ngandong crania. WLH 50 is by far the largest and thickest of the three and in this lateral view its sagittal contour is less evenly rounded; from the frontal to the nuchal plane it is more strictly divided into junctures of 5 distinct, flattened planes. In other comparisons such as thickness of the supraorbitals, expression of the angular torus, and flattening of the nuchal plane WLH 50 is more similar to Ngandong 1. Our contention is that their anatomical relationship is complex because Ngandong is only one of the ancestors of WLH 50, which in turn is only one of the ancestors of recent and living Australians such as the cranium shown here.

We also make some limited comparisons with later Australian fossil crania. These comparisons are not meant to be

systematic, but for the purpose of determining whether the anatomical features of WLH 50 also can be found within the later Australian fossil sample. We want to establish, within reason, whether WLH 50 is part of a normal range or an unusual, unexpected, or perhaps anomalous or pathological Australian fossil. Issues of the uniqueness and/or purported pathology or artificial alterations of WLH 50 are informed by comparisons with males from the large samples from Kow Swamp and Coobool Creek. Granted that these Kow Swamp and Coobool comparisons are sampled from one extreme of a wide range of anatomies, we believe they are sufficient to address the question of whether WLH 50 is normal or unique in demonstrating some Ngandong contribution to Australian ancestry. Although these data can also effectively address the hypothesis of an African source for indigenous Australians, no feature or combination of features seems to clearly demonstrate that an African source was the only, or the unique ancestor. We return to this question in our statistical analysis.

Where appropriate, we cite the observations on WLH 50 that Webb (1989) published; Webb also based his remarks on the study of the original specimen. Curnoe (2009, 2011) and Curnoe and Thorne (2006a) published additional comparisons with other Australian fossils. These also are cited as appropriate. Although lacking a systematic description, there has already been considerable discussion about WLH 50 and its place in human evolution (Curnoe 2009, 2011; Hawks et al. 2000; Miller 1991; Stringer 1998; Stuart-McAdam 1992; Webb 1989, 1990, 2006; Westaway and Groves 2009; Wolpoff et al. 2001).

PATHOLOGY OR ARTIFICIAL DEFORMATION AS EXPLANATIONS FOR THE ANATOMY OF WLH 50

Some authors recognize similarities in the anatomy of WLH 50 and the Ngandong crania, but attribute these to other causes than relationship. Key among these have been suggestions of local adaptive processes, age or size related ruggedness, artificial deformation, or pathology.

> "Perhaps Australia was a special case where local differentiation, cultural practices, or pathologies led in some cases to apparent evolutionary reversals" (Stringer and Andrews 1988: 1263).

Here we review these possibilities. We agree that WLH 50 could not validly inform phylogenetic hypotheses if the distinctive aspects of its anatomy are a consequence of unusual environmental or artificial influences.

Adaptive Explanations

Pardoe (2006) cites a fluctuating balance between microevolution and gene flow in the context of different ecological zones as an explanation for anatomical variation, including variation in patterns of ruggedness, among recent indigenous Australians. Bulbeck (1982, 2001) suggests that the robust anatomy of WLH 50 and some of the other robust Australian fossil crania could reflect adaptation to the deteriorating climatic conditions of the last glacial maximum, and others concur (Brown 1987; Stone and Cupper 2003). The underlying assumption of these contentions is that earlier dated "gracile" crania such as Mungo 1 and 3 (Bowler et al. 2003) represent the ancestral condition and later specimens such as WLH 50 (and even later (Macumber 1977, but see Stone and Cupper 2003) samples from Kow Swamp, Coobool Creek) evolved from this ancestral condition. This model has yet to be fleshed out in terms of how the cause (harsh Australian climate) might have led to the result (cranial ruggedness), or presented as a testable hypothesis.

Age or Size Related Ruggedness

Explanations for the WLH 50 morphology, especially its cranial thickness, include a combination of advanced age (cranial thickness increases with age) and normal population variation, in this case similarity to the wide ranges of variation in Australian fossil hominid samples such as Coobool Creek (Miller 1991). As noted above, however, the age of WLH 50 is not "advanced" but rather young to middle aged.

Curnoe (2009: 981) describes WLH 50, along with later remains from Kow Swamp, Cohuna, and Nacurrie as "characterized by thickly boned vaults, with marked frontal recession, strong postorbital constriction, well-developed ectocranial structures, relatively broad facial skeletons, high prognathism, and moderate to large dental size". He suggests (2009: 980) that this morphological complex, including cranial thickness:

> "might best be explained by four underlying factors: possession of a (1) large neurocranium, (2) narrow cranial base, (3) viscerocranium with considerable midfacial projection, and (4) large dentition, especially the cheek teeth, with their associated large jaws and high volume masticatory muscles" [We note that WLH 50 does not preserve numbers 3 or dental or gnathic evidence of 4].

Stuart-McAdam (1992) describes WLH 50 as a large individual with thick diplöe, but Curnoe and Green (2013) demonstrate that the WLH 50 relative diplöe thickness is not greatly different from the relative thickness of the WLH 3 diplöe, a specimen with a diplöe not considered unusual in its relative thickness.

Artificial Deformation of WLH 50—A Red Herring

Artificial deformation has often been raised as an explanation of some fossil Australian morphology, and as an example of the claim that "cultural practices" are responsible for key aspects of WLH 50 (Antón and Weinstein 1999; Stringer and Andrews (1988) as cited above). There are three questions here:

- is there evidence of past or present artificial deformation in Australia?
- are contentions of Australian similarities to Ngandong dependent on, or independent of cranial deformation?
- is there reason to believe WLH 50 has been artificially deformed?

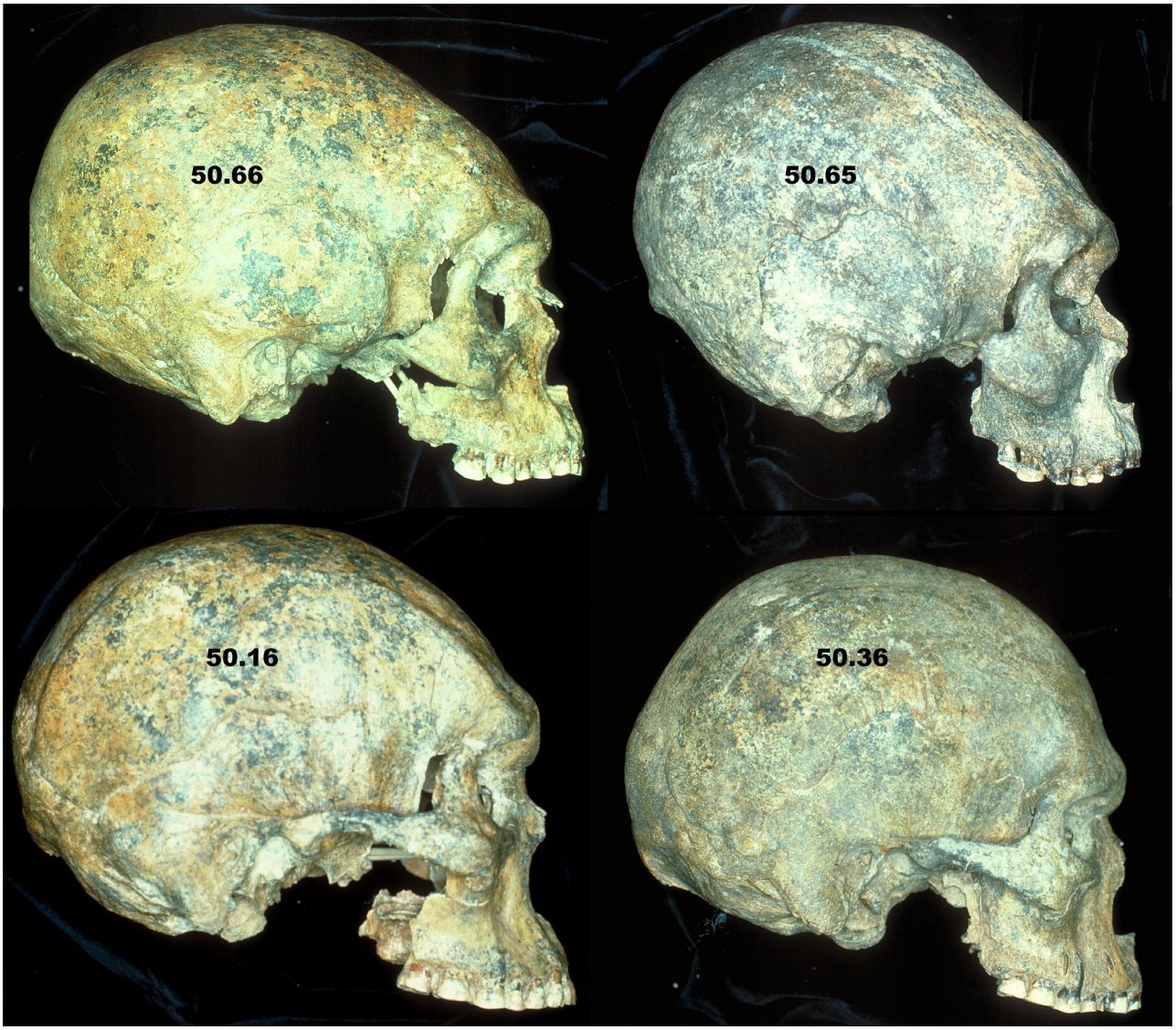

Figure 9. Some Australian fossil crania were artificially deformed. These four Coobool Creek crania are shown at the same size, facing in the same direction. They show marked variation in cranial shape, expressed in many ways that include frontal flattening. As in virtually all features, the variation is continuous through the sample (Brown 1989). Of these, Coobool 50.65 and 50.66 (above) have convincing evidence of artificial deformation according to Brown (1981, 1989). The lower two do not have evidence of deformation.

We can begin here—artificial deformation exists in Australia. There is convincing evidence (Figure 9) that some fossil and recent Australian crania have been artificially deformed (Clark et al. 2007), as Brown (1981, 1989, 2010) has consistently asserted. Brown (most recently 2010) maintained that this fact disqualifies certain features from being used in analysis. Durband (2008) also supports this position, and recently (2009: 8) stated:

> "the presence of artificial cranial deformation in some Pleistocene Australians … [calls] … into question the utility of certain features like flat frontal bones as indicators of continuity with Indonesian *H. erectus*."

However, as Curnoe (2009) and others have noted, that some fossil and recent crania show signs of artificial deformation *does not mean or imply that all do*. If artificially deformed crania can be identified, as we believe, comparisons based on the crania that are not deformed should not be disqualified. Since the existence of artificial deformation in Australia is widely recognized, it is not clear to us why this argument has persisted for so long.

Clark and colleagues (2007) quantified the identification of artificially deformed crania with a discriminant function using frontal, parietal, and occipital arc/chord indices. At Kow Swamp, the discriminant function indicated that cranium 1 was not deformed while cranium 5 was. We expect that KS 7 was deformed as well, as Brown suggests. Thus, there is convincing evidence of artificial deformation in some Australian crania, but not in others[13]. In the first publication on multiregional evolution, Thorne and Wolpoff (1981) used both Kow Swamp 1 and 5, the two best-preserved Kow Swamp crania, as examples of speci-

mens showing evidence of regional continuity. Once the validity of Brown's subsequent interpretations was evident, Kow Swamp 5 was no longer advanced as an example of expressing regionally predominant traits. But Kow Swamp 1 continues as such an example, because it lacks evidence of deformation (Clark et al. 2007; Curnoe 2009). KS 1 exhibits all of the regionally predominant features discussed in Thorne and Wolpoff (1981). The discriminant function also demonstrated that none of the Ngandong crania were deformed; there is no reason to doubt that their anatomy reflects their ancestry, as Weidenreich and others had supposed. In all, the Australian similarities to Ngandong can be demonstrated independently of deformation.

The discriminant function addressing deformity could not be calculated for the Coobool Creek crania. Brown (1989) published the only cranial measurements that exist for this sample, prior to their repatriation. Brown did not report all of the measurements required to apply the function that was later derived by Clark and colleagues (2007). Nevertheless, we concur with Brown (1981, 1989, 2010) that the artificially deformed Coobool crania are: 1, 41, 49, 65, 66, and 81 (see Figure 9). Characteristics of Coobool crania Brown identifies as artificially deformed, even those not obviously altered by the deformation, are not included in any of our analyses addressing relationships.

To our knowledge, only Bräuer et al. (2004) and Lieberman (1995) proposed that artificial deformation could specifically explain the anatomy of WLH 50. Lieberman contended: "while a few of the modern human fossils from Australia have thickened skulls (e.g. WLH 50), those fossils have pathological thickening of the diplöe that almost certainly resulted from cranial deformation (1995: 167). As Curnoe (2009: 982) puts it, no researcher who has studied the specimen has made a similar suggestion.

Pathological Explanation for Cranial Thickness

As noted above, several authors have questioned the phylogenetic utility of the elevated WLH 50 cranial vault wall thickness (see Table 6 below), suggesting it is invalid for addressing questions of relationship because it is pathological. There have been further suggestions that vault shape may somehow also have been altered by the pathology, although the details of the alleged alteration are generally not presented and no mechanism to accomplish this has yet been described. Explanations for the thickened WLH 50 vault as an adaptive response to some sort of chronic anemia or a related pathology are meant to exclude or replace an explanation of its shape and ruggedness based on ancestry. Brown (1989), Webb (1989, 1990, 2006) and Westaway (2006; Westaway and Groves 2009; Westaway and Lambert 2014) have each proposed a variant of a pathological explanation for WLH 50 cranial thickness, and others have cited pathology as the basis for discarding metric comparisons or morphological observations for WLH 50 (Bräuer et al. 2004; Lieberman et al. 2002).

Webb (1990) cites three observations to support his assessment of pathology—the thin cortex of the vault bone; uniformity of vault thickness; and, identification of the "hair-on-end" sign on lateral radiographs. He suggests (1989, 2006) that the cranial bone structure of WLH 50, marked by the presence of thin inner and outer cortical tables contrasted by thick diplöic tissue in between (see Figure 12 below), may be a "hematopoietic reinforcement in the cortical bone as a result of pathology" (Westaway and Lambert 2014: 2793). The proposed anemic condition which created this condition is perhaps closely related to, or a precursor to, modern genetically derived hemoglobinopathies, such as sickle cell anemia or thalassemia.

However, Webb's interpretation is constrained by the fact WLH 50 does not display other changes in its cranial bone similar to those observed in recent populations suffering from genetically determined anemias (Webb 1990). WLH 50 lacks any overt expression of symmetrical hyperostosis (Curnoe 2007; Curnoe and Thorne 2006b), *cribra orbitalia*, or localized bossing of the parietal or frontal squamae, which are the main paleopathological indicators of chronic anemia. If the diplöic thickening of WLH 50 had been the result of chronic anemia, the hemoglobinopathy responsible would have to be unlike any known today or throughout paleoepidemiological history. Moreover, Webb reports that the large percentage of diplöic bone in relation to total cranial thickness found in WLH 50 is not uncommon in the Willandra sample—the 73% WLH 50 value is equaled in (the much thinner) Mungo 3 vault, and is less than the diplöic bone percentage in several other Willandra specimens (data from Webb 1989: Table 3). We do not believe that a compelling case for a pathological explanation of the WLH 50 vault thickness has been made.

In further discussion of this question, Curnoe and Green (2013) systematically compared CT scans of WLH 3 and 50, two Willandra lakes males with markedly different cranial vault thicknesses. These provide a key comparison because they are two males differing in the robustness of cranial superstructures. Curnoe's earlier assessment (2011: 10) was that WLH 50 closely resembles WLH 3 in shape and proportions: "WLH50 simply presents as a more rugged version of the WLH3 morphology, the two resembling each other in their angle of the posterior part of the frontal squama and profile of the parietals and occipital."

To expand on their earlier comparisons, Curnoe and Green (2013) took thickness measurements in a number of regularly spaced positions along both the axial and coronal planes, creating a matrix of measurements for each specimen. The paired cranial bone thickness differences for these two specimens are significant; WLH 50 is thicker. And there are significant differences for the diplöic space and the inner and outer bone tables.

But the pathology question is over whether there are *differences in ratios* for the external bone tables and the diplöic space between them, and systematic differences are not evident for these. The diplöe's contribution to bone thickness is mostly greater in WLH 50. Curnoe and Green (2013) show all components of the vault except internal table thickness are significantly thicker in WLH 50 than in WLH 3, in both scanning planes. However, relative bone thickness, or proportion of total vault thickness for the

diplöic space, and of the total table, are not significantly different between the two Willandra vaults (WLH 3: 42.9–59.1%; WLH 50: 50.8–51.5%). Internal table thickness is also relatively greater in WLH 3 (WLH 3: 19.7–21.1%; WLH 50: 13.0–13.4%). While the relative thickness of the internal and external tables is very similar and statistically indistinguishable between WLH 3 and WLH 50 in the axial plane, it is significantly thicker for WLH 50 in the coronal plane.

Curnoe and Green (2013) addressed the issue of uniformity in thickness (raised by Webb 1995, in the context of whether the thickness was pathological). In all, they measured thickness at 37 points for WLH 3 and 31 points for WLH 50; most of these were in the same positions. The difference in the CV of the measurements for these crania is not significant. These comparisons show that, for all intents and purposes, WLH 50 and WLH 3 have similar patterns of vault thickness and its distribution.

Finally, WLH 50 cranial bone structure is like that of other recent and living humans, and the thicknesses of WLH 50 cranial bone are within the range of a recent Australian population (Coobool, see Table 6 below). We infer, as have many others, that a pathological explanation of the vault thickening in WLH 50 is not well supported (Curnoe 2009; Hawks et al. 2000).

Allometry?

Although incorrectly described by Curnoe and Green (2013: 1317) as "the largest individual recovered from the Pleistocene hominin fossil record" (see Table 1 below), WLH 50 is the largest known Pleistocene Australian vault. Curnoe and Green (2013: 1316) suggest a significant role for size-related allometry in explaining its greater thickness. They report a highly significant correlation for the geometric mean of five cranial dimensions versus thickness at bregma in sample averages for Pleistocene-Holocene and recent Australians (r^2=0.71). We concur that in the context of Australian fossils, the exceptional size of this specimen could contribute to its unusual cranial thickness, but there are problems in this interpretation.

Curnoe and Green (2013) also calculated the allometry for cranial vault bone thickness within the much smaller Ngandong sample. They found the relation of thickness to cranial size was *significant but negative*. Because of the different allometric relationships of the Ngandong and more recent human samples and the unusual cranial thickness of WLH 50, Curnoe and Green conclude that cranial thickness aligns WLH 50 with Pleistocene-Holocene and recent Australians and not with Ngandong. We do not agree with this phylogenetic assessment. The negative allometric coefficient for the Ngandong crania was only significant at 9% (Curnoe and Green 2013: 1317) and it would be more correct in our view to interpret the analysis to show that there was no demonstrable relationship between vault size and cranial thickness at Ngandong, a result in keeping with the very small Ngandong sample size.

Curnoe (2009, and as noted above) attributes the exceptional aspects of the WLH 50 anatomy to the consequences of allometry and a well-developed masticatory apparatus superimposed onto the population-specific attributes of Australian cranial morphology. There is evidence of a powerful WLH 50 masticatory adaptation found in the size and anatomy of the associated zygomatic fragment described below. But the fact that WLH 50 is similar to the Ngandong specimens in so many ways, but these crania are smaller compared to the large cranial size of WLH 50 (see Table 1 below), indicates that size-based allometry is probably not a key factor in explaining the similarities. And this table shows Pleistocene human crania larger than WLH 50 that do not have thick vaults, or share the other features described above as "robust," as would be expected from an allometric causation for the Ngandong-WLH 50 similarities we are discussing. Finally, the Coobool Creek crania are smaller than WLH 50; yet, the thickest crania within that sample reach or exceed WLH 50 thickness in comparable regions (see Table 6 below, Coobool data from Brown (1987)). As at Ngandong, the Coobool male cranial bone thicknesses do not scale allometrically.

No Compelling Explanations Replace Ancestry

We interpret the above to mean that no compelling evidence suggests WLH 50 was altered significantly by deformation or pathology (the same conclusion was reached by Curnoe 2009, among others), nor are anatomical similarities with Ngandong an obvious response to the large size of the WLH 50 vault or a consequence of similar (albeit, unknown) adaptations. We expect that the comparative anatomy of WLH 50 can validly address its ancestry, and be used to test hypotheses about it.

DESCRIPTION OF WLH 50 AND COMPARISON WITH NGANDONG SAMPLE

Condition and Preservation

The WLH 50 vault is comprised of a faceless and mostly baseless calotte reconstructed by Thorne (see Figure 7). Because the vault is incompletely preserved, we limit our comparisons, observations, and measurements to those aspects that can be directly ascertained for WLH 50. This might seem obvious, but we wish to be clear that this is the *only* factor delimiting the information we present[11].

The bone remaining is for the most part well preserved, although many portions of the outer bone table are abraded (Curnoe 2011, see Figure 5 and text), and other exceptions are noted below. With just a few gaps that have been filled with a red wax, bone surface extends continuously from the frontal, including most of the full supraorbital torus (see below for a description of this structure). A 22mm (length) by 31.5mm (maximum breadth) piece of the orbital roof is preserved adjacent to the lateral torus on the left side. On the vault, the external bone surface is mostly complete from a position at or very close[14] to glabella on the medial-most part of the right side of the supraorbital torus, posteriorly to the upper part of the nuchal plane of the occipital, 6mm beyond (anterior and inferior to) the *tuberculum linearum* on the superior nuchal line. The *tuberculum linearum* is defined here as the union of the superior nuchal lines at the mid-

line, where they meet the external nuchal crest.

The supraorbital torus extends laterally on both sides to a position not quite as lateral as the frontozygomatic suture. But, posterior to this, nothing is preserved of the orbital notch except just below the temporal ridge. Behind the supraorbital, the left (more complete side, shown in Figure 7) preserves a broken inferior edge that arches in parallel to the temporal ridge up to the position of the coronal suture, and then continues the arch posteriorly and inferiorly to a position 14mm anterior to the parietal notch (at the parietal mastoid angle).

The posterior portion of the temporal remains on the left side but without any of its petrous region or the root of the zygomatic arch; the posterior portion of the supramastoid crest is preserved on the right. The bone surface is preserved 25.6mm anterior to the front edge of the mastoid, this is the most lateral aspect of the roof (Weidenreich's *tegmen*) above the external auditory meatus and the ring of bone surrounding it, but there is nothing preserved of the external auditory meatus or any part of the tympanic. Most of the mastoid process remains on the left side, including its anterior and posterior edges, although it is not evident that the tip remains.

Behind this, the broken bone surface is an irregular arch across the nuchal plane of the occipital, nowhere preserving the inferior nuchal line, with its most posterior extent just anterior to the *tuberculum linearum*, as described above (and see Figure 12 below). The bone surface is clearly eroded across the cranial posterior, especially inferior to the supreme nuchal line. Effectively this means that the nuchal torus has lost an unknown amount of the outer bone table and with it the crania's posterior projection. Bone thickness measurements that are affected are not reported. The positions of the *tuberculum linearum* and inion can be easily approximated from the remaining anatomy. Inion as defined here is superior to it, the midline point at the level marked by a chord between the superior nuchal lines in their most superior position (lateral to the beginning of the downward arc where they dip down to form the *tuberculum linearum*). Bone thicknesses at the inion and *tuberculum linearum* positions are uncertain because of the bone erosion, but we are confident that the linear or arc measurements to these points on the external surface are close to their original values. It does appear that the top of the torus, effectively the supreme nuchal line, is preserved without significant erosion, although difficult to identify on photographs. Opisthocranion occurs on the supreme nuchal line and measurements to it are also close to correct. The internal occipital protuberance is coincident with the supreme line and we are confident of the thickness of the occipital at this position as well.

The inferior-most edge of the cranium is not as complete on the right side, from the position of the mastoid base anteriorly. The singular exception is a small portion of the posterior temporal squama extending 34.5mm anterior to the parietal notch, and 20mm superior to it. The posterior parietal here is not well preserved, with an irregular break more or less paralleling the lambdoidal suture for 62mm, about 30mm anterior to it. From its most superior extent the break is a jagged, zigzagging surface that continues anteriorly to the most lateral extent preserved of the right supraorbital surface, described as follows. The broken edge continues 63mm further anterosuperiorly, to a point in the middle of the parietal that almost reaches the sagittal suture. The broken surface then extends some 60mm inferiorly, irregularly for 34mm anterosuperiorly to the position of the temporal line, and irregularly for 88mm inferoanteriorly until reaching the broken lateral surface of the right supraorbital, as described above.

The internal surface of the vault is preserved in a corresponding manner. Its internal table is not complete on the preserved portion of the left temporal, and especially behind the supraorbital torus where 20mm of the left-most lateral portion of the orbital roof remains, extending 30mm to the supraorbital notch. The anterior surface of what appears to have been a frontal sinus is exposed for 32.5mm, to the midline. Webb (1989, p. 35) notes:

> "the size of the left sinus is estimated to have been about 6.8 cm^3. This is based on the following dimensions: 22 mm deep (anteroposteriorly), 28 mm wide and about 11 mm high. The form and size of frontal pneumatisation in WLH 50 corresponds more closely to that of the Ngandong crania … than it does with the small Choukoutien sample."

Vault as a Whole

As we have described it, WLH 50 is a large male calotte with an estimated cranial capacity of 1540cc (Curnoe 2009, citing Brown's web site: http://www-personal.une.edu.au/~pbrown3/palaeo.html). This is over 30% larger than the Ngandong male mean (1177cc, n=4) and larger than the biggest Ngandong male, Ng 10 at 1231cc. While on the large end of the recent indigenous Australian range, this size is not completely unexpected; for instance, lying 2σ above the mean male value of 1295cc reported by Morant (1927, Table VI) for a sample of 146 from Queensland, Victoria, New South Wales, South Australia and Western Australia. There is no compelling reason to believe the standard deviation of 120 reported for these Australian males could be used to estimate the male Ngandong standard deviation, but if for the sake of demonstration we made this assumption, WLH 50 would be 3σ above the Ngandong male mean. This comparison contrasts with the 2σ difference of WLH 50 from the recent indigenous Australian mean, we regard the larger estimated difference from Ngandong as significant. Simply put, the vault is quite large, but at approximately two standard deviations above the mean not so large that it would be unexpected among recent Australians.

Table 1 records two of the largest hominid crania from the Pleistocene fossil record that are larger than WLH 50 (Herto VP-16/1 and Amud). We note that, for the most part, neither of these larger crania has exceptional cranial thickness throughout the vault[15] (see Table 6 below), or shares any other of WLH 50's special features that align it with Ngandong crania. WLH 50 is significantly larger than the

TABLE 1. WLH 50 IS NOT THE LARGEST PLEISTOCENE HUMAN VAULT (length, breadth, and height dimensions (in mm) for WLH 50 compared with larger[a] crania in Pleistocene members of genus *Homo*).

	Cranial length	Maximum cranial breadth	Auricular height to bregma (in the sagittal plane)
WLH 50	212.2[b]	151.6	115.5
Herto VP-16/1	219.5	155.0	122.0
Amud	214.7	157.0	117.1

[a]"Larger" meaning exceeding WLH 50 in all three dimensions

[b]This measurement is possible with reasonable accuracy on WLH 50 because, as we note in the text above, the external bone surface is mostly complete from a position at or very close to glabella on the medial-most part of the right side of the supraorbital torus. Several different estimations resulted in close to the same result; the significant digits reported reflect our assessment of the precision. Curnoe and Thorne (2006a) also provide an estimated cranial length for WLH 50: "c212 mm".

Ngandong males (as described above, and in Table 2). This is one of the key differences between the Willandra calotte and those earlier remains from Ngandong. However, the hypothesis examined here, that the anatomy of WLH 50 indicates that Ngandong-like populations are among its ancestors, and thereby the ancestors of indigenous Australians, is not refuted by its larger size. Virtually all cranial samples of sufficient sample size more recent than the Ngandong sample are, on average, larger than it. Nor does the size of WLH 50 make its cranial thickness, or any other aspects of its cranial shape and anatomy, into exceptional or unexpected features requiring special explanation.

The thick vault is absolutely long, and compared to Ngandong relatively high and narrow (Table 3), with the position of maximum breadth low across the cranial base at the supramastoid crests. It is otherwise similar in shape and proportions in the occipital view to specimens from the Ngandong sample, although not exactly like any one of them. The posterior view of Figure 16 (see below) is standardized to cranial breadth and thereby illustrates the greater relative height of WLH 50. This vault shape can also be found among the Coobool remains—some of the larger specimens such as Coobool Creek 50.76 share a number of anatomical details, including sagittal keeling, and the cranial contour as seen in posterior view including low maximum breadth, and a prominent nuchal torus covering the entire cranial rear (Figure 10).

In fact, the length of WLH 50, over 212mm, is within

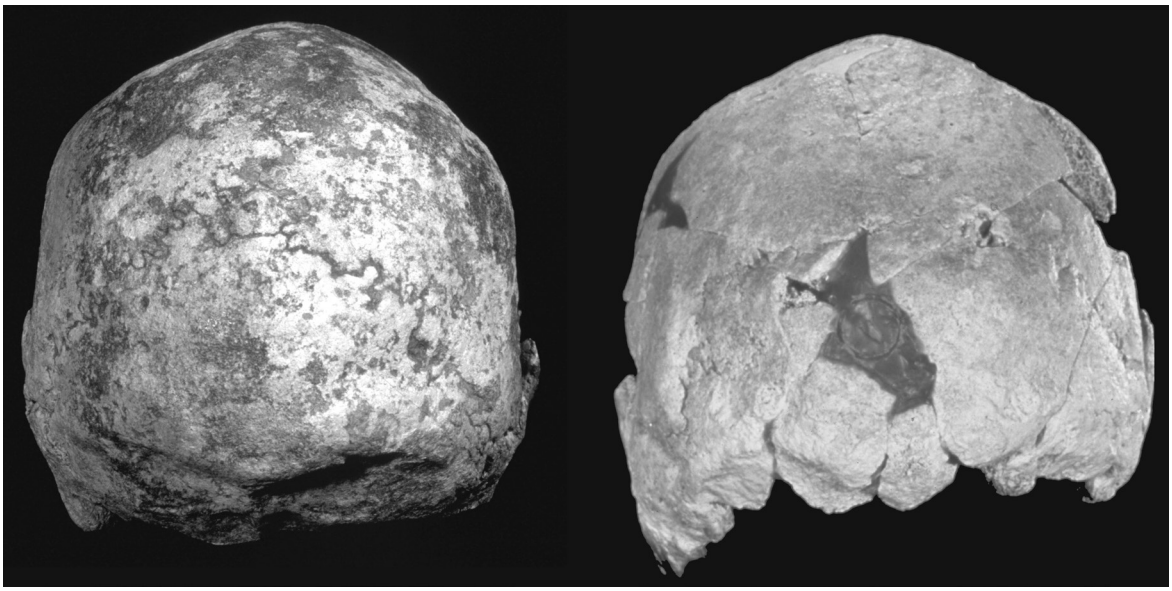

Figure 10. Similar cranial shapes. Posterior views of WLH 50 (right) and Coobool 50.76 show that the cranial shape, sagittal keeling, and the low position and relative magnitude of the WLH 50 cranial breadth can be matched in the Australian fossil record. When the effects of erosion are considered (see Figure 12), it is likely that the shape and position of the superior nuchal lines of these specimens are similar as well. WLH 50 is unusual in its combination of size, cranial thickness, and the development of some of its cranial superstructures, but it is not unique and is not the only fossil Australian with these attributes. The specimens are shown to approximately the same size to facilitate shape comparisons.

TABLE 2. CRANIAL CAPACITY AND KEY CRANIAL VAULT MEASUREMENTS (mm).
Ngandong sex is as attributed by Weidenreich, and cranial capacity is from Holloway (1980).

In this and all following tables, M## refers to the Martin number for the measurement (Martin 1928). These are reported when the measurements are taken as described by Martin. Measurement abbreviations are also following Martin's usage, as in "g-ast" meaning "glabella to asterion." *In this and all following tables, when there are sided measurements such as g-ast, if both left and right sides are well preserved and free of anomaly or damage, or when only the right is preserved, right is used. When only the left side is known or is better preserved, it is reported instead.*

	Sex	cranial capacity in cc (M38)	maximum cranial length (M1)	maximum cranial breadth (M8)	auricular height (au-br projected into the sagittal plane)	bregma-inion (br-i)	glabella asterion (g-ast)
WLH 50	M	1540	212.2	151.6	115.5	166.5	178.4
Solo 1	F	1172	195.6	150.2	96.9	142.0	163.5
Solo 5	M	1251	220.3	150.7	107.6	161.5	186.9
Solo 6	F	1013	191.9	147.4	100.8	141.5	167.9
Solo 9	M	1135	202.0	159.0	104.5	146.5	175.0
Solo 10	M	1231	205.0	158.5	108.9	148.6	176.2
Solo 11	M	1090	200.6	150.7	104.8	152.4	174.4

TABLE 3. CHORD AND ARC (measurements in mm, and ratios and shape indices for the cranial vault).

	glabella-opistho-cranion (g-op) arc (M23)	g-op arc/chord index	glabella-lambda g-l arc	g-l (M3)	g-l arc/chord index	breadth/ length index (B/L)	height/ length index (AuH/L)
WLH 50	338.0	159.3	278.0	207.0	134.3	71.4	54.4
Solo 1	285.0	145.7	232.0	186.2	124.6	76.7	49.5
Solo 5	293.5	133.2	233.5	197.0	118.5	68.4	48.8
Solo 6	271.5	141.5	214.5	175.8	122.0	76.8	52.5
Solo 9	280.0	138.6	221.5	183.0	121.0	78.7	51.7
Solo 10	280.5	136.8	228.5	184.0	124.2	77.3	53.1
Solo 11	278.5	137.3	212.0	177.9	119.2	75.1	52.2

the Ngandong range, exceeded by one of the six Ngandong crania (Ng 5, see Table 2). On the whole, the vault is more arched than the Ngandong crania, although as described below the arching is formed by three flattened surfaces rather than the more generally rounded surfaces of the Ngandong crania. Figure 11 illustrates these shape comparisons. The more vaulted cranial shape is described by the index for the arc to chord relation of glabella-opistho-cranion (see Table 3), above the Ngandong range. Most of this difference reflects curvature of the top of the vault. This is further demonstrated by the index for glabella-lambda that is also high relative to Ngandong, while the index for occipital curvatures from lambda are lower, within the Ngandong range (see Table 11 below).

To further quantify these aspects of cranial shape, distances are determined from the auricular point, projected into the sagittal plane (Table 4). Remembering that the WLH 50 vault is volumetrically larger than any from Ngandong, the auricular distances to glabella in the anterior and opisthocranion in the posterior lie within the Ngandong range, while the distances to the top of the vault, at bregma and lambda, lie above the Ngandong range. Once again, measurements show the top of the vault is higher and more rounded. The occiput is not especially projecting at the nuchal torus position (remembering that this structure is eroded away). But at its most superior position (lambda) the occiput projects more rearward than any Ngandong cranium. Thus, the posterior face of the occiput, along the occipital plane, is more vertically oriented than in any Ngandong cranium, and actually is a little backward leaning from lambda in our approximation of the Frankfurt Horizontal (Ng 1 is most similar in this regard, but differs in occipital plane orientation as described above). The surfaces of the Ngandong crania along the top of the vault on the midline are more-or-less evenly rounded, while, as noted, this surface in WLH 50 is comprised of three flatter portions—a frontal, top, and backward projecting rear aspect. For WLH 50 these surfaces meet at distinct angles; the frontal angle is at metopion, as described below, while the rear portion is the flattened posterior parietal region beginning some 57mm posterior to bregma and extending to lambda.

TABLE 4. DISTANCES FROM THE AURICULAR POINT (au) PROJECTED ONTO THE SAGITTAL PLANE (mm).

	glabella au-g projection	bregma au-br projection	lambda au-l projection	opisthocranion au-op projection	inion au-i projection
WLH 50	111.5	115.5	110.8	98.1	93.2
Solo 1	103.6	96.9	98.8	88.7	83.8
Solo 5	122.5	107.6	101.6	103.4	92.5
Solo 6	104.5	100.8	95.7	91.3	86.3
Solo 9	110.2	104.5	101.0	96.4	81.4
Solo 10	116.4	108.9	96.7	95.1	91.4
Solo 11	112.9	104.8	97.7	93.7	88.0

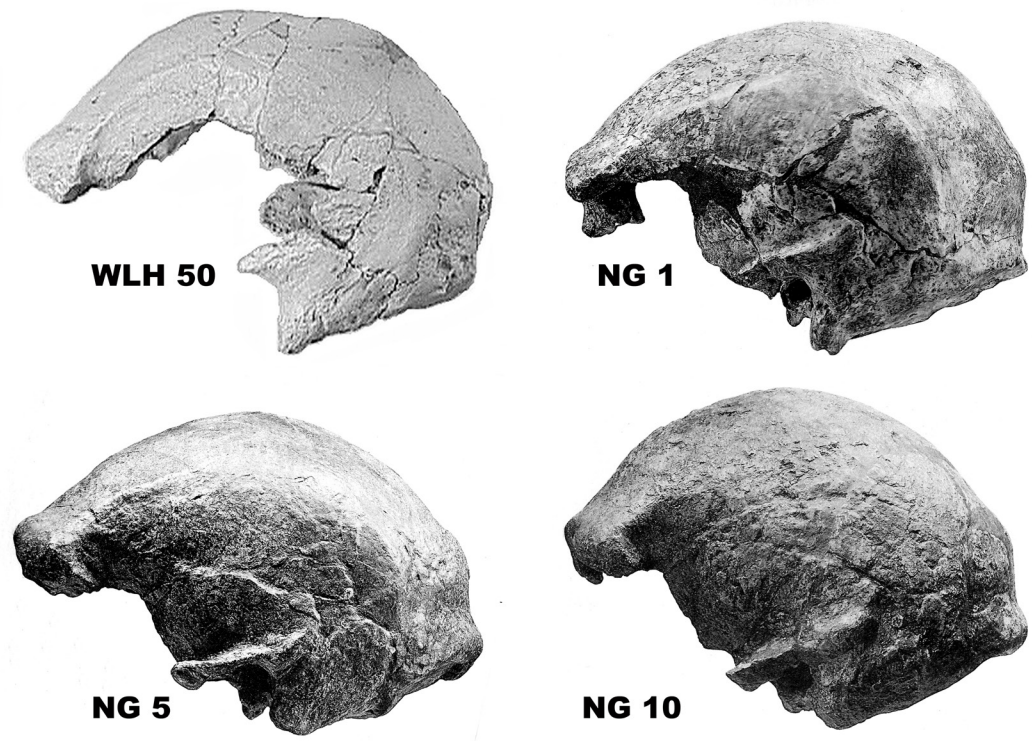

Figure 11. WLH 50 cast compared with three Ngandong adults, shown in lateral view and facing in the same direction (from Weidenreich 1951), and shown in the same approximate orientation and size to facilitate comparisons of shape (in reality WLH 50 is larger than any of the Ngandong specimens, see Table 1). In these and other lateral comparisons, the best-preserved side is shown, with images reversed as necessary. WLH 50 falls within the anatomical range of the Ngandong remains for most details, and one should remember that his nuchal torus appears to have been eroded away. For instance, the occipital plane form and verticality is most like Ng 1; the frontal angle to a glabella-opisthocranion line is most like Ng 10; the frontal flatness is most like Ng 5. The angular torus and mastoid expressions are most like Ng 1. Nevertheless, differences are evident in the greater relative cranial height of WLH 50, the difference in orientation of the occipital plane (in our approximation of the Frankfurt Horizontal), and the greater angularity of the portions of the vault along the midline. See the text for further details and discussion

These comparative details are clearly illustrated in Figure 11[16].

Cranial height can only be described from the auricular-bregma distance, projected into the sagittal plane (see Table 4). This measure of cranial height is larger than the Ngandong mean, actually well above its range (see Table 1; Figure 16 below), corresponding to comments made by other authors such as Brown (1992: 239), acknowledging "the vault is long, but also extremely high". The WLH 50 height/length index calculated from auricular-bregma distance (54.4, see Table 3) is larger than any from Ngandong [48.8–53.1, n=6] although just barely so—Ng 10 is almost as relatively tall. The cranial shape similarities of WLH 50 and Ng 10 are evident in Figure 11, where comparisons of the crania shown at the same size allow a visual assessment of shape. The position of the maximum cranial height in WLH 50 is at bregma, the condition in some (Ng 5, Ng 10) but not all of the Ngandong crania.

Contrasting with its greater height, the WLH 50 cranial vault is narrow compared with the Ngandong specimens; its maximum cranial breadth, maximum parietal breadth, biauricular breadth, and biasterionic breadth are all within the lower part of the Ngandong range, but always above the minimum (Table 5). As in the Ngandong crania, the maximum cranial breadth is low on the vault (see Figure 16 below) and is substantially larger than the biparietal breadth. WLH 50 maximum cranial breadth is the closest cranial breadth to the corresponding Ngandong mean, just a little more than a millimeter less. Four Ngandong crania are narrower, two are broader. Table 3 shows that cranial breadth relative to length is similarly below the Ngandong mean but encompassed within the range.

Relatively narrow (or dolichocranic) as well, the WLH 50 breadth-length index of 71.4 (see Table 3) is less than all the Ngandong crania except for number 5, and only Ng 5 is dolichocranic while the others are mesocranic. Although the greatest breadth of the cranium as seen from above is far to the posterior (see Figure 13 below), it is no more so than Ngandong crania such as Ng 5. The basic WLH 50 vault shape in this view appears as elongated, not tear-dropped as in more brachycranic specimens. Thus, the minimum frontal breadth is more similar to the greatest cranial breadth than is usual at Ngandong; ratio of the minimum frontal breadth to greatest cranial breadth (calculated from Table 5) is 75.9, slightly greater than the Ngandong maximum [68.9–73.7, n=6]. The relative breadth of the cranial base (biauricular breadth/cranial length) also reflects narrowing; it is relatively narrower than Ng 5, and,

TABLE 5. CRANIAL BREADTHS (mm).

Maximum frontal and biauricular breadths for WLH 50 estimated using mirror imaging, repetition of the estimates show that the former is less accurate (to the nearest millimeter) than the latter (to the nearest half-millimeter).

	maximum cranial breadth (M8)	maximum bi-parietal breadth	bi-asterionic breadth (M12)	bi-auricular breadth (M11)	nuchal plane breadth	minimum frontal breadth (M9(1))	post-orbital breadth at temporal lines (ft-ft) (M9)	maximum frontal breadth (co-co) (M10)
WLH 50	151.6	142.0	123.0	137.5	111.0	115	112.0	124
Solo 1	150.2	147.5	131.0	134.0	106.7	105.0	103.5	119.0
Solo 5	150.7	144.6	128.0	147.5	107.0	111.0	101.5	123.5
Solo 6	147.4	141.8	120.5	138.2	102.9	106.6	102.1	117.5
Solo 9	159.0	151.3	123.9	146.5	101.5	109.6	102.2	120.5
Solo 10	158.5	148.1	128.2	149.7	101.5	114.0	104.0	123.1
Solo 11	150.7	142.0	126.7	143.4	108.3	107.1	100.3	120.3

in fact, relatively narrower than all earlier hominids of the genus *Homo*, although OH 9 is almost as relatively narrow (see endnote 17).

There is a low, broad sagittal keel beginning anteriorly at the bregma position and extending posteriorly for 57mm. Anterior to it, there is no keel on the frontal. The keel is bordered by basically flat, very slightly concave surfaces to either side, in totality forming the roof of the vault. All of the Ngandong crania have some kind of sagittal keeling pattern, none precisely the same. Ng 9 is similar, and Ng 11 appears to be the same as WLH 50, though its frontal anatomy is somewhat obscured by healed wounds. Ng 9 has a distinct sagittal keel beginning at bregma and extending posteriorly to where the posterior flattening begins. Many sizes and shapes of sagittal keeling are found throughout the Pleistocene fossil record, and while Wu (1998) reports the North Asian form of the keel in the Middle Pleistocene differs from South and Southeast Asia, Balzeau (2013) notes that the sagittal keeling in *Homo erectus* is not an autapomorphy.

The flattened portion of the superior surface of Ng 9 is triangular in shape and covers the back of the parietals and the upper portion of the occipital plane. Behind the sagittal keel of WLH 50, as noted above, the back of the parietals is similarly flattened in a triangular form with the apex at the above-described point at the end of the sagittal keel and the base roughly along the lambdoidal suture. While the flattened region for WLH 50 extends to the lambda position, there is no prelambdoidal depression such as found in Ng 11 and the other Ngandong crania as described by Weidenreich (1951). According to him, a prelambda depression also is found in some recently living indigenous Australians. Below and behind this flattened area the posterior face of the WLH 50 cranium defined by the occipital plane is as discussed above, tall and more or less vertical, extending some 45mm from the most posterior part of the lambdoidal flattening to the top of the supreme nuchal line. This is quite to the rear of the Ng 1 cranium (see Figure 11).

The posterior flattening of WLH 50 creates the superficial appearance of an occipital bun, and Curnoe (2009: 984) describes the specimen has having one. We do not agree. In the Neandertal chignon the lambdoidal flattening extends onto the occipital leaving it a much shorter vertical face than WLH 50 shows. The sides of the Neandertal bun, when it is present, are often defined by a vertical flattening of the posterior parietals, also extending onto the occiput. None of these appear on WLH 50. Instead of a vertical flattening, the cranium lateral to the vertical rear is rounded, although not evenly. On the posterior border of the angular torus, left side of WLH 50, there is a large, shallow lateral fossa with what appears to be a resorptive surface encompassing the suture and extending medially for 34mm, up to a slight vertical elevation, or ridge, that separates it from and forms the lateral border of the suprainiac fossa (Figure 12), described below in the occipital section. The lateral fossa, bordered medially by the angular torus, is 24mm in height above the supreme nuchal line, thereby incorporating most of the lateral-most lower corner of the occipital plane. Because the fossa extends to the angular torus, a small section of the lambdoidal suture is incorporated in it, coming as close as 14.8mm from asterion. There is no corresponding fossa on the right side. Ng 9 is strikingly similar in this anatomy, with fossae on both sides of the cranial rear that closely correspond to the WLH 50 condition, except they are larger and deeper in Ng 9. Ng 10 and 11 also are similar to WLH 50 in this region; in these Ngandong crania the tori and ridges, described above, are strongly developed and the fossa is deep and extends medially. In these three Ngandong crania, the sides are symmetric. Ng 5 has a similar though not as extensive fossa bordering the angular torus on the left, this is barely visible on the right so that like WLH 50, the sides are asymmetric.

Other tori, ridges, and muscle-related features are well developed. The supraorbital torus/superciliary arch, described below in the frontal section, is prominent. The nuchal torus, as defined by the supreme and superior nuchal lines, was tall and appears to have been substantial, although its surface, as described below in the occipital section, is eroded so that torus thicknesses cannot be ascertained (Table 6) and the appearance of the torus is misleading.

The temporal line, also best preserved on the left side, extends posteriorly from the temporal notch as a raised ridge, or crest, and flattens to a barely discernible line across the parietal. Toward the posterior aspect of the bone it becomes a prominent, well-developed but less sharpened ridge, and ultimately is expressed as an angular torus, as it curves downward and approaches but does not quite reach the lambdoidal suture. In this most posterior position the angular torus is prominent and thickened, about 15mm superior to asterion with its posterior border 4.8mm anterior to the lambdoidal suture. The back of the angular torus extends downward and slightly anteriorly from the most posterior projection of the torus; its posterior border travels along the lambdoidal suture with the toral structure ending at asterion where the occipitomastoid, parietomastoid, and lambdoidal sutures come together. The anterior border of the angular torus, the superior temporal line, continues to arc toward the parietal mastoid angle, its most anterior extent ending 4.5mm short of it. Along the parietomastoid suture, the base of the angular torus, so defined, extends 20mm anteriorly from asterion.

In the Ngandong crania the angular torus most closely approaches the lambdoidal suture in a lower position (closer to asterion) than it does in WLH 50. But there is more similarity in how closely the angular torus approaches the lambdoidal suture. Kaifu and colleagues (2008: 576) describe "the anterior shift of the posterior end of the superior temporal line and resultant marked separation of it from the lambdoidal suture" as a Ngandong autapomorphy, but in fact not all of the Ngandong crania have this character state. The Ng 9 temporal line reaches the lambdoidal suture as an angular torus. In Ng 1 the angular torus is weakly developed but the temporal line also extends back to the lambdoidal suture, albeit close to asterion. Ng 5 on the right has an expression of this feature very similar to WLH

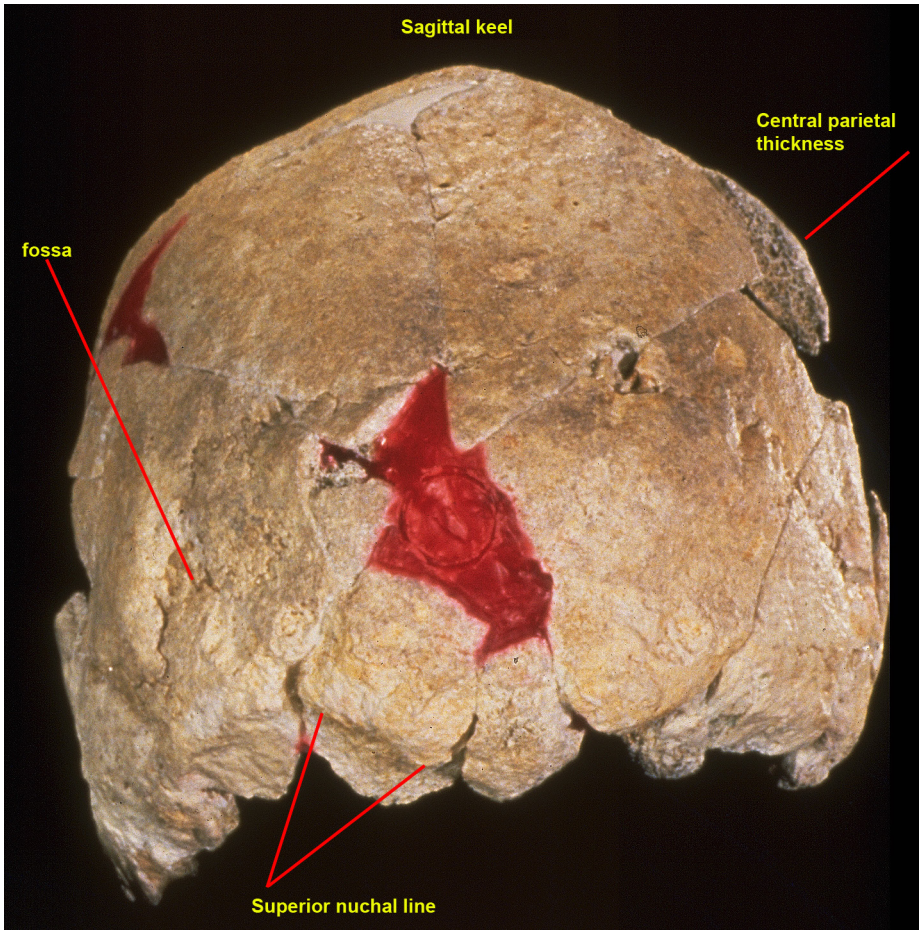

Figure 12. Posterior of WLH 50 showing parietal thickness in cross-section, the low sagittal keel, the superior nuchal line defining the inferior border of the nuchal torus, and other details described for the cranial posterior. The eroded condition of the bone surface at the nuchal torus position is visible and the supreme nuchal line delineating its superior border cannot be easily seen in this photograph.

50. The distance between the back of the angular torus and the lambdoidal suture is 4.8mm in WLH 50 and 6.7mm in Ng 5. Thus, while the anatomy described for Ngandong does not characterize WLH 50, as we note above, this anatomical description is not consistently expressed in the Ngandong sample, which actually encompasses WLH 50 in its range. The recent/modern human range for these anatomies in Australia is quite similar; note that in Figure 9 the most posterior aspect of the temporal line touches the lambdoidal suture in Coobool 50.16, but is anterior to it in Coobool 50.36.

Like the Ngandong remains, the WLH 50 cranial vault, as seen from the rear, has the form of a house with a gabled roof and curved sides slightly inward-slanting from the cranial base, where the cranium is broadest (see Figure 16 below). The parietal walls inferior to the temporal line are evenly curved and lack any boss development (see Figure 12). Beginning with the distinct angle at the temporal ridge, the cranial roof is gabled up to its peak where there is a low and wide parietal keel on the anterior portion of the parietal, as described above. These details of the cranial rear are found in the Ngandong sample, the greatest similarity is with Ng 5.

Apart from its larger size, WLH 50 is similar to the Ngandong cranial sample in many of its details; with exceptions or specifications as noted, most of the character states of WLH 50 are a good match within the Ngandong sample in the sense of falling within the range of the individual specimens (see Figures 8, 10, and 12). Those features that differ from the Ngandong sample, such as the enlarged cranial size, higher and more rounded sagittal contour of the cranial vault, reduction of supraorbital structures and their division into central and lateral structures, and greater contribution of the diplöe to vault bone thickness, reflect evolutionary changes of the Late Pleistocene that to some extent characterized all regions of the world. In WLH 50 these result in anatomical details that are much like other fossil and recent Australians. The existence of detailed anatomical similarities with some or all of the Ngandong crania, including various measures of ruggedness, suggests that its neurocranial size alone cannot be the cause of these anatomical similarities (*contra* Curnoe[17] 2009).

Cranial Bone Thickness

One of the most notable features of WLH 50 is the marked cranial wall thickening (see Table 6), discussed above as a possible pathological condition and illustrated in Figure 12. It is notably thicker than the next thickest Willandra speci-

TABLE 6. CRANIAL VAULT BONE THICKNESS (mm).

Substantially different WLH 50 vault thickness measurements were published by Webb (1990), Curnoe and Thorne (2006a), and Curnoe and Green (2013). The probable cause of differences in reported thickness measurements for WLH 50 is the extreme sensitivity of position in thickness determination[18] (Marsh 2013), and with the exception of parietal thickness at the middle eminence, a position possible to measure with a caliper because of the breaks, the thickness reported in the table are at standardized and easily replicable measuring points. The WLH 50 measurements reported here were published by Curnoe and Green or taken by one of us (MHW) on the original specimen, as were the Ngandong measurements that were not published by Weidenreich (1951). The Herto 16/1 thicknesses are from White et al. (2003, supplement). The maximum thickness dimensions at Coobool are from Brown (1987).

	frontal at bregma	parietal at bregma	parietal at lambda	parietal at middle eminence	parietal at asterion	occipital at lambda	occipital at inion	occipital at internal occipital protuberance
WLH 50	14.0	14.9	15.0	16.0	17.0	16.2	>18.0[a]	>20.0[a]
Coobool Creek max	14.1	15.4				17.1	23.0	
Herto 16/1		10.0		7.0	11.0	7.0	18.0	
Solo 1	9.5	7.9	10.9	7.0		8.0	18.8	18.5
Solo 5	8.8	11.5	12.5	9.5	17.0	15.0	25.0	20.0
Solo 6			12.1					
Solo 9	11.5	7.6			14.5		20.0	17.0
Solo 10		10.1	9.9	9.0	16.0	8.5	22.0	16.5
Solo 11	9.0	9.2	12.0				25.0	

[a]These are less than the true values by an unknown amount. The external bone surface is eroded away in this region (see Figure 12) and the thickness measures of the nuchal torus are not preserved. Even still, the bone that remains is significantly thickened here.

men (Webb 1989: Table 7), and in a measure of thickness averaged throughout the vault (not including the supraorbital and nuchal tori), WLH 50 is on average 1.8 times thicker than the other partially complete Willandra male, WLH 3 (Curnoe and Green 2013). Its thickness lies well above the means of recent Australians from Kow Swamp, Coobool, and the collection from Murray Valley (Brown 1987). However, WLH 50 cranial thickness is within the recent Australian range, if barely. It is not as thick as the thickest specimens from Coobool (see Table 6) reported by Brown (1987). Where comparisons can be made, for most thickness measures on the cranial squama WLH 50 is thicker than any specimen from Ngandong (see Table 6).

To a large extent thickness is accomplished by a greater relative and absolute thickening of the diplöe in WLH 50, and in this regard WLH 50 resembles other recent and modern human crania (Curnoe and Green 2013; Kennedy 1991; and see below). In contrast, in the Ngandong crania it has been reported that generally the compact outer and inner tables contribute more to total bone thickness than is normal in recent crania. In the cranial vault thickness of Ngandong, as in the earlier remains from Sangiran and Zhoukoudian:

> "all three constituents of the [cranial vault] bone take equal part in the thickening, the two tables slightly more than the diplöe (Weidenreich 1943, p. 164). This pattern is typical of vault construction in other middle and upper Pleistocene crania, as well as those individuals from the Ngandong series. The pattern in WLH50 is quite the reverse" (Webb 1995: 64).

More than any other comparison, issues have been raised about whether cranial bone thickness comparisons of WLH 50 and the Ngandong crania are between homologous characteristics, and therefore whether cranial thicknesses can be validly compared. While the internal anatomy of the WLH 50 cranial bone is well-described and known at many positions (Curnoe and Green 2013), the internal characteristics of cranial bone can differ considerably from one position to another (Marsh[18] 2013) and comparable data have not been published for the individual Ngandong crania. Balzeau (2006) reported general observations on the contribution of inner and outer tables and diplöe to cranial bone thickness in *Homo erectus*, Ngandong, and fossil and recent modern humans. Balzeau found that in virtually all specimens studied the diplöe contributes to more than 50% of the thickness. We have observed that the diplöe in WLH 50 is not exceptional in its relative thickness relative to other Australian fossils. Combined, these observations challenge previous assertions that Asian *Homo erectus* and Ngandong differed in these regards, and support the assessment of homology for cranial bone structure, providing validity for our cranial bone thickness comparisons.

Frontal Bone

The angled forehead is long, flattened, and thick. Its gentle curvature is even along the midline from the glabella position to the metopion position (metopion is the highest point above the nasion-bregma line), about 3cm anterior to the posterior border at bregma, where a strong angulation separates what is basically the front of the cranium from its top. Metopion is not always delineated as a distinct angulation in the sagittal plane on Ngandong crania, as in Ng 1 and 5 (see Figure 11). In Ng 10 there is an angulation in the metopion position but unlike WLH 50 it is more anterior, at about the center of the frontal squama. WLH 50 appears to have something like a prebregmatic eminence, and has been described as such (Curnoe 2011: 10). But this is not an eminence in the sense of bulging outward from the cranial surface, but rather is the point of angulation described above, between the top of the cranium and its front defined by the slope of the forehead.

WLH 50 frontal length, whether described as a chord or an arc, is substantially greater than in the Ngandong crania (see Table 7 below for this and following comparisons except as noted). WLH 50 frontal length relative to cranial length is 60.6%; this greatly exceeds the relative frontal length for the Ngandong sample [50.4–56.8%, n=6]. However, although most human frontals are not as long, relatively long frontals are found through the Late Pleistocene fossil record everywhere—Cro Magnon 3 and 8 (61.1, 62.9), Předmostí 22 (60.5), Pavlov 1 (60.3), and Liujiang (61.8). An elongated frontal is unusual but not unknown in the Late Pleistocene.

In contrast,, flattening of the WLH 50 frontal squama is similar to the Ngandong specimens. The chord/arc index for frontal length (107.6) is close to but very slightly above the range of 103.2–106.2 for the four Ngandong males. The WLH 50 frontal is thicker at bregma than the Ngandong crania (see Table 6). Bregma thickness is the only frontal squama comparison we report; while many cranial thickness comparisons suffer from problems of identifying the same position on different crania (Marsh 2013)[18], those taken at defined points are most likely to be comparable. The squama is evenly curved transversely, the sagittal keel of the parietals does not extend on to the frontal as it does in Ng 5, nor is there a frontal boss similar to that of Ng 11. In these respects WLH 50 is most similar to Ng 1 and 10.

Posteriorly on the frontal squama there is a very broad bulging surface involving approximately the middle half of the frontal at the coronal suture, narrowing as it passes anteriorly to the supraorbital region. To its sides the frontal squama is shallowly concave to the temporal ridges—this development varies in Ngandong; WLH 50 closely resembles Ngandong 10 in it. The WLH 50 lateral torus has a poorly developed frontal trigone at its lateral edge on the left, a smaller but otherwise similar structure to the Ngandong crania; in particular, very similar to that in Ngandong 9 (the trigone of Ngandong 9 is larger). The supraorbital torus just medial to the trigone on the left is 9.6mm in thickness (height); at the trigone the thickness is 12.6, a relationship of greater thickness at the corner that is similar to Ngandong. The superior surface of the lateral torus is not distinguishable from the frontal squama; this part of the torus could be described as a thickening at the end of the long, flat squama.

The postorbital constriction is pronounced, although not as much as in the Ngandong mean. Whether measured across the temporal fossae or across the temporal ridges, the postorbital constriction is most like Ngandong 10, both absolutely and relative to maximum frontal breadth. The latter is also very similar to Ngandong 10. WLH 50 minimum frontal breadth is only 1mm greater than the Ngandong maximum (see Table 5), not unexpected given the similarities in cranial shape and how much larger the Australian is. Relative to the maximum frontal breadth (calculated from Table 5), WLH 50 is relatively less narrow than any Ngandong cranium; but again, the difference is slight as its 92.7% value is little different from the Ngandong maximum (for cranium 10, it is 92.6%). In all, WLH 50 is quite like Ng10 in these absolute and relative breadths, in general above the Ngandong mean.

The distance between the temporal lines at the temporal fossa (where they are actually ridges) is 112mm, significantly exceeding the Ngandong condition where the lines (ridges) are higher on the cranium at this position, and thereby closer together—a range of 100mm to 104mm. The anterior portion of these ridges projects from the frontal and there is a distinct angulation of the bone inferior to them, where the bone surface along the inferior border of the ridge is more sculpted out and concave than in any of the Ngandong crania (in Ngandong the ridge is less distinct and the inferior border along it convex in all cases). Posteriorly on the WLH 50 frontal, the ridge becomes less prominent, as does the angulation it defines, and the temporal ridges gradually soften to indistinct lines as they cross the coronal suture posteriorly. Their vertical position on the cranium changes as well, more posteriorly the lines rise to a higher position on WLH 50, reversing the relationship with Ngandong even though the Willandra cranium is by far the largest. The 98.2mm distance between the temporal lines where they cross the coronal suture is below the Ngandong range (101.3–113.5mm), this despite the fact that the maximum frontal breadth is just barely above than the Ngandong range (see Table 5).

Supraorbital Region

The WLH 50 supraorbital region is mostly preserved externally but not internally, as noted above and illustrated in Figures 7 and 11. In WLH 50:

> "the flat frontal squama is associated with a large and anteriorly projecting supraorbital torus, and this feature results from anterior placement (growth) of the orbit relative to the frontal squama. The anterior point of the superior orbital plate is located well anterior to the angulated plane of the frontal squama" (Curnoe 2009: 984).

Webb (1989) describes (and illustrates, his Figure 9) the WLH 50 torus as comprised of both superciliary ridges

and a middle section that is "as large or larger, implying a partial torus" (p. 30). We believe the issue of whether the WLH 50 condition can be described as supraorbital torus or as superciliary ridges (or arches) is complex, not the least because of differences between the left and right sides, as described below.

The WLH 50 torus is an osseous bar that extends across the frontal. It projects from the frontal squama, but the direction of the projection is almost parallel to the squama so that only a weakly developed *fossa supraglabellaris* occurs, similar to the Ngandong condition[19] (and unlike earlier Indonesian crania). It is especially similar to the left side of Ng 5 where the *fossa supraglabellaris* also extends in a lateral and superior direction across the entire front face of the torus. Whether or not the osseous bar is continuous across the midline is unclear because the central portion across a portion of 11mm at the top of the torus is missing, except for its very top that is at, or almost at, the midline position. There is a suggestion of a glabellar notch similar to Ngandong, and it is possible, but far from certain, that there was a broad groove at glabella separating the two sides. Insofar as this notch is (weakly) expressed, it differs from Ngandong 5 but is similar to Ng 11 (Figure 13).

Laterally the bone surfaces are continuous from this break to the lateral-most preserved positions, not quite at the suture with the zygomatic but lateral enough for the temporal line to parallel the top of the torus surface. The preserved bone surface indicates that there was some glabellar projection, as seen from above. In frontal view, the torus surface on both sides dips inferiorly at the most medially preserved positions. There are centrally located supraorbital notches, or incisura, on the superior rim of the orbit on both sides of the frontal, a condition that can be seen on some (e.g., Ng 11) but not all Ngandong crania.

There are two ways to interpret the anatomy of this osseous bar as it is expressed in WLH 50, and it would be fair to say that both the Webb and the Curnoe descriptions above are correct. On the one hand, both sides of WLH 50 preserve a continuous toral surface, making it reasonable to describe the structure as a supraorbital torus, as Curnoe suggests. But on the other, there is the appearance of strongly developed broad, vertically tall superciliary arches, weakly distinguished from lateral tori by an abrupt change from greater medial projection to weaker and less vertically tall lateral projection, as Webb describes. This is more distinct on the left than the right side. The juncture between these is easily visible on the left and could be described as a weak superolaterally oriented supraorbital groove, although it is not so much a furrow as the conjunction of two different surfaces. Nor does the supraorbital notch position correspond to the tallest part of the superciliary arch, as is common.

As seen from the superior surface (see Figure 13), the torus extends across the front of the Ngandong crania in what is a virtually straight line for all but its more lateral aspects. The superciliary arches project more anteriorly than the lateral tori which angle more posteriorly than the straighter lateral supraorbital aspect in Ngandong. Only in Ng 4 and10 do the sides angle somewhat posterolaterally, away from the center. WLH 50 is most like Ng 10 in this regard; while it is difficult to measure accurately, and the preservation of Ng 10 is not complete, WLH 50 seems to have about the same angulation.

The anatomy of the WLH 50 supraorbital region is not quite like any other Late Pleistocene fossil sample. Smith and Ranyard (1980: 589) describe the Neandertal supraorbital torus as:

> "… basically an osseous bar, extending continuously across the inferior margin of the frontal bone. The torus forms an arch over the superior margin of each orbit and appears depressed superiorly in the midline by the presence of a supraglabellar fossa."

WLH 50 preserves a structure that is in some ways similar, but not the same. Nor does it closely resemble the classic supraorbitals of Zhoukoudian, and it also differs somewhat from the Ngandong condition (see Figure 15 below) as described above. However, whether or not WLH 50 has a true supraorbital torus is not a key diagnostic issue, because true supraorbital tori can be found in recent Australians. For instance, the supraorbital torus in Coobool 50.35 is thick and evenly developed (Figure 14) and unlike WLH 50 there is not even the most incipient division of the structure into superciliary and lateral elements, in spite of the orbital notch. In contrast, however, no Coobool or Kow Swamp cranium has as strong a frontal trigone expression as even the weakest development in the Ngandong sample.

In Late Pleistocene/Recent Australian adult samples such as Kow Swamp and Coobool Creek, the anatomy of the supraorbital region varies across the full range of possible expressions seen in Pleistocene and recent times, and WLH 50 fits within this range:

- a classic, thick, continuously and evenly developed supraorbital torus (for instance, as in Kow Swamp 15; Coobool 50.16, 50.75, 50.76, 50.82, and 50.35 (see Figure 14));
- a classic, thin, continuously and evenly developed supraorbital torus (Kow Swamp 14; Coobool 50.38);
- continuously expressed tori with thinning at the midorbital position (Kow Swamp 5; Coobool 50.29, 50.65);
- continuously expressed tori thinning laterally (Kow Swamp 1, 3, 4, 7, 8; Coobool 50.9, 50.28, 50.37, 50.41, 50.45, 50.46, 50.49, 50.66);
- division of the torus into superciliary arches and lateral tori (Kow Swamp 154; Coobool 50.10, 50.12, 50.13, 50.23, 50.36, 40.47(R), 50.50, 50.51, 50.65(L), 50.71); and,
- virtual or full absence of toral structures (Kow Swamp 2, almost adult; Coobool 50.2, 50.7, 50.61).

Arguably the most unusual morphology of the Ngandong supraorbital tori are the knobby frontal trigones found at their most lateral extent, making the torus thickness in this position (reported in Table 7 below) the greatest for any part of the structure (Weidenreich 1951). The temporal line emerging from the temporal fossa forms the lateral side of the trigone. The apex of the trigone is created by

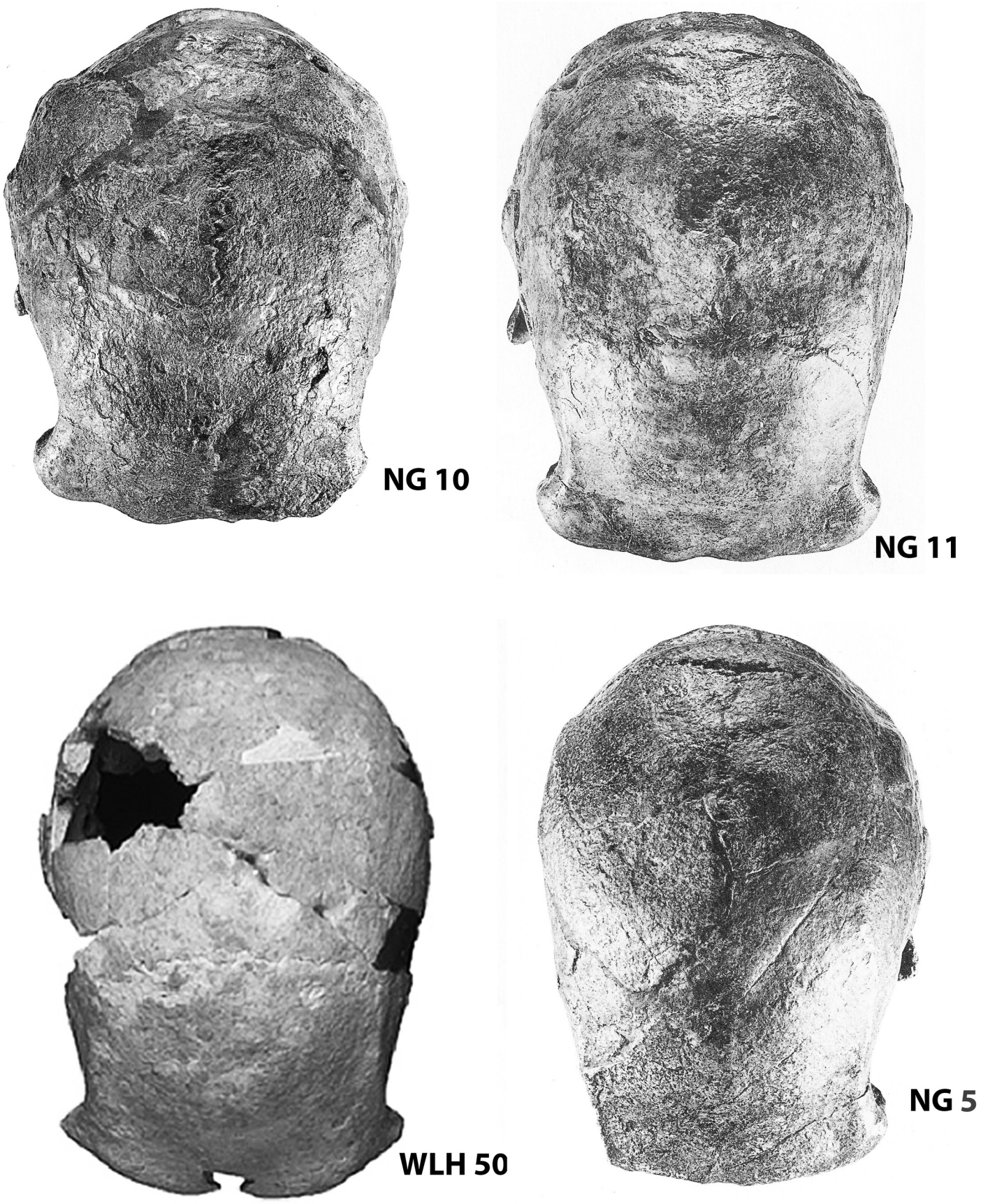

Figure 13. WLH 50 (from Curnoe and Green 2013) compared with three Ngandong adults, seen in superior view at approximately the same size. WLH 50 cranial shape in this view is most like NG 5, which is relatively narrower, the rounding of the cranial rear is most like NG 11, but none of the Ngandong crania have so strong a posterior angulation of the superior orbital border.

Figure 14. Coobool 50.35 has a classic supraorbital torus, and not separated superciliary arches. The torus is thick and close to evenly developed, extending across the entire frontal without break or interruption. Unlike most Pleistocene expressions of supraorbital tori, the supraorbital foramina are opened as notches on the superior orbital margins.

the temporal line. This line changes into a ridge as it swings posteriorly. The medial side of the trigone is the distinct top of the supraorbital. WLH 50 has part of such a trigone preserved on its right side, but it is much smaller and less prominent than any of the Ngandong structures, and more like the structure as it is found in the Kow Swamp sample. Table 7 (below) measures lateral height as it is preserved in WLH 50, at what Weidenreich refers to as the "corner portion[20]" since it is just above the superolateral corner of the orbit. As Table 7 (below) and Figure 15 show, lateral height taken there is the thinnest of the supraorbital height measurements, and its lateral torus length, from the temporal ridge to the orbital border on the side (see Table 7, footnote c, below), is also smaller. In these observations WLH 50 is quite different from the Ngandong condition. Yet, the Ngandong condition is not completely lost in the Australian fossil record. A number of the later adults from Kow Swamp and Coobool have special thickening at the outer corner of the torus, forming a frontal trigone similar to that at Ngandong although, again, not as strongly expressed—Kow Swamp 5, 8, 14; Coobool 50.10(R), 50.12, 50.15, 50.29, 40.41(L), 50.49, 50.65, 50.66, 50.76.

Webb (1989: 31) states: "the anterior brow morphology of the Willandra series (WLH 18, 19, 50, and 68) seems to be, in its general form, closer to that of the Choukoutien sample than it is to Ngandong."

We agree that the anterior brow region in some Pleistocene fossils is more similar to WLH 50 than Ngandong is. While this is not the case for the Zhoukoudian remains, in later Middle Pleistocene Asians such as Dali there are sig-

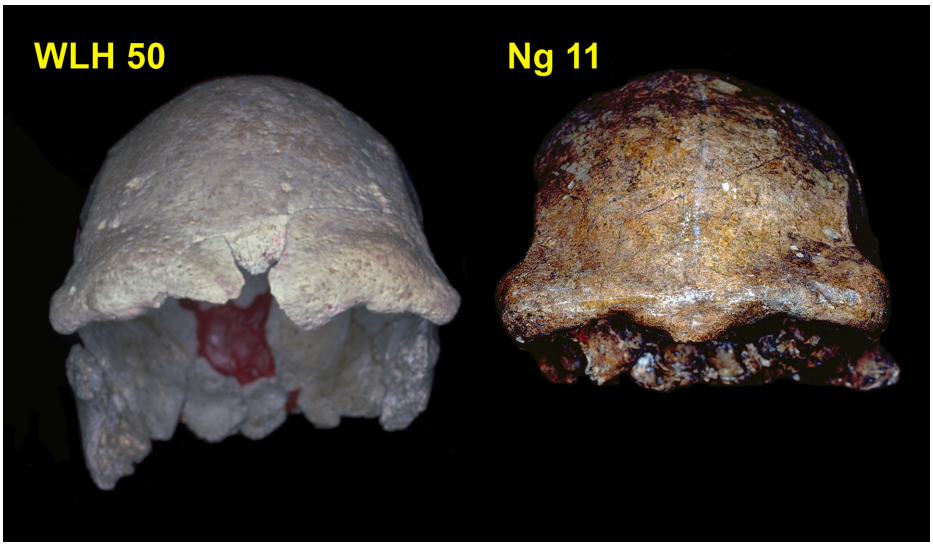

Figure 15. WLH 50 (left) compared with Ngandong 11 in frontal view, shown to the same approximate size. Many of the details that can be seen are similar, including the distinct supraorbital notch in close to the same position, and the flatness of the frontal squama between the temporal ridges. The supraorbital structures are quite thick in both cases. The most significant difference is the classic supraorbital torus in Ngandong 11 that, like many from Ngandong, is thickest at its most lateral extent, where there is a frontal trigone. In contrast, WLH 50 has thick and well-developed superciliary arches, slightly divided from the lateral torus by a weak supraorbital groove (see text for further details). Like most other differences discussed in the text, the WLH 50 condition is within the normal recent/modern anatomical range in Australia.

nificant similarities to the WLH 50 anterior brow (Wu and Athreya 2013). Dali also has a continuous osseous bar of the same basic shape as WLH 50, in this case across the midline because the region is preserved. There is significant arching corresponding to a superciliary arch and a more lateral portion that is not as vertically tall and has a flat superior surface that is continuous with the frontal squama. But unlike WLH 50, Dali has no supraorbital trigones or notches, nor do the surfaces of the two structures—the superciliary arches and the lateral tori—meet along a juncture of two different shapes forming the sides of a groove, they are continuous and even in curvature.

Posterior to the torus, and in addition to it, Weidenreich (1951: 249) considers "the manner in which the torus portion is connected with the squama *frontalis*" as one of the two special features of the Ngandong crania, the other being the torus itself. As Weidenreich (1951: 251) describes the region:

> "contrary to the conditions in *Sinanthropus*, the tori are not separated from the squama by a distinct sulcus *supraorbitalis* and *glabellaris*, but continue into the squama itself without any demarcating impression, except for the lateral halves of the supraorbital tori where they build the zygomatic process."

The condition he portrays is quite similar in WLH 50, where no true sulcus appears behind the supraorbitals but rather the surface slopes almost evenly up the frontal squama. In WLH 50 and the Ngandong crania, there is a top to the supraorbital tori but this cannot be described as a combined, continuous supraorbital sulcus and glabellar prominence because it does not extend across the midline of the frontal. Instead, the supraorbital sulcus alone exists, increasing in extent from the middle of the frontal, where it does not exist, to the most lateral position, where there is an elongated surface between the rim of the torus and the beginning of the frontal squama that is the external manifestation of the top of the orbit.

Another way to describe this anatomy in WLH 50 and the Ngandong crania is that the anterior face of the frontal squama is strongly curved in the horizontal plane, such that at the middle of the bone it is directly over the glabella position, but as it retreats from the torus laterally, an increasingly longer superior orbital roof is created. Bearing in mind that the roof is not angled strongly relative to the frontal squama, as it is (for instance) in the Zhoukoudian crania described in the Weidenreich citation above, at the lateral-most position the length of this roof, from the anterior face of the squama to the superior supraorbital border, can be measured at about 32mm in WLH 50, similar to 29mm in Ng 11 where it is arguably most distinct among the Ngandong crania.

Internal Surface

Weidenreich (1951: 250–251) describes the internal surface of the Ngandong frontals thusly:

> "on the cerebral side of the frontal squama of all the skulls a broadly based frontal crest has developed … it rises from a point … at about the level of the metopion region. In all cases the ridge is very pronounced but

TABLE 7. MEASUREMENTS OF THE FRONTAL BONE (mm), WITH SOME ARC/CHORD INDICIES.

	glabella bregma (gl-br)	g-br arc	g-br index	frontal squama breadth (st-st)[a]	mid-torus length[b]	lateral torus length[c]	medial supra-orbital thickness (height)	central supra-orbital thickness (height)	supra-orbital thickness (height) at the highest point on the torus	supra-orbital thickness (height) at the corner[d]
WLH 50	128.3	138.0	107.6	98.2	26.0	13.0	24.0	21.5	21.5	12.6
Solo 1	111.1	117.5	105.7	113.5	27.0		20.2	13.0	14.7	
Solo 5	111.0	114.5	103.2	108.0	27.5	17.0	21.3	14.5	17.9	19.2
Solo 6	107.2	112.0	104.5	111.0	20.7		16.5		14.0	18.0
Solo 9	106.3	112.5	105.8	106.2	22.0	14.2		12.0	15.9	18.0
Solo 10	112.1	119.0	106.2	101.3	18.5	12.8	15.4	9.0	9.0	18.5
Solo 11	104.7	108.5	103.6	105.3	21.6	15.2	17.6	13.9	12.2	22.0

[a]Bistephanion breadth is across the temporal lines where they cross the coronal suture.

[b]The length measure is the projection of the supraorbital torus in front of the frontal squama, as defined by Weidenreich, taken from the most anterior point of the torus at its middle, parallel to the flat base of the sulcus up to the place where the frontal squama begins its ascent above it.

[c]The distance from the most anterior point of the torus at its most lateral extent to the temporal line behind it. This is not in the same position as the slightly smaller fmo-fmt diameter, not preserved on WLH 50.

[d]The "corner position" as in Weidenreich (1951: Table 6), to be distinguished from the lateral thickness (height) of the torus, which is not preserved on either side of WLH 50.

TABLE 8. PARIETAL MEASURES (mm) AND INDICES FROM BREGMA.

	bregma-lambda (br-l) (M30)	br-l arc (M27)	parietal curvature (br-l) index	bregma-asterion (br-ast)	br-ast arc	br-ast index	bregma-parietal mastoid angle (br-pma)	br-pma arc	br-pma index
WLH 50	128.5	140.0	108.9	150.0	167.0	111.3	140.0	158.0	112.9
Solo 1	105.9	114.5	108.1	125.7	142.0	113.0	118.9	140.0	117.7
Solo 5	113.2	119.0	105.1	138.4	157.5	113.8	129.2	147.5	114.2
Solo 6	97.6	102.5	105.0	132.8	144.5	108.8	123.2	143.0	116.0
Solo 9	103.8	109.0	105.0	134.2	153.0	114.0	129.8	146.0	112.5
Solo 10	105.3	109.5	104.0	139.0	156.0	112.2	130.5	145.0	111.1
Solo 11	98.8	103.5	104.8	134.4	149.5	111.2	126.6	142.5	112.6

somewhat rounded. Contrary to the condition in modern man, there is no trace of a division into two lips allowing space for the sagittal sinus."

The WLH 50 frontal crest, as preserved, is shorter than in the Ngandong adults, and neither as projecting nor as sharp-edged. Its maximum height at the most anterior point that is preserved is 8.2mm. The frontal crest extends posteriorly for about 33mm, followed by a sagittal sulcus that develops into a low torus up to the position of the coronal suture, which cannot be discerned internally. This low internal torus, about 14mm wide, is bordered by shallow pitted grooves on both sides, about 13mm apart at the coronal suture position. But whereas the Ngandong condition lacks a sagittal sulcus posterior to it, in WLH 50 a sagittal sulcus with its division into two lips begins immediately posterior to the frontal crest, 35.5mm behind the most anterior part of the crest that remains, or just about 68mm posterior to glabella. The lips of the sulcus continue posteriorly to the approximate position of metopion (endometopion), diverging slightly with a barely projecting plane between. Posterior to the endometopion position the structure continues to the coronal suture as a low torus some 10mm in breadth, bordered on either side by a pitted sulcus. Most of the pacchionian pits on the endocranial surface of the frontal are along these sulci. Asymmetrically expressed meningeal grooves are preserved to about 25mm superior to the broken edges of the bone, in a very anterior position.

The anterior of the frontal crest in WLH 50 is broken at the frontal sinus so that its lower termination cannot be seen. On the midline a small 6.5mm piece of the anterior face of the sinus remains, about 8.5mm anterior to the frontmost extent preserved of the frontal crest. There is a much larger portion of the anterior face of a second sinus attached to it. Addressing its estimated size, Webb (1989: 41) notes: "the frontal sinus of WLH 50 is large by any standard and makes a striking contrast to almost all other individuals in the [Willandra] series." Exposed by the broken internal surface on the left side, the sinus extends laterally from the midline for 34.5mm, the external wall in its most medial position preserved, some 6mm lateral to the midline, is 4.7mm thick.

Parietal Bones

Neither of the WLH 50 parietals is complete. They share a full sagittal edge, and on the left there is more-or-less continuous bone from the coronal to the lambdoidal sutures, excepting some red wax patchwork visible in Figure 7. The left side is complete to asterion and the parietal notch. Anterior to this is about 25mm of the superior 20mm of the parietal's bevel for the temporal squama, but, anterior to that, the broken arc of the remaining bone's border is superior to this bevel and no indication of the position of the temporal border of the parietal is preserved. The superior 90mm of the coronal suture to bregma remains. On the right, the full lambdoidal border also remains, but otherwise the bone is not as complete. Unless noted otherwise the parietal description is of the left bone, and only the left side is illustrated in the (sometimes reversed) figures.

WLH 50, like the Ngandong crania, lacks distinct parietal bosses. The superior temporal line is barely discernible on the bone surface from the coronal suture to the area 86mm posterior where the angular torus (described above) begins. Even here, where the angular torus is most weakly developed, a significant sulcus follows its superior border, and this sulcus continues for the full extent of the torus, to the lambdoidal suture which the sulcus follows to a position some 10.5mm above and behind asterion.

Parietal size is reported in Table 8; Table 11 (below) reports dimensions of the shared occipital border; and, Table 6 (above) reports the bone thickness. The WLH 50 parietals are notably larger than those of Ngandong, where they can be compared, and slightly more curved in the sagittal plane. As described above, a low, broad sagittal keel extends for

TABLE 9. A PARIETAL TRIANGLE
(formed by the three chords connecting at bregma, lambda, and asterion [given in mm]).
The dimensions are specified for the other figures reported.

	bregma-lambda (br-l) (M30)	lambda-asterion (l-ast)	bregma-asterion (br-ast)	area of included triangle (mm^2)	angle at bregma (degrees)	angle at lambda (degrees)	angle at asterion (degrees)
WLH 50	128.5	92.8	150.0	5926	38.0	83.7	58.4
Solo 1	105.9	87.6	125.7	4574	43.4	80.4	56.2
Solo 5	113.2	85.3	138.4	4822	38.0	87.2	54.8
Solo 6	97.6	86.4	132.8	4213	40.6	92.2	47.3
Solo 9	103.8	80.5	134.2	4174	36.6	92.6	50.6
Solo 10	105.3	84.4	139.0	4435	37.3	93.6	49.1
Solo 11	98.8	85.2	134.4	4201	39.3	93.6	47.2
Ng mean	104.1	84.9	134.1	4403	39.2	89.2	50.9
Ng adult σ	5.6	2.4	4.8	259			

57mm down the anterior half of the WLH 50 parietals; behind it, the bone surface angles from where the keel ends and flattens to lambda, these factors together creating the slightly elevated curvature index along the superior surface of the parietal. This is much like the Ngandong 9 condition. The parietal curvature index for Ngandong is low (mean of 105.3), unchanged from the index in earlier Indonesians from Sangiran (Bapang-AG) and Sambungmachan (Kaifu et al. 2008), and the WLH 50 parietal curvature index (108.9) is almost as low as the Ngandong maximum (108.1). Across the bone transversely (bregma to asterion or the parietal notch), the WLH 50 parietal is also flattened and the curvature index is within the Ngandong range and below the Ngandong mean. Curvature along the posterior border (see Table 11 below) also does not differ from the Ngandong condition.

The three preserved sides of the parietal define the surface of an irregular triangle, with three included angles (Table 9). The dimensions of the three sides for WLH 50 exceed all of the Ngandong crania and the area of the included triangle is 35% larger (5.9 σ^{21}) than mean value at Ngandong. The difference for the dimensions of the preserved triangle is greatest for the superior surface (bregma-lambda, WLH 50 is 4 σ larger. Transversely the WLH 50 parietal is also larger, but not as much so (for bregma-asterion, WLH 50 is 3.3 σ larger). The shape difference reflects a relatively elongated parietal bone. The included angles of the irregular triangle are similar, in that the WLH 50 values can be found within the Ngandong range for the angles at bregma and lambda. However, the WLH 50 angle at asterion is above the Ngandong range, reflecting the comparisons of the triangle sides, above, wherein the WLH 50 bregma-lambda length has the greatest difference from the Ngandong specimens. Bregma-lambda is the side opposite the asterion angle in the irregular triangle.

Vault thickness varies greatly across the bone (see Table 6). Where comparisons can be made, WLH 50 parietal thickness is exceptional and exceeds the Ngandong maximum at every measurement point except asterion, where it matches the maximum. At some places away from the standardized points thickness is somewhat less; for instance, attaining only 7.7mm at the posterior lower border of the bone at the superior anterior position remaining on the bevel for the temporal, 30mm anterior and superior to the parietal notch.

On the endocranial surface, the sagittal sinus continues behind the coronal suture for greater than half the parietal's length, corresponding to the external portion of the parietal that is keeled. The sinus is double lipped for that length. Pits occur along it and to either side. There are some details of the impressions of the anterior middle meningeal artery on both endocranial sides; where the sides can be

compared, the arterial impressions differ. But the considerable breakage internally, as well as the broken edges of the preserved bone, make it difficult to clearly discern the full pattern of branches and ramifications on either side. The internal position of lambda and the course of the lambdoidal suture near it can be seen, but for the most part the endocranial portions of the lambdoidal and sagittal sutures are closed and obliterated.

Temporal Bones

The temporal bones are only preserved posteriorly and mostly externally; neither the petrous portion nor the anterior squama remains, though on the right side there is posterior squama extending some 36mm anterior to the parietal notch and 22mm above it, and, on the left, a 21mm length of the most posterior aspect of the 14.6mm tall beveled surface on the left parietal shows where the posterior temporal squama had been. The internal surface is sheared away on both sides, exposing the internal pneumatised structure of the mastoid region described below. Slightly more of the internal bone surface remains on the left, but here too the petrous pyramid is gone. Neither temporal is complete enough for length measurements. Whether the WLH 50 temporal bones show any of the unique temporal bone-related aspects described for Ngandong relative to earlier Indonesians (Kaifu et al. 2008) can only be addressed for the mastoid process and a small part of the region around it.

Where comparisons are possible, the remaining portions of temporal bone in WLH 50 are similar in size to the Ngandong specimens. The left temporal is more complete, comprised of the rear-most 65mm of the bone, extending to asterion, absent any of the petrous portion, external auditory meatus, or glenoid area. An arc formed by the edge of the preserved bone continues from the anterior face of the mastoid, extending along the side of the temporal just below the position of the root of the zygomatic arch to the approximate position of the auricular point which is the most anterior point preserved (see Figure 7); we do not believe it extends as far anteriorly as the anterior rim of the external auditory meatus. No evidence is preserved that would indicate whether or not there was a postglenoid process. Along this arc the bone surface is preserved externally but not internally. None of the zygomatic root is preserved on this side. However, on the right side the posterior 41mm of the supramastoid crest is preserved on the temporal squama, its most posterior aspect 18mm above the mastoid notch.

At the equivalent position on the left, the outer bone surface of the temporal squama is sheared away; however, it does appear that the more anterior part of the lower border of the sheared area corresponds to the position of the supramastoid crest on the right. This reaches the lower border of the preserved bone at the position we attribute to the auricular point; immediately above and actually bordering what may be the supramastoid crest, the outer bone surface is sheared or broken away; below it the surface is preserved as described above. Given its larger cranial capacity, what remains of the WLH 50 temporal is not especially large (Table 10). Parietomastoid suture length is smaller than any Ngandong specimen. The 58mm distance from the approximate position of the auricular point to asterion, at the back of the bone, is only slightly larger than the 57.2mm Ngandong mean. In another comparison, the distance from the front edge of the mastoid process at its base to the most anterior point preserved where we believe the auricular point lies in WLH 50 is about 20mm; the equivalent distance measured to the auricular point on Ng 5 is 17mm.

TABLE 10. MEASURES OF THE TEMPORAL BONE (mm).

	au-ast	parieto-mastoid suture length: ast-pma
WLH 50	**58.0**	**27.0**
Solo 1	**48.2**	**31.0**
Solo 5	**60.7**	**32.0**
Solo 6	**57.4**	**29.0**
Solo 9	**64.6**	**34.0**
Solo 10	**57.7**	**31.0**
Solo 11	**55.1**	**31.0**

Most of the external portion of the mastoid process remains on the left; it is short and triangular. The process is more anterior-posteriorly narrowed and more pointed than in the Ngandong mastoids. In general, while there is considerable variation in the anatomy of the lateral mastoid face at Ngandong, the left mastoid of WLH 50 most closely resembles the left side of Ng 10 (see Figure 11). However, the external face of the WLH 50 structure is curved and cants medially to a slight degree although it is basically oriented vertically. In all of the Ngandong mastoids the external face is more curved and cants even more strongly medially, as seen from the rear (Figure 16). A low mastoid crest extends down the middle of the external surface of the WLH 50 mastoid; as described below, it is formed by the superior branch of the nuchal ridge.

A short portion of the posterior aspect of the digastric sulcus remains, defining the medial and posterior borders of the mastoid process. As preserved, the mastoid process projects some 5.5mm inferior to the floor of the digastric sulcus, but this is not a true value, as an unknown portion of the mastoid's tip appears to be missing. Measurements to *mastoidale* are not reported, as the correct position of this point is unclear. The digastric sulcus is preserved for its distal-most 9mm. This portion is shallow and broad, definitely broader than in any Ngandong specimen, but the angulation of the sulcus relative to the cranial midline is close to the same as in the Ngandong specimens that preserve

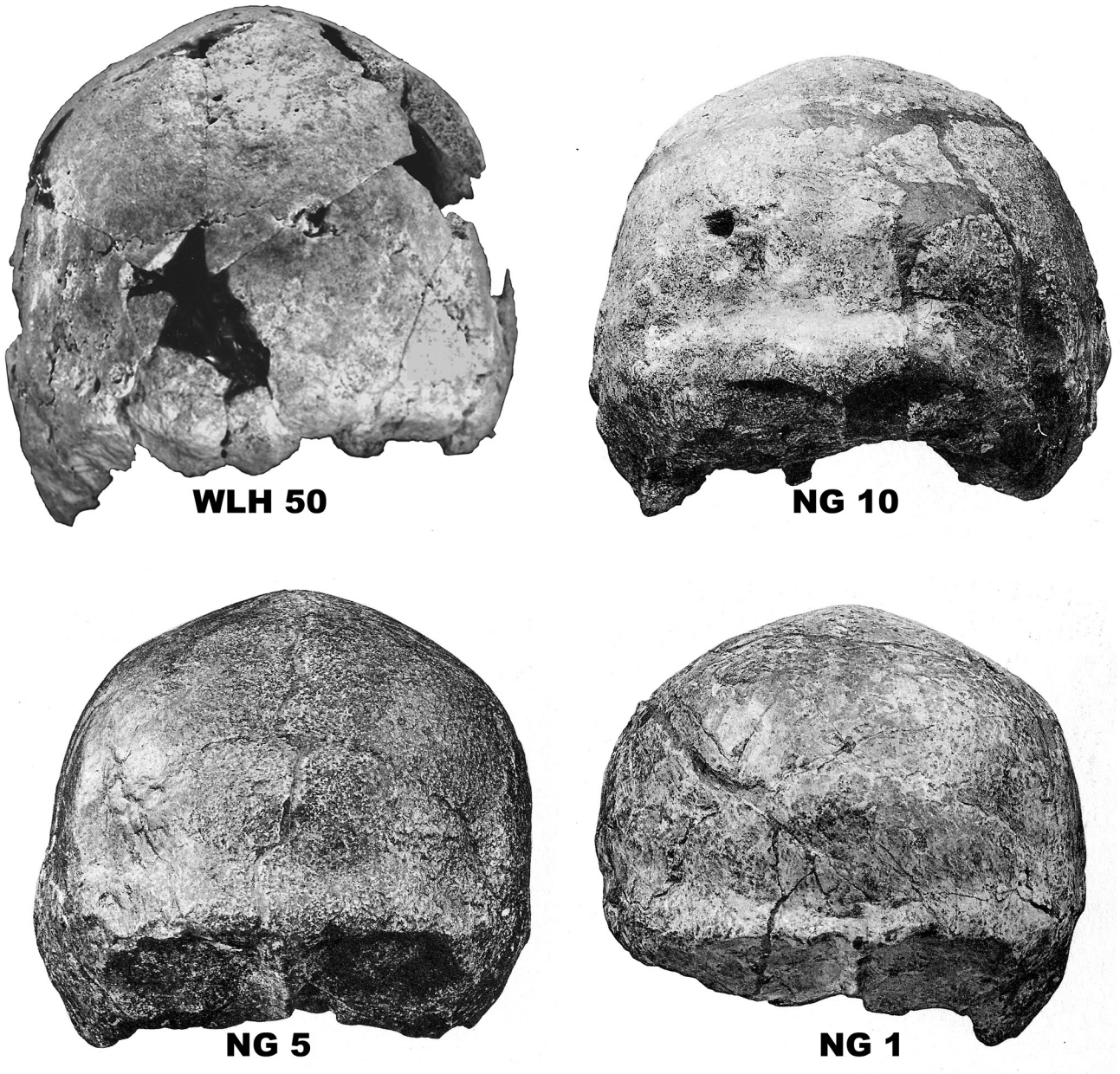

Figure 16. Posterior contour of WLH 50 is similar to the Ngandong crania, but the Australian vault is markedly taller. Shown are views of three Ngandong crania and WLH 50, approximately scaled to the same maximum cranial breadth (WLH 50 maximum cranial breadth is very close to the Ngandong mean), but in this comparison WLH 50 is more tilted backwards (on a transverse axis). The greatest breadth of the WLH 50 vault is at its base, across the supramastoid crests, and other details of WLH 50 can be found in each of the Ngandong crania. WLH 50 has a similar angulation between the parietal walls (higher and more vertical than in Ng) and the similarly gabled roof. The walls themselves are gently curved in a similar manner. The eroded nuchal torus of WLH 50, with its prominent tuberculum linearum, on inspection also closely resembles Ngandong crania, especially Ng 10. But the supreme nuchal line delineating the top of the WLH 50 torus cannot be easily seen in this photograph or in Figure 12.

it. For the posterior portion preserved, a low and narrow ridge, the lateral juxtamastoid, borders it medially. No cortical surface is preserved more medially.

The pneumatisation is extensive. As described by Webb (1989: 41):

> "it extends posteriorly to the occipitomastoid border, superiorly to the parietal notch and anteriorly above the supramastoid crest. The cells themselves are uniformly large, the largest being 13.9 mm at its greatest diameter. Medial portions of the mastoid region are missing, making any comment about their spread in this direction impossible. It is likely, however, that the extent of pneumatisation in this direction was commensurate with that observed in other robust individuals."

TABLE 11. MEASUREMENTS (mm) AND INDICES OF THE OCCIPITAL BONE.

	lambda-asterion (l-ast)	l-ast arc	l-ast index	lambda-to inion (l-i)	lambda to lowest inion	inion-asterion	lowest Inion-asterion	nuchal torus midline height	height lateral to inion
WLH 50	92.8	101.0	108.8	66.0	79.5	72.6	68.6	34.0	18.0
Solo 1	87.6	95.0	108.4	52.7	54.4	77.8	76.9	16.0	11.0
Solo 5	85.3	95.0	111.4	62.4	67.9	73.2	70.7	26.4	16.3
Solo 6	86.4	90.0	104.2	59.7	59.7	73.3	73.3	14.0	10.5
Solo 9	80.5	87.5	108.7	61.8	66.2	79.5	76.8	20.7	13.2
Solo 10	84.4	91.0	107.8	55.1	55.1	67.3	67.3	22.3	18.0
Solo 11	85.2	92.0	108.0	69.6	72.5	76.4	73.5	21.0	14.0

Occipital

The occipital bone is only partially preserved. Virtually all of the occipital plane remains, but only small portions of the nuchal plane are preserved (much of which is incomplete or broken), and as noted above, erosion has destroyed the outer bone table and an unknown amount of diplöe across the nuchal torus. The bone is large but comparatively narrow, relative to the Ngandong occipitals. Biasterionic breadth is less than all the Ngandong males, and only Ng 6 is smaller (see Table 5). Distances from lambda to inion or asterion average about 10% greater than the Ngandong mean (Table 11), although lambda to the lowest inion position is markedly larger, reflecting the significant downward turn of the superior nuchal lines at the midline to form a prominent *tuberculum linearum*. No extrasutural bones occur at lambda, but some large ossicles are incorporated in the lambdoidal suture.

As described above, the superior portion of the occiput has a close-to vertical occipital face (see Figure 11). The vertical face is formed by the bulge below lambda extending through the upper portion of the occipital plane that helps create the 29mm tall vertical surface reaching the superior edge of a tall, elliptically rounded suprainiac fossa. A similar bulge appears on most Ngandong crania, but the surface below it, while straight, is outwardly angled. Only Ng 1 is similar to WLH 50 in this region (see Figure 11). The WLH 50 suprainiac fossa is 35mm in breadth, extending for 19mm above the supreme nuchal line, and deepest just above its inferior border (the supreme nuchal line). In fact, the supratoral depression that extends along the supreme nuchal line is limited to the base of the suprainiac fossa and unlike the Ngandong condition, does not extend across the entire width of the bone. Also unlike most of the Ngandong crania this depression dips inferiorly (with the supreme nuchal line) at the midline[22]. The WLH 50 suprainiac fossa is larger and more distinct than on any Ngandong specimen, but Ng 9 is similar and smaller fossae can be found on Ng 6 and 11. The Ngandong fossae resemble the Neandertal condition (Caspari 2005, and *contra* Trinkaus 2004) in that they appear as an elliptical shape on a flattened somewhat concave surface above the superior nuchal line, transversely elongated, with a rough, pocked surface. WLH 50 shares these similarities. Lateral to the suprainiac fossa on the better-preserved left, a supratoral sulcus continues to border the superior surface of the nuchal torus, extending to the position where the supreme and superior nuchal lines converge to almost meet. This is 46mm from the midline of the occiput, measured along the bone surface.

As noted, the external surface of the nuchal torus is eroded between the distinct superior and supreme nuchal lines, and at first glance this obscures some of the similarities with nuchal tori in the Ngandong remains. It also makes it inaccurate to determine the thickness of the torus or arc lengths to inion that include the distance over the torus. But even comparisons of the incomplete thickness dimensions that are preserved on the remaining bone of WLH 50, to Ngandong or the Herto cranium (see Table 6), strongly suggest the full thickness in this region would have been quite exceptional.

While quite large, the WLH 50 nuchal torus does not fully extend from one side of the occiput to the other. The torus occupies the middle 70mm of the bone and was significantly tallest at the midline because of the vertically prominent *tuberculum linearum*. The full extent of its projection away from the bone is unknown because of erosion, as noted, but the large, downward pointing triangle of the

TABLE 12. ZYGOMATIC THICKNESS MEASUREMENTS (mm) FOR WLH 50 COMPARED (comparisons are with Australian fossils and other hominids at the extremes for dimensions where WLH 50 is unusual).

The breadth of the frontal pillar of the zygomatic is measured as the distance from the orbit rim to the posterior of the pillar above jugale. The thicknesses are taken along the base of the zygomatic.

	frontal pillar breadth	zygomatic thickness at *zygomaxillare*	maximum thickness of the masseter attachment
WLH 50	17.9	14.0	12.0
Cohuna		13.1	12.4
Kow Swamp 1	12.2	11.6	7.8
Klasies 16651	17.8		
Sangiran 17 (earlier regional)	21.9	13.3	11.5
OH 5 (broadest pillar)	29.4	14.4	14.0
SK 46 (thickest at zm)	11.7	16.3	8.5
ER 13750 (thickest at masseter attachment)	14.0	12.8	14.5

tuberculum linearum almost doubles vertical height of the torus at the midline, and the torus is vertically taller than any of the Ngandong crania, to a considerable degree (see Table 11). What remains of the WLH 50 nuchal torus appears much like Ngandong 5, but markedly larger. The torus and the *tuberculum* are vertically taller in WLH 50 than in any Ngandong specimen.

Only part of the posterior aspect of the nuchal plane is preserved, including its lateral border up to the mastoid on the left side. Lateral to the nuchal torus, the supreme and superior nuchal lines converge but do not quite meet. They delineate what we describe as a nuchal ridge (or much smaller torus) just under 6mm in height (i.e., the lines are about 6mm apart) that arcs from the nuchal torus laterally across the occipital, crossing the occipitomastoid suture on to the temporal 14.7mm inferior to asterion on the left. WLH 50 lacks the retromastoid process that Weidenreich describes and illustrates for the Ngandong crania. Had there been one, we believe it would have been on the nuchal ridge we describe here, most probably at or close to the position where it bifurcates.

Three elements combine to obscure some details in this region or make them difficult to define: (1) the condition of the bone surface, (2) a significant (repaired) break, and, (3) the loss of most of the nuchal surface. Along the nuchal ridge on the occipital is the attachment area for a large *splenius capitis* and *sternocleidomastoid* more laterally. The nuchal ridge appears to bifurcate on the occipital, 4.6mm posterior to the occipitomastoid suture. Almost exactly at this point the 12mm segment of the *linea obliquus* that remains extends anteromedially as the lateral border of the *semispinalis capitis* insertion.

The superior branch of the nuchal ridge on the lateral occipital continues anteriorly onto the mastoid process and, turning inferiorly, becomes the mastoid crest, as described above. The inferior branch travels 24mm in a parasagittal direction to the broken edge of the nuchal plane. Although key portions of the region are missing, we believe its anatomy would have most closely resembled the anatomy of Ng 11[23], and that (had it been preserved) the inferior branch extended to form a medial juxtamastoid process. None of the medial juxtamastoid process was preserved, apart from the 9 anterior-most millimeters preserved of the inferior branch that becomes markedly taller and more crest-like.

Medial to the mastoid process, a small portion of the lateral juxtamastoid appears to remain (again assuming an anatomy similar to that of Ng 11), separated from the mastoid by a shallow digastric groove. Thus as we reconstruct the region, including its missing portions, there were both medial and lateral juxtamastoid processes divided by an occipital groove on the left side of the WLH 50 cranial base.

Zygomatic Bone

A part of an associated cheek bone was recovered, most of a large zygomatic bone fragment (Figure 17) with a bone thickness of 14mm at the base of the zygomaxillary suture, and a maximum thickness of the masseter attachment on the lower border of the bone of 12mm. This is an exceptional thickness, greater than other Australian fossils (Table 12) and a large dimension for hominid fossils generally[24]—only robust australopithecines are thicker in this region. A linear dimension we have comparative data for is the breadth of the frontal pillar, the minimum distance from the orbital rim to the posterior of the zygomatic column, just above the *jugale* position. This dimension is larger than in any recent human observed and in the Late Pleistocene

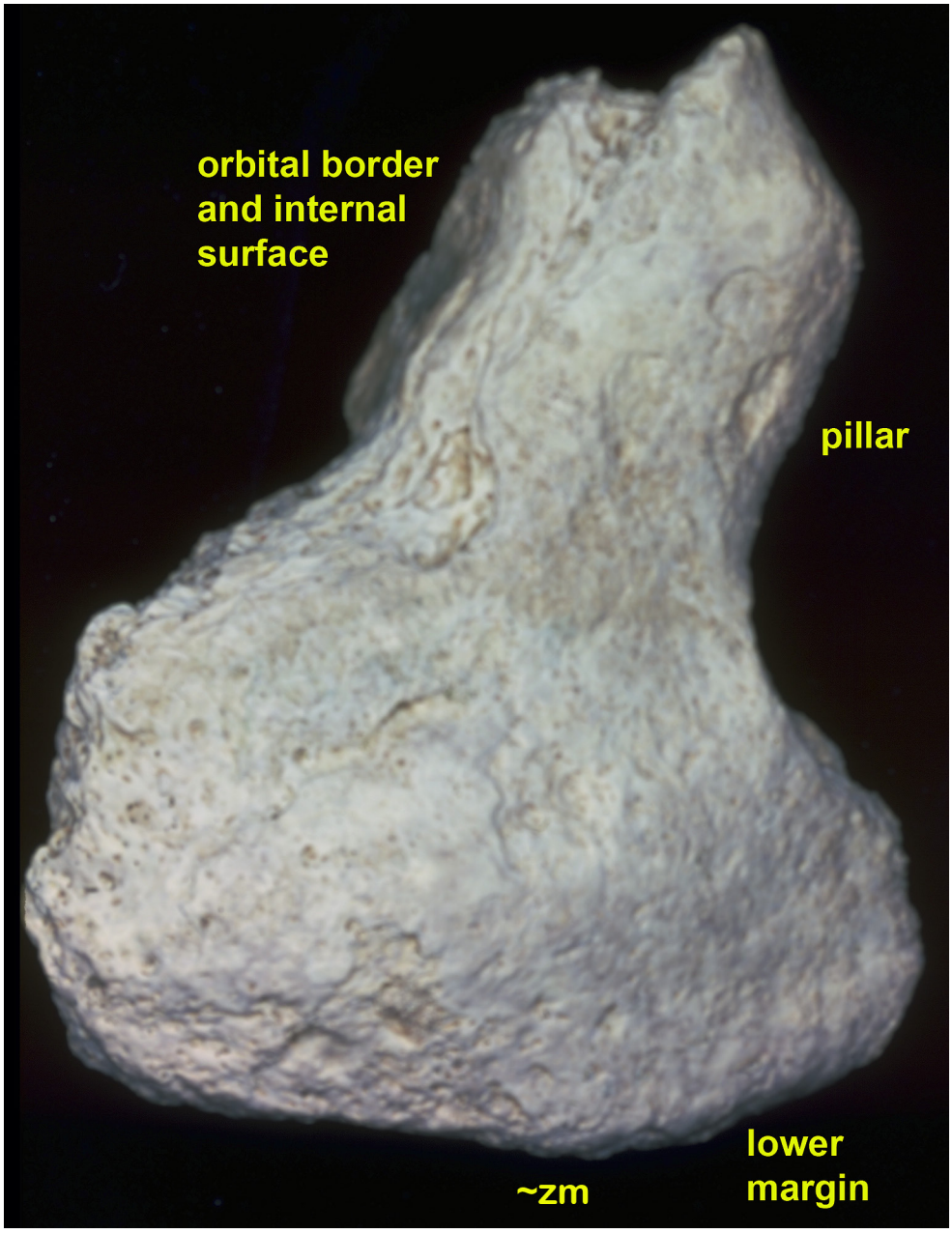

Figure 17. Left partial zygomatic bone preserving much of the pillar with an eroded orbital border, some internal orbital surface, the jugal notch, part of the lower border to the approximate zm position, and a small portion of the temporal process.

it is only matched by the large Klasies 16651 partial zygomatic. Among earlier remains, WLH 50 is matched by the KNM-ER 3733 zygomatic dimension, and exceeded by archaic specimens such as Kabwe and Sangiran 10 and 17, and greatly so by OH 5. The largest earlier zygomatic bone from the region is that of Sangiran 17, a specimen with an exceptionally broad face and large cheeks. The Sangiran male has a broader frontal pillar, but the zygomatic thicknesses are slightly less than WLH 50.

In an unusual anatomy, there are two ridges paralleling the zygomaxillary suture, one above it and the other below.

It would be foolhardy to reconstruct the face from this information about part of a zygomatic bone, but WLH 50 clearly had a large cheek, one of the largest known from the Late Pleistocene, with support for masseter muscles providing significant masticatory strength. As noted above, powerful mastication might contribute to the cranial vault thickness of the specimen.

STATISTICAL APPROACHES

The observations and comparisons described above, and many of the questions they address, are amenable to statistical analyses. These include both standard multivariate approaches and testing that takes the characteristics of the samples themselves as its basis. It is reasonable to expect that if Australian populations descended from a mixture of distinct ancestral groups from different geographic sources, this should be demonstrable in a testable statistical manner. This frames our approach to examining questions

TABLE 13. SPECIMENS IN THE COMPARATIVE GROUPS (for research reported in Hawks and colleagues [2000]).

Ngandong	Late Pleistocene Africans	Levantines
1	Jebel Irhoud 1	Skhul 5
4*	Jebel Irhoud 2	Skhul 9
5	Laetoli 18	Qafzeh 6
6	Omo 1*	Qafzeh 9
9	Omo 2	
10	Singa	
11		

* Used only in the non-metric analysis

about the ancestry of WLH 50; most importantly, **whether Ngandong-like populations are among the ancestors of WLH 50, and by inference of indigenous Australians.** The outcome is fundamental for evaluating hypotheses of Australian ancestry, which themselves inform our knowledge of the pattern of human evolution.

Although this is a question about ancestry, we do not address it phylogenetically for reasons noted above—the samples are too closely related under any hypothesis of relationship. In fact, we believe both WLH 50 and its immediate ancestors are most probably samples of potentially interbreeding populations and thereby both lie within the species, *H. sapiens*[25]. The basis for this assessment is in research comparing the time of divergence of known mammalian species and measures of their interfertility (Curnoe and Thorne 2003; Holliday 2006). Even under the most generous interpretations of lineage divergence, different putative ancestors of WLH 50 have not been separated for long enough for significant reproductive isolation to be expected. This assessment is also supported by the analysis of nDNA discussed below, and by observed mixtures of both Neandertal and Denisovan nDNA with each other and in many human populations.

This is why phylogenetic analysis is not appropriate. The approach relies on the parsimony principle; when two specimens have the same character state, the most probable explanation is that they both inherited it from a last common ancestor with the same character state. The limitation for specimens of close relationship is that *the parsimony principle cannot be validly evoked when gene flow is also a potential source of shared traits*. Gene flow would be a different source of similarity and its probability in any particular case is not possible to assess. Therefore, our approach to assessing these close relationships is to evaluate limited hypotheses of ancestry based on patterns of similarity in metric and non-metric comparisons.

We are not the first to approach the relationships of WLH 50 in a multivariate manner. Stringer's analysis (1998) was the earliest to provide a phenetic analysis of WLH 50. He did a Penrose size and shape analysis for 11 measurements, that indicated WLH 50 was most similar to Skhul-Qafzeh, and most different from Ngandong. When the size component is separated out, his analysis places the specimen closest to Skhul-Qafzeh and the recent Australian samples, further from the African "archaics" he considered, and furthest from Ngandong. Stringer also used a Principal Component Analysis to take the correlations between the measurements into account.

In our discriminant function analysis reported below, we also evaluate metric relationships with a standard multivariate approach. However, we also report on tests for similarity based on non-metric observations that we and our colleagues developed to test predictions for patterns of phenetic similarities coming from hypotheses of ancestry when a phylogenetic approach is inappropriate or cannot be used. Some of these analyses were reported in Hawks and colleagues (2000), with additional details in Wolpoff and colleagues (2001).

DISCRIMINANT ANALYSIS OF METRIC DATA

Our metric evaluation is based on discriminant function analysis of the metric observations preserved in WLH 50, and best differentiating its potential ancestors from Africa, the Levant, and Ngandong (Table 13). The function determined to discriminate these three samples was used to assess the group affinity of WLH 50. In this instance we take similarity to be a reflection of affinity, although there is no possibility that WLH 50 actually belongs to any of these three groups.

Using SPSS version 8.0.0, Hawks and colleagues calculated a stepwise discriminant function using the Wilks' Lambda statistic for a set of 21 measurements present in the three samples and WLH 50. The advantage of this commonly used test statistic is that at each step it maximizes the cohesiveness within each group without affecting the separation between groups (Klecka 1980). The function (Table 14) correctly classified every member of the three groups. These classifications of known specimens were without exception robust to cross-validation using the other known specimens, confirming the utility of this set of measurements for determining geographic origin.

The discriminant analysis resulted in two functions

TABLE 14. UNSTANDARDIZED DISCRIMINANT FUNCTION COEFFICIENTS (for the 5 variables chosen in the stepwise analysis to separate the three groups samples from Indonesia, Africa and the Levant [Hawks et al. 2000]).

Calculations are based on the Wilks' Lambda statistic, and the functions are normalized around the origin. These values reflect the absolute importance of the independent variables in contributing to discrimination.

Variable (mm)	Discriminant Function 1	Discriminant Function 2
cranial length	0.396	-0.075
glabella-bregma	0.318	0.207
bregma-asterion arc	-0.721	0.021
central parietal thickness	0.988	0.190
medial supraorbital height	-0.508	0.039
(constant)	2.368	-13.541

that together correctly assigned all the specimens into their geographic group, based on five of the original 21 variables (Figure 18). The first discriminant function accounts for 99.1% of the among-group variance, and is highly significant ($p<0.001$, Wilks' Lambda test). The second discriminant function accounts for the remaining 0.9% of the among-group variance, but is not significant ($p=0.192$, Wilks' Lambda test).

These variables sort WLH 50 with the Ngandong group to the exclusion of either the African or Levantine group (see Figure 18). For the first discriminant function, the squared Mahalanobis distance from WLH 50 to the Ngandong centroid is 18.15, while that to the next closest group centroid, Africans, is 74.48. Including the second discriminant function, though it is not significant, tends to pull WLH 50 away from all of the groups somewhat. The high score on this discriminant function for WLH 50 appears to reflect principally the long frontal length (glabella-bregma distance) for this specimen, which though it exceeds every other specimen in the analysis, is most similar to the value for the largest African specimens.

For both functions taken together, the squared Mahalanobis distance from WLH 50 to the Ngandong centroid is 42.5, while that to the centroid of the next closest group, Africans, is 91.7, more than double. Based on these data, the position of WLH 50 is significant at the 0.001 level. WLH

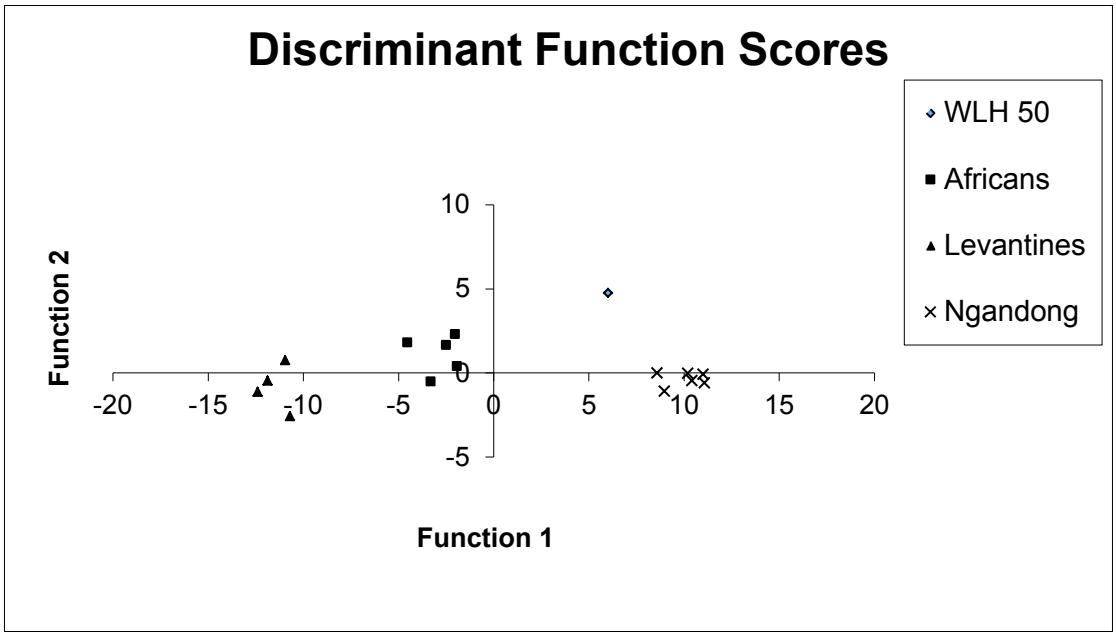

Figure 18. Discriminant function scores, from Hawks and colleagues (2000). Function 1 accounts for 99.1 percent of the among-group variance, and is highly significant ($p<0.001$, Wilks' Lambda test). Function 2 accounts for the remaining 0.9 percent of the among-group variance, but is insignificant ($p=0.192$, Wilks' Lambda test). Classification of WLH 50 with the Ngandong group is significant at the 0.05 level.

50 is unambiguously and significantly closest to the Ngandong sample, according to this analysis. The point is not whether WLH 50 is a Ngandong cranium, we know it is not. The conclusion is that WLH 50 has significant phenetic similarity to the Ngandong remains, and we interpret these in the context of ancestry as framed by Ngandong's earlier date and close geographic proximity to WLH 50.

PAIRWISE DIFFERENCE ANALYSIS USING NON-METRIC DATA

The second test we report was a pairwise difference analysis using non-metric observations (from Hawks et al. 2000). The numbers of differences of individuals compared with WLH 50 for each of the traits studied were counted. This both ignored each specimen's *a priori* group assignments, and avoided problems that could arise from scaling (Smith 1996), since WLH 50 is significantly larger than the Ngandong specimens. Difference analysis provides an approach to validly examine hypotheses of ancestry below the level of species, where phylogenetic analysis is not appropriate. In this case, *it also has the advantage of using non-metric data.* This allows us to compare specimens of various sizes without attempting to compensate for size differences, since compensation often creates more problems than it solves because of the assumptions size compensation approaches often require.

For this test, 16 non-metric traits as described in Table 15 were scored for their presence or absence in each specimen. The traits were chosen with the goal of clearly describing the various anatomical features of WLH 50. To maximize the data set Hawks and colleagues (including MHW) developed, a complete list of features that could be scored with good replicability and were homologous for the crania studied. There was no *a priori* limitation to the number of observations analyzed[11] and they were not "cherry-picked" out of a larger set. The problems inherent in these data, as with most fossil data, come from the lack of data, not its overabundance.

A count was made of the number of differences in these scores comparing WLH 50 and each of the 17 other specimens (the 10 from Africa and the adjacent Levant, and seven from Ngandong shown in Table 13). For instance, six of the 16 traits were scored differently in WLH 50 and Omo 1 and this is reflected in Figure 19, which presents the comparisons in order of difference, from the least different to most different. More individuals could be included in this analysis than in the discriminant function analysis because it is tolerant of missing data, as long as the missing data are randomly distributed as is the case for these groups of specimens (Kruskal-Wallis test, chi square=0.126, p=0.939). In cases where a trait could not be scored on a specimen, the trait was treated conservatively, as showing no difference in comparisons involving that individual.

Figure 19 shows that six of the seven Ngandong crania are less different from WLH 50 than any other specimens are, and the seventh Ngandong cranium is only separated from the others by one specimen (Skhul 9). On average, WLH 50 has strikingly fewer differences from the Ngandong group (3.7 mean pairwise differences) than from either the African group (9.3 mean differences) or the Levantine group (7.3 mean differences). This pattern is statistically significant, using the Wilcoxon-Mann-Whitney test. WLH 50 is unquestionably less different from the specimens from Ngandong than from any other group in its non-metric traits. In the light of these significant statistics, it is difficult to explain how such a pattern of differences could appear by chance. Any (or all) of these groups are potential ancestors for WLH 50; the minimum interpretation of our analysis is that Ngandong is *one of the ancestors* of WLH 50.

Hawks et al. first presented this pairwise test in 2000. Several papers from around that time and since have advanced arguments that pairwise analysis is not valid; the Hawks et al. paper addressed one of these at length (Stringer 1998). Since 2000, Bräuer et al. (2004), Collard and Franchino (2002), and Gordon and Wood (2013) presented arguments addressing the validity of pairwise analysis for phylogenetic issues. Gordon and Wood (2013: 465) "address (1) whether these particular methods do what they claim to do, and (2) whether such approaches can ever reliably address the question of conspecificity," and they conclude that the methods do not do what they claim to do, and furthermore, any effort is futile because: "no pairwise method can reliably answer the question of whether two fossils are conspecific."

We agree; as a general proposal this must be the case, as the existence of sibling species (Mayr 1963) demonstrates. However, for us, the more relevant issue is whether pairwise methods can be used to address questions of ancestry below the species level. We do not need pairwise comparisons to test phylogenetic hypotheses. There is already an established procedure to do this—cladistics—and the question of whether a phenetic approach is more appropriate than phylogenetics to resolve issues of phylogeny has, in our opinion, been resolved long ago. We need not repeat this debate here, and besides if we did, we would not be on the side of phenetic analysis at and above the species level. Our use of pairwise methodology is and has been to ascertain differences *below the species level* where phylogenetic analysis is not always valid because of reticulation, and to address hypotheses of ancestry. This aspect of our analyses has not been addressed, let alone invalidated.

Gordon and Wood (2013) are critical of pairwise analyses because they are (p. 473): "highly dependent on the number of variables involved in the comparison, … and on the specific set of variables considered". We agree with these assessments (Lee 2011) and have addressed them in this and other research by including all of the variables that are homologous and can be compared in our analyses.

STET (STANDARD ERROR TEST)

Unlike the pairwise difference analysis described above, STET (Lee and Wolpoff 2005; Wolpoff and Lee 2001, 2006) is an approach based on comparing linear homologous measurements. STET compares pairs of specimens using all of the measurements they have in common, in an approach

TABLE 15. NON-METRIC OBSERVATIONS USED IN THE FIGURE 19 PAIRWISE DIFFERENCE ANALYSIS (from Hawks and colleagues [2000]).

The traits were chosen to represent all regions of the WLH 50 vault, be homologous and clearly definable on all of the specimens, and be accurately replicable by different observers. The list of traits was finalized before there was any analysis.

1.	**Transversely Extensive Nuchal Torus:** This feature is scored as present if a distinct nuchal torus defined by superior and supreme nuchal lines extends transversely across the entire occipital bone.
2.	**Sulcus Dividing the Medial and Lateral Elements of the Supraorbital Torus / Superciliary Arches:** This feature is scored as present if a clear sulcus can be identified that divides the supraorbital torus or superciliary arches, whatever the case may be, into medial and lateral elements.
3.	**Frontal Sagittal Keel:** A thickening along the midline of the frontal bone anterior to bregma. The feature is scored as present if it can be either seen or felt. It need not extend along the entire length of the frontal bone.
4.	**Parietal Sagittal Keel:** A thickening along the sagittal suture. This feature is scored as present as long as it can be identified anywhere along the suture.
5.	**"Rolled" Superior Margin of the Orbit:** Scored as either blunt (present) or sharp (absent). If the margin is blunt then the supraorbital surface grades evenly into the inferior surface of the frontal bone.
6.	**Suprainiac Fossa:** An elliptic depression on the occiput above the superior nuchal line.
7.	**Temporal Line forms a Ridge:** This feature is scored as present if the temporal lines form a ridge along the frontal bone posterior to the post-orbital constriction.
8.	**Projecting Inion:** This feature is scored as present if the nuchal torus/line projects posteriorly at the most inferior midline point along the superior nuchal lines.
9.	**Pre-Bregmatic Eminence:** This feature is scored as present if a distinct eminence can be visually identified anterior to bregma when viewing the specimen in Frankfurt Horizontal. If the frontal bone and the parietals form an even curve in Frankfurt Horizontal then the feature is scored as absent (0).
10.	**Angular Torus:** This feature is scored as present if the posterior temporalis muscle attachment forms a raised and thickened ridge at its furthest backward extent.
11.	**Post-lambdoidal Eminence:** This feature is scored as present if a distinct posteriorly projecting eminence can be visually identified immediately posterior to lambda when viewed in Frankfurt Horizontal.
12.	***Linea Obliquus*:** This feature is scored as strongly developed if there is a clear line or ridge extending inferiorly and anteriorly from the lateral portion of the nuchal line/torus.
13.	**Lateral Frontal Trigone:** A backward-facing triangular development at the lateral-most portion of the supraorbital torus. The apex is created when a prominent temporal ridge meets a clear line on the anterior lateral portion of the supraorbital torus.
14.	**Mastoid Crest:** This feature is scored as present if a distinct bony crest can be identified that extends inferiorly and slightly anteriorly from the top of the mastoid process towards the tip of the mastoid process.
15.	**Supramastoid Crest:** This feature is scored as present if a distinct bony crest can be identified that curves posteriorly and slightly superiorly from the root of the zygomatic arch on the temporal bone above the mastoid process.
16.	**Coronal Keel:** A thickening of raised bone extending transversely from bregma along the coronal suture.

similar to the *Q*-mode approach Lovejoy (1979) proposed. STET provides a method for quantifying similarity or difference for pairs of specimens within a species or between closely related species where there are insufficient data for a valid phylogenetic analysis.

The different comparisons addressed by STET need not involve exactly the same set of measurements, but they do require a minimum number of shared measurements (Lee 2011) for accuracy. The STET statistic is the uncertainty in the value of the slope of the regression line calculated for the measurements that are shared. This uncertainty provides an estimate of the phenetic similarity between a pair of specimens. The requirement of a minimum number of shared measurements addresses the accuracy of this uncertainty. STET is tolerant of missing-data and it is comparable for different pairs of comparisons of sufficient size. Thusly, STET does not require that each comparison in a study be based on exactly the same set of shared measurements.

This analysis of variation is pairwise, in that we compare individuals two at a time. This provides a statistic that can be used in evaluating null hypotheses (Figure 20; see also Figure 21 and Tables 16–19 below). We may compare all the specimens in a sample to each other for an assessment of sample variation (e.g., see Table 16), a single specimen to all the specimens in a sample (e.g., see Table 18), or all the specimens in one sample to all the specimens in another (e.g., see Figure 20) to understand the pattern of difference.

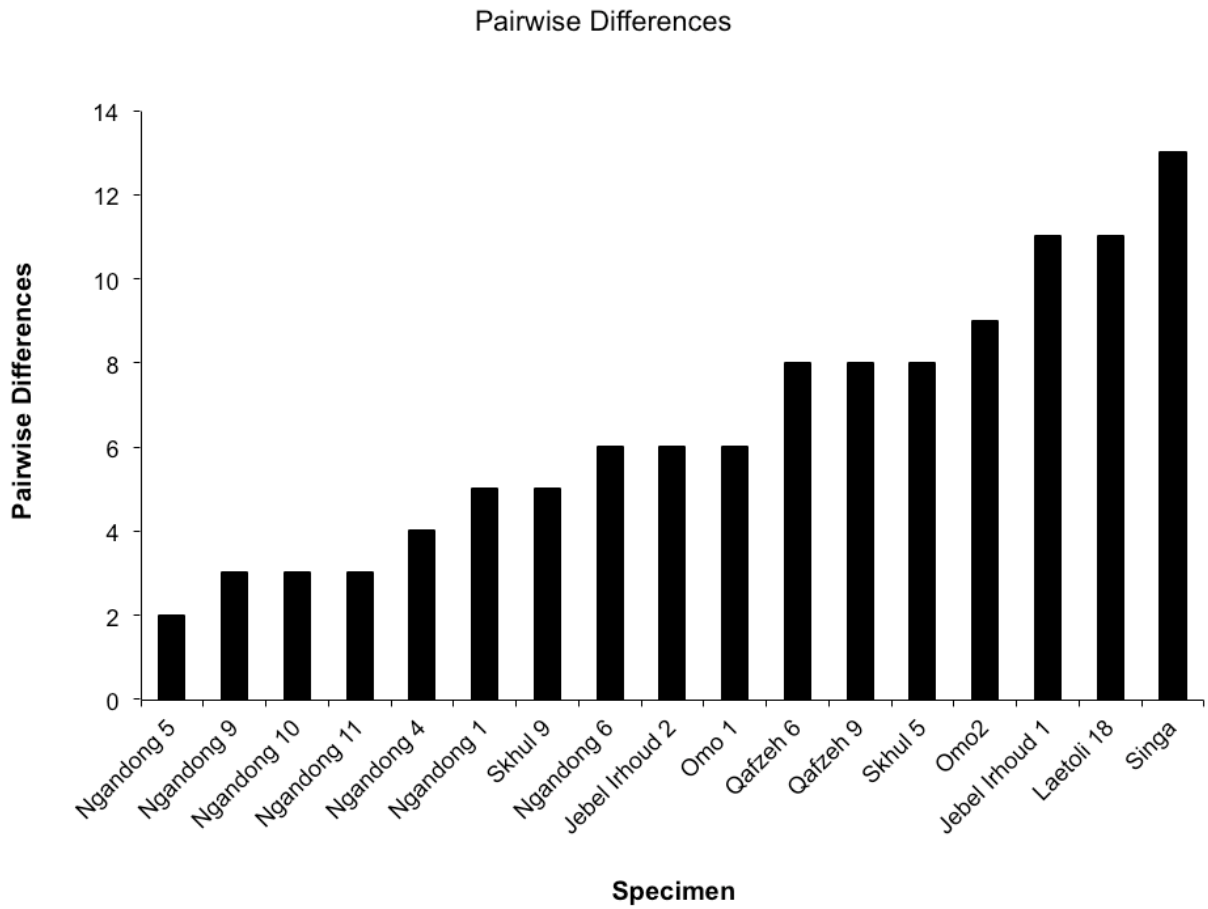

Figure 19. Pairwise comparison of WLH 50 to Indonesian, African and Levantine specimens (Hawks et al. 2000) based on non-metric observations (see Table 15). The comparisons are in order of the number of differences from WLH 50—Ngandong 5 (furthest left) has only two differences from WLH 50 while Singa (furthest right) has 13. The difference comparisons indicate the least differences, by far, are with the Ngandong sample. Mean pairwise differences between Ngandong and African, and Ngandong and Levantine groups are statistically significant at the 0.05 level (Wilcoxon-Mann-Whitney Test).

Standard Error of the Regression Slope

STET is calculated from the linear regression analysis for bivariate comparisons between sets of homologous linear measurements of individual specimens. The standard error of the regression slope (s.e.m) is a measure of its uncertainty. Thus, contra Gordon and Wood (2013) STET reflects the consequences of variation in both size and shape and measures uncertainty, not deviation, in that STET reflects the effects of "both geometric and allometric shape similarities between crania rather than just geometric shape similarity" (Aiello et al. 2000: 180). There are many cases where the bivariate comparison is not symmetric around a linear regression line, the regression of X on Y differs from the regression of Y on X and the standard errors of the regression slopes differ as well. We calculate standard errors of the regression slopes (s.e.m) for the linear regression of X on Y, and again for Y on X, and combine these as the square root of the sum of the squares of the two. One could think of STET as a hypotenuse joining the sides of a triangle determined by the two orthogonal standard errors.

$$(1)\ \mathrm{STET} = 100[(\mathrm{s.e.m}_x)^2+(\mathrm{s.e.m}_y)^2]^{1/2}$$

STET has several advantages. It does not require any assumptions about the sample distributions; in specific, it does not assume normality in the measurements compared. Perhaps most importantly, STET tolerates missing data and does not require their estimation. Lee (2011: 260) notes: "because STET compares each pair of specimens using the measurements that are available for that particular pair, not all specimens in a dataset need to have all the variables preserved." In STET, comparisons of specimens that do not preserve all the same anatomical regions are possible as long as each comparison also involves a sufficient number of observations from shared anatomical regions.

Does STET "Work"?

Similar to disputes about pairwise difference analysis, some authors argue that STET does not "work" (Gordon and Wood 2013). This, of course, depends on what one means by "work." Gordon and Wood, in the aforementioned reference, maintain that shape similarity does not imply conspecificity: "no pairwise method can reliably answer the question of whether two fossils are conspecific" (2013: 465). We agree. This is evident in cases of sibling spe-

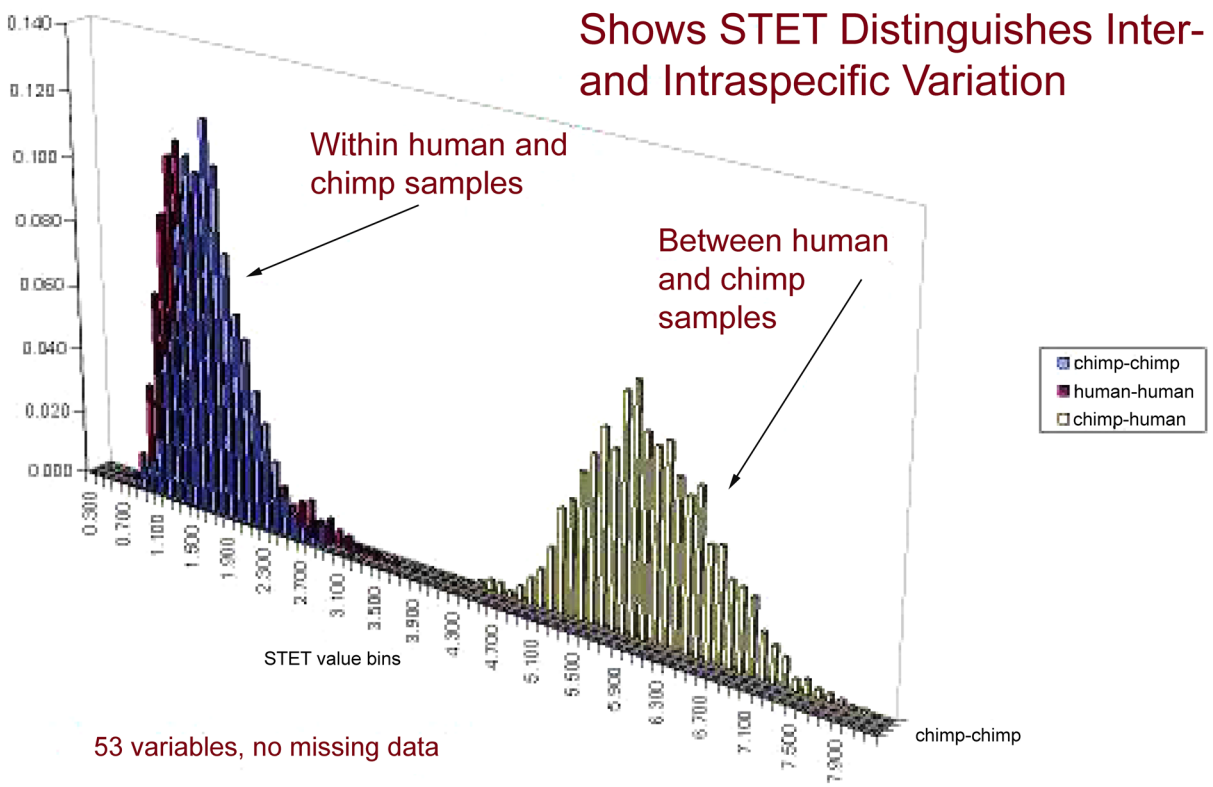

Figure 20. STET values for 53 variables within samples of Homo and Pan, and for a sample consisting of Homo-Pan pairs. These are not constrained to the measurements known for WLH 50. From Wolpoff and Lee (2006).

cies (Mayr 1963), cases of mimicry (Jiggens et al. 2001) and certain other cases of closely related groups (Kimbel and Martin 1993), and of course has been evident to us:

> "STET can only be used to refute the hypothesis of no difference. The fundamental precept is asymmetrical: sufficient difference can refute the same-species hypothesis but similarity cannot refute the hypothesis of different species" (Wolpoff and Lee 2001: 295).

STET, like the pairwise difference analysis, is a tool for quantifying variation below the species level (Tables 16 and 17) or in closely related species (see Figure 20). STET comparisons at this level result in STET magnitudes that reflect widely acknowledged similarities and differences[26]. Each of the analytical approaches we discuss here is based on different data sets and, in some cases, makes different assumptions. But when they address hypotheses of ancestry, for the most part, they provide the same results.

STET Analysis

Here, we use STET to examine hypotheses about ancestry within a single evolving hominid lineage (c.f. Wolpoff et al. 1994). STET helps this evaluation of ancestry for WLH 50 by providing an opportunity to refute the hypotheses of a unique African ancestry for WLH 50, or a unique Ngandong ancestry for it. In this use, STET is treated as a statistic of variation, combining all the measurements possible on each specimen. The relation of specimens in pairs provides a way to examine variability in many interrelated metrics at the same time, without making any assumptions about which measures have greater importance. A classic multivariate approach would weigh the measurements by their contribution to the total variance, an approach that might be indicated when sample sizes are large. However, in these fossils, the sample sizes are so small that they cannot be used to reliably estimate the form of the variance/covariance matrix, and estimating the missing data or copying the variance/covariance matrix from a larger sample will bias the results and make them dependent on the matrix used, and not on the variation of the sample (Ahern et al. 2005). The comparison of STET values between samples is an approach that avoids making these assumptions.

African ancestry was evaluated from similarities with the Later Pleistocene African remains earlier than WLH 50, attributed to early modern humans. Without measuring the plaster part of the reconstruction, Omo 1 is too incomplete for these comparisons, and while Herto BOU-VP-16/1 is largely complete, not enough measurements are published to calculate STET with accuracy (Lee 2011). Inclusion of this key cranium awaits a more detailed publication, or availability of an accurate cast. The remainder of the African sample is reported in Table 18.

Ngandong ancestry was evaluated by first calculating STET from paired comparisons of crania within the Ngandong sample (see Table 16) for a sense of STET variation

TABLE 16. STET VALUES WITHIN THE NGANDONG SAMPLE.

The number of measurement pairs in these comparisons ranged between 48 and 56, numbers limited by the variables that could also be observed for WLH 50.

	Ng 1	Ng 5	Ng 6	Ng 9	Ng 10
Ng 5	2.28				
Ng 6	2.30	2.66			
Ng 9	2.47	1.74	2.34		
Ng 10	2.39	1.77	1.99	1.37	
Ng 11	2.68	2.06	1.81	1.97	1.94

TABLE 17. STET VALUES WITHIN SAMPLES AND COMPARING SAMPLES.

The Ngandong comparison (from Table 16) is constrained to use only the measurements known for WLH 50, the others are not. CMNH is the Cleveland Museum of Natural History.

	Mean	Maximum	Minimum
WITHIN			
H. sapiens (CMNH sample)	1.50	4.11	0.59
Pan	1.68	3.10	0.82
Ngandong	2.12	2.68	1.37
Skhul and Qafzeh	2.34	4.30	1.13
Sterkfontein	2.45	3.25	1.34
Swartkrans	2.46	3.89	1.77
BETWEEN			
African-Ngandong	2.92	4.41	2.12
Pan-Homo	5.98	8.03	3.86

TABLE 18. STET VALUES FOR FOSSIL AUSTRALIAN AND FOSSIL AFRICAN COMPARISONS WITH NGANDONG.

Red indicates the specimen STET value is larger than the WLH 50 STET.

If WLH 50 and the older African sample were on a lineage that was divergent from the lineage including Ngandong, we would expect WLH 50 to be the most different from Ngandong because the genetic distance from Ngandong to WLH 50 would be the genetic distance from WLH 50 to the last common ancestor plus the genetic distance from that last common ancestor to Ngandong. However, WLH 50 is not the most different from Ngandong.

	Ng 1	Ng 5	Ng 6	Ng 9	Ng 10	Ng 11
WLH 50	3.20	2.51	4.00	2.79	2.93	3.25
Omo 2	2.97	2.17	3.40	2.56	2.72	2.49
LH 18	2.87	2.54	4.41	3.42	3.22	4.03
Jebel Irhoud 1	2.49	2.27	2.76	2.13	2.41	2.78
Jebel Irhoud 2	2.70	3.08	3.47	2.72	3.01	3.42

TABLE 19. STET VALUES FOR AFRICAN FOSSILS PAIRED WITH WLH 50.

	WLH 50	Omo 2	LH 18	Jebel Irhoud 1
Omo 2	1.86			
LH 18	2.65	3.08		
Jebel Irhoud 1	2.89	2.66	2.59	
Jebel Irhoud 2	3.47	3.45	3.56	2.04

within the sample. The measurements used in this and all other STET comparisons are constrained by the measurements that can be taken on WLH 50, except when indicated, so that the data are comparable. The comparisons ranged between 47 and 56 homologous linear measurements from the original Ngandong specimens. The specific measurements from the WLH 50 measurement set used in each pairing, of course, depend on the preservation of the two specimens being compared, but the comparisons mostly overlapped.

STET values within the Ngandong sample (see Table 16) ranged from 1.37 to 2.68, with a mean of 2.12 (see Table 17). This is a bit larger than the *Pan* (1.68) and *Homo* (1.50) within-sample means (each of these represented by 53 measurement pairs), but well within their individual ranges. Earlier (Wolpoff and Lee 2001), we reported on STET values within the Skhul and Qafzeh sample (n=6, 11 paired comparisons with sufficient sample size), and a similar number of comparisons for Swartkrans and for Sterkfontein (Wolpoff and Lee 2006). These are also shown in Table 17 and are similar to Ngandong. In marked contrast, the mixed *Pan-Homo* STET average was much larger—5.98 (range of individual paired values: 3.86–8.03).

One might expect the STET values comparing every individual within the Africans sample with every individual within the Ngandong sample to be unusually high, if these represented the end-points for different, diverging lineages, according to some researchers separated for as long as 600,000 years. As it turns out, these STET values are not as high as the STET values of the mixed *Pan-Homo* sample, although they do exceed the values for any individual sample (see Table 17). We take these comparisons to indicate that the STET values for the groupings used here and in other analyses are not unexpectedly great.

How Similar is WLH 50 to Ngandong and to the African Sample?

STET analysis provides a way of comparing WLH 50 to the crania from Ngandong (see Table 18) and to the earlier Africans (Ngaloba (LH 18), Omo 2, and the two Jebel Irhoud crania [see Table 18; Table 19]). Figure 21 combines the information in these tables. The critical information is not in the individual comparisons with WLH 50, but in their pattern of variation. The resulting pattern of STET values ad-

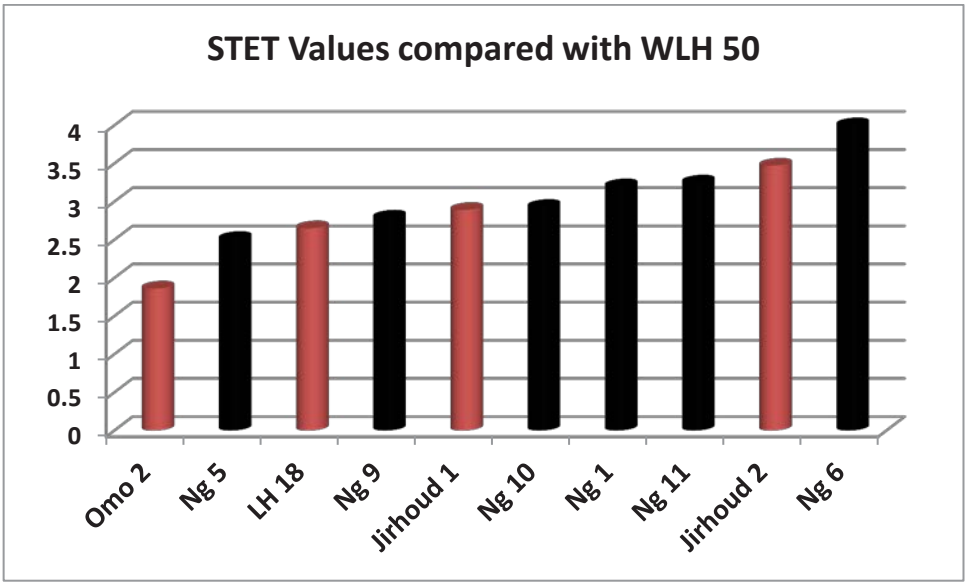

Figure 21. Combining the information in Tables 18 and 19, STET values are shown for WLH 50 individually paired with African (red) and Indonesian (black) specimens. The resulting pattern of STET values addresses hypotheses of ancestry of WLH 50. A Sample Runs Test comparing African and Ngandong values does not reject randomness to this order at ≤0.05; neither sample is a unique ancestor.

dresses whether a unique African ancestry (red bars) or a unique Ngandong (black bars) ancestry for WLH 50 can be refuted. A unique African ancestry would be suggested if most or all of the small STET values were with the African specimens, a unique Ngandong ancestry would be suggested if most or all of the small STET values were with the Ngandong specimens. Neither is the case. Taking all the comparisons into account, there is no pattern to the order of which crania are more similar to WLH 50—Africans or Ngandong. A Sample Runs Test does not reject randomness to this order at $p \leq 0.05$. This provides a good case for rejecting both hypotheses; the implication is that WLH 50 has a mixed ancestry.

SUMMARY OF RESULTS FROM THE STATISTICAL APPROACHES

In Some Tests Reported Above, WLH 50 is Most Like the Ngandong Sample

The discriminant function (see Figure 18) determined from the metric data preserved in WLH 50 that best differentiates earlier crania from Africa, the Levantine, and Ngandong, correctly assigned all specimens into their group. The function used five of the original 21 variables. It sorts WLH 50 with the Ngandong group to the exclusion of either the African or Levantine group. For the first discriminant function, accounting for 99.1% of the among-group variance, the squared Mahalanobis distance from WLH 50 to the Ngandong centroid is 18.15, while that to the next closest group centroid, Africans, is 74.48.

In the pairwise difference analysis (see Figure 19) using non-metric data from the crania, six of the seven Ngandong crania have fewer differences from WLH 50 than any other specimens, and the seventh Ngandong cranium is only separated from the others by one specimen (Skhul 9). On average, WLH 50 possesses fewer differences from the Ngandong group (3.7 mean pairwise differences) than from either the African group (9.3 mean differences) or from the Levantine group (7.3 mean differences) groups. This pattern is significant—WLH 50 is unquestionably less different from the Ngandong crania than from any other group in its non-metric traits. It is unlikely that the pattern of differences is due to chance.

In Other Tests, the Hypothesis of Multiple Ancestry (Africans and Ngandong) for WLH 50 Cannot be Rejected

The Standard Error Test (STET) provides comparison of pairs of specimens using all of the measurements they have in common, without stipulating that each comparison involves exactly the same set of measurements. It estimates the similarities of specimen pairs by measuring the uncertainty in the value of the slope of the regression line calculated for the measurements that are shared in each case. STET comparisons of the Ngandong crania to each other provided values similar to those within living taxa and less than those from other fossil samples such as Skhul and Qafzeh, or the Sterkfontein hominids.

When the African and Ngandong STET comparisons with WLH 50 are illustrated in an ordered pairwise distribution (see Figure 21), a Sample Runs Test does not reject randomness to this order at $p \leq 0.05$, indicating the hypothesis of a mixed ancestry of Africans and Ngandong for WLH 50 cannot be rejected.

GENETIC BASIS FOR MIXED AUSTRALIAN ANCESTRY

Ancient DNA has not been successfully extracted from WLH 50, and current knowledge suggests it is unlikely that it ever will be. But it is possible to discuss the position of WLH 50 in the framework of what is known of the genetic history of Australia, and the regions nearby. Many of the earlier hypotheses about the pattern of migrations to the continent and the sources of the migrants have been confirmed by genetic analysis, including paleogenetics. Analysis of the 100 year old nuclear genome (nDNA) reported for an Australian male, chosen to minimize the chances of European admixture (Rasmussen et al. 2011), concludes that the ancestors of this individual, and possibly of many other Australians, were part of an Asian lineage that separated from the gene pool of all other contemporary non-African populations approximately 70 kyr ago. Other genetic evidence now available demonstrates mixture for this, and other lineages: "it is becoming increasingly difficult to imagine a structure model that can fully explain the complex pattern of archaic ancestry in non-Africans without invoking any restricted admixture events with archaic humans" (Skoglund and Jakobsson 2011: 18305). Explanations of human prehistory assuming the Eve replacement theory can no longer be considered.

> "The recent finding that significant interbreeding occurred between Neanderthals and modern populations refutes the long-standing model that proposes all living humans trace their ancestry exclusively back to a small African population that expanded and completely replaced archaic human species, without any interbreeding" (d'Errico and Stringer 2011: 1060).

This is compatible with the conclusions we have reached here.

The research reported here based on anatomical comparisons independently suggests that mixed ancestry is a well supported interpretation of indigenous Australian anatomical variation, in the same sense that mixed ancestry is a well supported explanation for recent European variation (Wolpoff et al. 2001). The recent genetic history of Europe largely reflects the dispersals of hunter/gatherers into Europe as the ice age came to an end, and later of farmers into Europe from portions of western Asia. The indigenous European hunter/gatherers of the Late Pleistocene had relatively little input into the gene pool of Neolithic Europeans. In southern and southeastern Asia, the recent genetic history similarly reflects mixture with successive Late Pleistocene and Holocene dispersals across Asia. Agriculture did not reach Australia at this time, although domestic dogs

did, minimally by 3,450 bp ± 95 (Milham and Thompson 1976).

Earlier in the Pleistocene history of these regions, Europe is also a good analogy for Australia, in the sense that the Late Pleistocene populations there are a consequence of mixture. In both regions there is a historic confusion of geographic source with evolutionary status. For Australia this has meant confusing an indigenous Indonesian source with "robust" and "archaic" cranial anatomy; in Europe this has meant an indigenous European source with introgression from (what was thought of as) a different (Neandertal) species. The many interbreeding events that are now understood to have taken place across Eurasia during the Late Pleistocene, from Europe to Australia (Wolpoff et al. 2001; Wolpoff and Lee 2012), means adaptive genes were able to disperse widely, under selection, between populations (Hawks 2013). Many, if not most, of these adaptive genes originated in African populations, as the majority of genes in the human gene pool today are of African origins.

In some discussions of Australian prehistory it has seemed important that the earliest dated crania were recognized as gracile (i.e., "modern") and not robust (i.e., "archaic"). This was taken as a disproof of an evolutionary sequence from a robust condition to a more gracile one, similar to other parts of the world, and indeed it would have been a disproof! But in Australia the robust crania were not more "archaic," and they did not evolve into more gracile (="modern") populations. The robust crania differed because they included some ancestors from different places; we have argued here from skeletal evidence that one of these different places was very likely Pleistocene Indonesia. Every known Australian fossil sample of more than one or two individuals has combinations of anatomical features that indicate ancestors from several geographic regions. This reflects a history of mixture of populations from different sources.

One implication is that as Howells (1967: 339) noted early on, the *sequence* of dispersals from different source populations does not matter. The differences between populations entering Australia, *contra* Webb and others, are not of evolutionary grade ("modern" or "archaic" species), but of source area (for instance China or Indonesia[27]). And for this reason, the question of which region the *earliest* migrants were from[28] is not pertinent; this is solely an archaeological and historical issue. The question important in earlier discussions—which migrants were first—is not relevant in the context of evolutionary processes described this way.

MTDNA

Current archaeological reconstructions of the peopling of Australia and nearby lands indicate numerous and complex events (Balme 2013; Bednarik 2003; Bellwood et al. 1995; Davidson 2010; Flood 2006; Hiscock 2008; O'Connell and Allen 2004, 2012; Webb 2006). One driving factor was no doubt the "huge sea-level rises that flooded much of Greater Australia, reducing it to the present day archipelago" (Hill et al. 2007: 40). We believe complexity is also indicated in mtDNA studies. The strongest signals from the post-glacial world "appear to result from the movement and expansion of indigenous, rather than introgressive, mtDNA lineages (*op. cit.*)." Along with the rest of the world, the region also was subject to both earlier and ongoing population dispersals as the world population increased. Paleogenetics is a useful approach for evaluating these reconstructions based on current genetic diversity.

MtDNA (as well as Y haplotype) analysis supports a generally Asian source for Australian and New Guinean populations, but does not indicate that there was a single source population (Jinam et al. 2012; van Holst Pellekaan 2012). One possibility is that there was an early migration to New Guinea, followed by a second migration from Southeast Asia (van Holst Pellekaan and Harding 2006) prior to the compacting, following reductions in habitable land areas as sea level rose at the end of the ice age. Some of the oldest haplotypes are shared in both Australian and New Guinean peoples, while others are specific to each place (Friedlaender et al. 2007), a consequence of the most recent period of isolation during higher sea levels. The problem is that it is hard to distinguish the various models of migration source or sources from mtDNA alone. McEvoy and colleagues used a suite of genome-wide SNPs to argue:

> "The clear phylogenetic grouping of the Aboriginal Australians with other Near Oceania samples, from New Guinea and Melanesia, favors the common origin hypothesis for the original settlement of the Pleistocene Sahul continent. … The most parsimonious explanation is a single settlement of the Sahul, … followed by differentiation into subregional populations. However, **we cannot formally distinguish between this and an initial separation and isolation of the proto-Sahul population in mainland Eurasia followed by multiple ancient migrations to various locations in the Sahul**" (McEvoy et al. 2010: 303), emphasis added.

Across the region there is evidence of a high level of mtDNA lineage diversity (Smith et al. 2007), and much as the reconstructions of Australian habitation have converged on the models of numerous migrations, mtDNA shows the history of the whole region to be far more complex than first thought (Hill et al. 2007; van Holst Pellekaan 2012; Xu et al. 2012). A complex genetic history suggests multiple geographic sources and several migrations.

> "Collectively, these [archaeological and genetic] data suggest that the cultural and genetic history of Australasia is more complex than a single dispersal model such as "Out-of-Africa 2" allows" (Smith et al 2007: 298).

In living Australians, mtDNA variation reflects the pattern of Australian migrations in a broad regional context. Bellwood (1997) suggests Island Southeast Asia (Indonesia, East Malaysia, and the Philippines) was colonized at a time similar to the time of the first Australian migrations, by peoples "related to the indigenous people of Australia

and New Guinea … [in the] mid-Holocene immigration of the ancestors of most of the present-day inhabitants" (Hill et al. 2007: 29). Some of the migrants to the Australasian region came in earlier (10–30 kyr) migrations from the Asian mainland (Jinam et al. 2012).

Reich and colleagues (2010) showed mtDNA also addresses earlier issues in Asian and Australian prehistory. The Denisovan mtDNA identified from the Siberian finds, is markedly different from Neandertal and recent human mtDNA. Within the Denisovan mtDNA, Susanna Sawyer from Pääbo's lab showed that that the mtDNA from one of the teeth indicates greater Denisovan mtDNA variation than is known for either Neandertals or living humans (Pennisi 2013). Even older mtDNA on the Denisovan clade was recovered (Meyer et al. 2014) in specimens from the 430 kyr[29] Spanish site of Sima de los Huesos (SH).

Our comparisons of WLH 50 with some of the earlier inhabitants of Indonesia, described above, suggest that anatomical variation in Australia today reflects a mix of sources, just as the genetic evidence does (this is a conservative interpretation of the mtDNA [Huopenen et al. 2001]). Mixed ancestry is directly reflected in the pattern of nDNA variation.

NDNA

The Denisovan mtDNA clade is a sister group to the mtDNA clades of Neandertals and recent/living humans (Meyer et al. 2014). But, mtDNA alone is not necessarily sufficient to examine hypotheses of relationship above the population level (Ballard and Whitlock 2004; Eyre-Walker 2006). The fact that the Sima de los Huesos mtDNA is on the Denisovan mtDNA clade and not the Neandertal mtDNA clade has seemed inexplicable since the abundant Sima de los Huesos skeletal remains share features with later European Neandertals that are uniquely common in the Neandertal sample (Arsuaga et al. 1997; Martinón-Torres et al. 2012). The Sima de los Huesos hominids are unquestionably one of the ancestors of the later Neandertals. We believe absence of mtDNA continuity, in the face of these anatomical similarities, indicates a pattern of reticulation in the nuclear genome that cannot be reflected in mtDNA. Nuclear and mtDNA give different phylogenies for the same specimens because of their different patterns of evolution; mtDNA evolves with branching and extinction of lineages because the entire mtDNA genome is inherited as a whole, while nDNA both branches and reticulates so that gene flow is a powerful mechanism altering the structure of population relationships. Besides, Denisovan mtDNA, like the Neandertal anatomical form, can no longer be found.

The comparison of nDNA analyzed from the Denisova Cave specimen with Neandertal mtDNA shows that Neandertals and Denisovans together are a sister group to recent and living humans (Prüfer et al. 2014). The implications of nDNA studies to date were summarized by Hawks (2013: 441):

> "The pattern of variation outside Africa appears to reflect interbreeding among populations that were much more separate during the period before 100,000 years ago, including the Neandertals and Denisovans. This historical pattern is not uncommon among mammals (Hawks & Cochran 2006), for which reproductive incompatibility has rarely evolved in a period shorter than one million years (Holliday 2006). … the recurrence of this pattern within and outside Africa and the geographic specificity of Denisovan and Neandertal descendants both show that interbreeding among these ancient people recurred within their habitats. **Neandertals and Denisovans were part of the biological species *Homo sapiens*. Today's people around the world are a relict mixture of populations from an ancient species much more genetically and morphologically diverse than now**" (emphasis ours).

We agree with this appraisal (Wolpoff et al. 1994). Accepting that Neandertals and Denisovans are sister groups within the species *Homo sapiens*, there remains a fundamental difference between them. As far as the fossil record is concerned, we cannot identify who the Denisovans are (Wolpoff 2014). While there are almost certainly Denisovan fossils in the hands of paleoanthropologists today, we cannot recognize them, and it is even possible that there never was a recognizable sample of Denisovans in the sense that there is a recognizable sample of European Neandertals. Reasons for this are discussed below. In our view none of the skeletal remains of the Late Pleistocene (<50 kyr: Prüfer et al. 2014) hominids from the Denisova cave have diagnostic anatomy. Only limited inference is possible from the range of modern human populations containing detectable frequencies of Denisovan nDNA, almost invariably from Island Southeast Asia, Australia, and Oceania (Reich et al. 2011), where the frequencies of Denisovan genomes are between 1% and 6%.

We describe the problem this way. There is no disparity between the phylogenies describing Neandertal mtDNA and their nDNA relationships, as evidenced by the fact that even the toe phalanx from the Denisovan cave with mtDNA close to that of European Neandertals also has a nuclear genome that closely resembles European Neandertals (Prüfer et al. 2014; Skoglund et al. 2014). This is not necessarily because the mtDNA and nDNA relationships are fundamentally different in Neandertals and Denisovans, but because the groups themselves, Neandertals and Denisovans, were quite differently defined historically. For more than 150 years, Neandertals have been identified by their skeletal anatomy as expressed in Western and Central Europe. In more far flung places near the observed edges of the Neandertal range their diagnosis is not always clear, as discussions about specimens from the Levant (Amud, Tabun), North Africa (Jebel Irhoud 1,2) and Central Asia (Teshik Tash) demonstrate. Each of these examples has been diagnosed as Neandertal by some authors, and as somewhat different from Neandertals by others. But this is rarely the case for skeletal remains in Western and Central Europe, where anatomical identification as Neandertal has been unambiguous and for the most part without controversy. Having made these anatomical identifications, the mtDNA subsequently recovered thus far from Euro-

pean and Asian (anatomically identified) Neandertals are branches of a single mtDNA clade.

Denisovans, on the other hand, have not been described anatomically. Their phylogenetic relationships are based on mtDNA alone, portrayed by the position of a hand phalanx and two molars from the Denisovan Cave in Siberia on an mtDNA tree (Krause et al. 2010). But the subsequent high-coverage nDNA sequence (Meyer et al 2012) shows more complex phylogenetic relationships. And the relationship of specimens with Denisovan mtDNA to Neandertals on the tree of mtDNA relationships (Meyer et al. 2014) differs from the relationship that anatomy suggests when Sima de los Huesos is also considered. As noted above, anatomy indicates that Sima de los Huesos is one of the ancestors of European Neandertals, but not necessarily of all living humans (Arsuaga et al. 1997; Martinón-Torres et al. 2012). We do not know whether fossil specimens with Denisovan mtDNA are anatomically similar to each other, in the sense that European Neandertals are (Wolpoff 2014).

WHO THE DENISOVANS MIGHT HAVE BEEN

We propose that the problem of identifying Denisovan anatomy can be indirectly addressed. The modern frequencies of Denisovan nDNA are highest in Australia (Cooper and Stringer 2013). For a good portion of Australian prehistory the continent appears to have only been sparsely inhabited[30], and significant expansions to late Holocene population levels began less than 10,000 years ago (Williams 2013). The key importance of low Pleistocene population sizes for most of Australian prehistory is in the potential effects of even a low magnitude of gene flow on the current nDNA variation[31]. The significant population size expansions in the late Australian Holocene are similar to population histories in most regions of the world (Cochran and Harpending 2009; Hawks et al. 2007; Wolpoff and Caspari 2013). This is one of the reasons we expect that however low the magnitude of Australian gene flow from the rest of the world may have been, many of the genes that entered Australia were adaptive genes that dispersed quickly under selection through Australian populations[32].

From past Siberia to present Australia, we can infer that Denisovan haplotypes were quite wide-ranging in the Late Pleistocene.

> "Denisovan genetic material [is] present in eastern Southeast Asians and Oceanians (Mamanwa, Australians, and New Guineans). … Our evidence of a Southeast Asian location for the Denisovan admixture thus suggests that *Denisovans were spread across a wider ecological and geographic region—from the deciduous forests of Siberia to the tropics—than any other hominin with the exception of modern humans*." (Reich et al. 2011: 23; our italics)

During the earlier period of low population levels, in one of the earlier dispersals of the Late Pleistocene, some of the ancient nuclear haplotypes known across Asia must have reached the Australian continent in sufficient numbers to remain today despite later dispersals (Reyes-Centeno et al. 2014). We posit that haplotypes remaining in Australia from this time include Denisovans, now at 6%. But there are also Neandertal haplotypes found across East Asia.

Frequencies of Neandertal genes across Asia do not differ much from those across Europe. East Asians must surely be the source of the Neandertal haplotypes in Australia. In mainland East Asia there are also adaptive introgressions from Denisovans (Huerta-Sánchez et al. 2014), although overall, there is only a ~0.2% Denisovan contribution to populations from both mainland Asia and the Americas (Prüfer et al. 2014). Even at the ~40 kyr Tianyuan site near Zhoukoudian in China (Shang et al. 2007), nDNA from the skeletal material lacks discernible Denisovan DNA (Fu et al. 2013). The Denisovan contribution to nDNA of populations from New Guinea and Australia is some 25 times greater than the above-mentioned contributions to mainland Asia and the Americas (Prüfer et al. 2014). Meyer and colleagues (2012) demonstrated that the highest frequencies of Denisovan nDNA in living populations are found in indigenous Australians (~6%) and similar or slightly less in New Guineans. More broadly, current populations with significant amounts of Denisovan nDNA are only found east of Wallace's Line (Cooper and Stringer 2013). Sequencing of the nDNA for a 100-year-old indigenous Australian (Rasmussen et al. 2011) revealed a mix of Denisovan and Neandertal haplotypes in his ancestry. Admixture with Neandertals was at about the same proportions as Neandertal admixture found in Asian sequences, but there was much more Denisovan admixture in this Australian than in continental Asians.

Cooper and Stringer (2013: 322) write: "The apparent absence of Denisovan introgression in current mainland populations is most easily explained through overwriting by the DNA of incoming East Asian populations in areas other than Island Southeast Asia". Our expectation is the presence of Denisovan introgression in indigenous Australians and New Guineans represent descent from an earlier Australian population with significant Denisovan presence. Rasmussen and colleagues conclude: "Our findings support the hypothesis that present-day Aboriginal Australians descend from the earliest humans to occupy Australia[33], likely representing one of the oldest continuous populations outside Africa" (Rasmussen et al. 2011: 94). Australians today descend from both these earlier Australians, and from a number of other Asian populations that later entered the region, as described above.

We cannot be sure who the earlier people carrying Denisovan haplotypes to Australia were. As noted above, there are no diagnostic skeletal remains from the Denisova cave to help with this, and only limited inference is possible from the Denisovan range. But if we begin with the assessment that the immediate ancestry of Australians is from populations inhabiting regions closest to Australia, one of the key conclusions of this research, and are mindful that the Denisovan haplotypes are unlikely to be from East Asians or Southeast Asian populations as they are constituted today, the other potential nearby source of Denisovan haplotypes would be from the Ngandong folk. *We have*

no Ngandong DNA, but in view of the anatomical comparisons we have presented, and the geography of the region, ***where else could the significant Denisovan contribution have come from?***

SUMMARY AND CONCLUSIONS

The appearance and evolution of modern human populations in Late Pleistocene Australia was part of one of the last chapters in the long history of human evolution. In this study we have focused on one key specimen, WLH 50, and concluded that the Ngandong folk, or a population similar to them, were *one of the ancestors* of WLH 50, and thereby of later Australians. We do not suggest these phylogenetic relationships as a hypothesis; it cannot be tested, at least with current technology. We propose it as an explanation that is compatible with the existing anatomical evidence and observations, and optimistically hope that testing will be possible some day. If significant Denisovan ancestry for the Ngandong folk is a reasonable interpretation, the implications are far-reaching.

> "Until the Denisova genome was found, many paleoanthropologists assumed that South and East Asian populations of the early Late Pleistocene were relict populations of *Homo erectus*, representing a relatively static population history from the initial human habitation of Asia. The Denisova genome appears inconsistent with that static model" (Hawks 2013: 441).

TAXONOMIC ASSESSMENT

The taxonomic assessment for WLH 50 is straightforward to evaluate, and universally accepted—WLH 50 is an example of Late Pleistocene *Homo sapiens*. The comparisons discussed here confirm this diagnosis, although they raise issues of taxonomy for our comparative sample from Ngandong. From their study of Indonesian hominid evolution leading to the Ngandong sample, Kaifu and colleagues (2008: 776) characterize the concluding portion of this evolution as follows: "Javanese *H. erectus* [including Ngandong] evolved along a somewhat different path from the lineage that led to *H. sapiens*." Others who have studied the Indonesian remains also regard Ngandong as *H. erectus*, a late surviving lineage of Indonesian hominids (Antón 2003, Antón et al. 2007; Huffman et al. 2010; Indriati et al. 2011; Rightmire, 1990).

We do not believe there is anything wrong with the logic of this position, as far as it goes. But none of these research papers included comparisons of Ngandong with human remains from Pleistocene Australia. We contend that if they had it done so, a different interpretation of the place of Ngandong in human evolution is possible. The similarities that WLH 50 and certain other Australian fossils have with Ngandong include aspects of the Ngandong remains that Kaifu and colleagues consider unusual or unique in the region. This supports the contention that Australians have some of their ancestry from these Indonesians, or a population similar to them. At the very least, these resemblances create a phylogenetically ambiguous situation. Unless one is willing to consider the possibility that all of these samples of early-to-late Pleistocene *Homo* are in the species *H. sapiens*, the description that the Ngandong remains are both *H. erectus* (from the demonstration of similarities to Sangiran) and *H. sapiens* (from the demonstration that Ngandong is one of the ancestors of WLH 50 and other Australians) defines a lineage that is difficult to name, because no evidence places fossil Australians in *H. erectus*.

Instead, every modern scientist who is familiar with the Australian fossil record agrees that by virtue of *all of* their anatomy, and the time, place, and cultural associations where they are found, every Australian fossil now known is unquestionably *H. sapiens*. If similarities indicate that Ngandong, or a population like it, is among the ancestors of Australians, including WLH 50 and other Australian fossil remains, **the evolutionary pathway that Kaifu and colleagues, Antón, and others describe in Australasia cannot be portrayed as "a somewhat different path from the lineage that led to *H. sapiens*" because this path *did demonstrably lead to H. sapiens*.**

This is a phylogenetic interpretation that is based on evidence of reticulation. It creates a taxonomic problem that disappears if *H. erectus* and *H. sapiens* are recognized as two successive species on a lineage without cladogenesis—in this case Ngandong would both be legitimately and necessarily classified as *H. sapiens* (Wolpoff et al. 1994).

THE ROLE OF WLH 50 IN UNDERSTANDING HUMAN EVOLUTION

WLH 50 is the ~26,000 kyr (16.5–37.4 kyr) year old calotte of a 1540cc young-to-middle-aged modern human male found in dune deposits near one of the Willandra lakes in New South Wales, Australia. It is not deformed, or otherwise altered by pathology, and most of its characteristics can be individually found in other Late Pleistocene/Holocene Australians. This large vault is key to the understanding of how Australia informs the worldwide pattern of Pleistocene human evolution. It is the focus of this work because of its long-recognized similarities to the crania from Ngandong, the sample older in time and closer in space than any other outside of Australia.

We have striven to provide a description and comparative analysis of WLH 50 addressing both issues of its normality and similarity to other Australian fossil remains, and the specific question of whether anatomical comparisons demonstrate a disproof of the hypothesis that Ngandong, or a sample like it, is one of its ancestors. Our evaluation shows that WLH 50 demonstrates reticulation, in that the preponderance of comparisons show significant similarities between WLH 50 and one or more of the Ngandong crania, some unique to this comparison. No other cranium or group of crania from outside of Australia or Indonesia has nearly as many similarities to WLH 50.

But WLH 50 is not actually a member of a Ngandong-like population. No Ngandong specimen is exactly like WLH 50, the size difference alone assures this. All crania have idiosyncrasies, but the ways in which WLH 50 is *not* similar to the Ngandong sample, for the most part, are

in characteristics for which it resembles recent and living populations, including Australians. Some but certainly not all of these are related to its large cranial capacity. We **conclude** from our comparisons and statistical analyses that there are anatomical details sufficient in form and number to strongly suggest that a Ngandong-like population is one of its ancestors; in other words, the hypothesis of Ngandong ancestry for WLH 50 cannot be disproved. We **imply** from our comparisons and statistical analyses that because the pattern of cranial evolution in Australia resembles that in other parts of the world at the same time, there was sufficient continuing gene flow from the rest of the world to allow adaptive genes to reach the Australian continent, where they dispersed.

As for the particular pathways of descent in Australia, the discussions of the anatomical features of WLH 50 and their comparisons with the Ngandong remains reveals both a number of specific resemblances to one or more of the Ngandong crania, and other comparisons that indicate how WLH 50 differs from all of the Ngandong remains. These were reviewed in a statistical manner, in the section on STATISTICAL APPROACHES. The comparative samples were both from Ngandong, and from earlier Africans and, in some comparisons, cranial remains from the Levant. In some tests WLH 50 is most like the Ngandong sample, while in others a hypothesis of multiple ancestral sources for WLH 50 could not be rejected. In no case was the African or Levant sample most similar to WLH 50, and no other Asian population fills this role. While Africa is the ultimate source for all human lineages and their populations, the fact that no Pleistocene African or West Asian sample is demonstrated to be a unique ancestor of WLH 50 addresses the long-disputed hypotheses of Australian origins—at least in this case we can say with the degree of certainty that these small samples allow, Australian ancestry is from multiple regions, and is neither directly nor uniquely African.

Are these conclusions surprising? Our work suggests that some Pleistocene Australian remains show evidence of a mixture of ancestors, which has long been suspected. Anatomical and genetic comparisons show that the immediate ancestors of Australians are from populations geographically closest to Australia, the Indonesians from Ngandong, and nearby populations of East Asia. Ngandong is only one thread of many ancestors that can be inferred, but it is an interesting one because it might also account for the relatively high percentage of Denisovan genes found in Australia, compared with other regions around the periphery of Asia (Cooper and Stringer 2013). The people who migrated to Australia were mixed, and their ancestry was mixed. There are, after all, Neandertal genes in Australia, even though no Neandertal ever lived there and the same is most likely true of Denisovans. The anatomical comparisons, the main part of this work, suggest that in spite of these ancient mixtures, the populations having the greatest influence on Australian anatomical variation were the closest—Pleistocene Indonesians, and Pleistocene populations from East Asia.

In the broader context, the pattern of complex ancestry and the direction of evolution for WLH 50 are compatible with the hypothesis of multiregional evolution (Caspari and Wolpoff 2013; Thorne and Wolpoff 2003; Wolpoff and Caspari 1997). For the most part, the present work has not been about this wider issue, but focuses on the comparative anatomy of WLH 50, and the specifics of its place in Australian and Australasian prehistory. But the context for the significance of WLH 50 is in the broader discussions of human evolution that acknowledge the key importance of gene flow and mixture.

The Australasian situation is not fundamentally different from that of Late Pleistocene Europe or of other peripheries. After the initial Early Pleistocene dispersals, evidence from the peripheries demonstrates the consequences of continued, significant, and numerous cases of mixture, as populations entering peripheral regions encountered populations evincing local ancestry (Thorne and Wolpoff 1981; Wolpoff et al. 2001). This is a pattern found all across the human range during the Pleistocene. Evidence of introgressions with older populations is found in both perhipheral and more central groups indicating that all human populations carry evidence of mixture with other human lineages (perhaps in some cases subspecies, Wolpoff 2009), some ancient and some contemporary to them. There have been many pathways leading to modern humanity, because all human populations share modernity through their interconnections (Caspari and Wolpoff 2013).

ACKNOWLEDGEMENTS

MHW acknowledges his debt to the late Alan Thorne for allowing research on WLH 50 and the Kow Swamp specimens in his laboratory at the Australian National University (Canberra), and also to both the late G.H.R. von Koenigswald at the Natur-Museum and Forschungs-Institut Senckenberg (Frankfurt) and the late T. Jakob at the Universitas Gadjah Mada (Jogjakarta) for permission to study the Ngandong crania. Peter Brown was instrumental in arranging permission for a brief study of the Coobool Creek crania, immediately before their repatriation. MHW thanks the National Science Foundation and the National Academy of Sciences for generous support that allowed significant data collection in Indonesia and Australia, including BNS 76-82729, and grants from the Australian National University Research School of Pacific Studies (Canberra) and the University of New England (Armidale). We thank Rachel Caspari for her insightful discussions on the anatomy preserved on the WLH 50 cranial rear and base, and Colin Pardoe for information and helpful insights. We are deeply indebted to our editor Karen Rosenberg, and to the four reviewers for their comments and suggestions.

ENDNOTES

1. In this paper we use Weidenreich's cranial numbers for the Ngandong crania, in Arabic form.
2. Curnoe (2011: 3) writes that Birdsell (1967b) cited a personal communication from Weidenreich that shows he "changed his mind late in life and also thought Australians had a dual ancestry." But Birdsell was incorrect. This was not a change of mind; as we show in the citation quotes (Weidenreich 1943: 248–250), Weidenreich had clearly

published his assessment of a dual ancestry for Australians earlier, as he developed his model of how human evolution worked.

3. Modern authors such as Westaway and Groves (2009) who continue to describe Weidenreich's position as "linear evolution in the region" (p. 91) are inaccurate, in that they ignore Weidenreich's own writings on the issue as cited above, as well as the publications of others who detailed the fallaciousness of this assertion (e.g., Caspari and Wolpoff 1996; Wolpoff and Caspari 1997).
4. The addition of more than 22 specimens from Kow Swamp, the Willandra Lake sample of more than 133 specimens, and Coobool Creek (n=126), to the handful of specimens known to Weidenreich dramatically increased the Australian fossil record, and more have followed these discoveries. Many of the cataloged specimens are small fragments or individual teeth, but a good number are mostly or partially complete crania and thus amenable to comparative analysis.
5. Although Webb (2006) posits the opposite order of colonization.
6. We believe that "robustness" is an overused and imprecise description in paleoanthropology. Over the years it has come to mean "strong," "large," "rugged," "well-developed," "powerful mastication" as in robust australopithecines, "thick" as in robust mandibular corpus that is broad relative to its height, "with strong ridges and tori," or in this case, "similar to Late Pleistocene Indonesians."
7. Possible exceptions are Kow Swamp 8 and WLH 3.
8. We do not choose to describe this as hybridizing; the populations involved are not as distinct as Neandertals were from penecontemporary Africans, a case of mixture that has been described as hybridization (Wolpoff 2009).
9. According to Kennedy (1991: 390): "the ectocranial keels may be characterized as discrete linear areas of thickened bone, not associated with muscle attachments, situated along suture lines and radiating from bregma". Balzeau (2013) notes "keels or the bregmatic eminence defined by external vault surface observations **do not always correspond** to a real vault thickening" (emphasis added). Sagittal keels are not all the same; in *Homo erectus*, for instance, the Chinese specimens tend to have transversely narrower and vertically taller keels (Wu 1998) compared to the Indonesians. By these definitions and descriptions, the WLH 50 sagittal keel is especially similar to specimens from Ngandong, and the structures observed are homologous.
10. Huffman and colleagues (2010) establish that the Solo River deposited most or all of the Ngandong crania in the basal bone bed of the Ngandong formation. The evidence they cite suggests a single depository event, and that most or all of the individuals died not long before it and were not transported far. Indriati and colleagues (2011) report an $^{40}Ar/^{39}Ar$ age estimate of 546±12 kyr from water-borne particles of pumice from the bone bed the hominids were associated with, and of 143 kyr +20/-17 kyr from ESR/U-series analysis of fauna from the bed.
11. Our approach has been to take every measurement and observation that is possible with reasonable accuracy and replicability on WLH 50, and compare these with the homologous measurements and observations on Ngandong.
12. We follow Weidenreich's (1951) terminology throughout.
13. This has not prevented some authors from continuing to maintain that cranial deformation in the Australian fossil record prevents researchers from validly testing hypotheses of relationship; for instance Lieberman (2011), who incorrectly asserts "several studies have shown that these more recent fossils look superficially archaic because of artificial cranial deformation" (p. 560). In fact, the studies Lieberman cited are those also cited in this text that demonstrate while some Australian fossil crania show evidence of artificial cranial deformation, others do not. Among those crania that *lack evidence of artificial deformation* are specimens that are key to the ancestry discussions, including KS 1 and WLH 50.
14. Glabella, the most anterior point on the cranial vault in approximate Frankfurt Horizontal, is on the superior border of the supraorbital torus, and it is the superior border that extends most medially on both sides of the preserved anterior of WLH 50. Our identification of the glabella position between the preserved halves of the structure is accurate; the cranial length determined from it (see Table 2) is the same as the cranial length reported by Curnoe and Thorne (2006a: Table 1), and only one mm greater than the length reported by Stringer (1998).
15. Herto BOU-VP-16/1 (see Table 6) is thicker than Amud 1, but it does not come close to the WLH 50 thicknesses except for the thickness at opisthocranion, which is 18mm in the Herto cranium and greater than 18mm by an unknown amount in WLH 50.
16. Here and in other comparative discussions, it is best for the reader to access the relevant figure or figures to better understand details as they are described. This makes best use of the comparative figures.
17. Curnoe (2009, 2011) attributes the great robustness of WLH 50 to a combination of its large neurocranial size and its narrow cranial base, admitting that other factors such as its sex and age contributed to a lesser degree as well. But there is a problem. Narrowing in these cases is described by the ratio (index) of biauricular breadth to cranial length (2009: Table 2). The 65.1 index Curnoe gives for WLH 50 is unlike his "*H. erectus*" mean of 72.6 and similar to his "early anatomically modern *H. sapiens*" mean of 65.7, allowing the WLH 50 vault to be described as relatively narrow. However, a number of archaic specimens with smaller neurocrania have similar relative cranial base narrowing with robust superstructures, indicating that the *combination* of size and cranial base narrowing is not causal. These individuals and their ratios are: Kabwe (64.4), Ng 5 (67.0), and Dali (67.2). OH 9 (67.3) is an equally narrow "*H. erectus*" specimen, the relatively narrowest in the sample.
18. Marsh (2013) demonstrated that cranial thickness measurements are sensitive to position. In comparing crania, homologous points must be accurately determined. Otherwise, comparisons may incorporate variation from inaccurate positioning that does not reflect specimen differences or similarities. Her solution was to superimpose grids over crania scaled to cranial length, to determine homologous points. That is not possible in these comparisons, and thickness evaluations at defined osteometric points such as lambda or bregma provide us with the basis for the greatest accuracy in comparisons.
19. Weidenreich writes (1951: 225): "the *fossa supraglabellaris* is absent in the Ngandong skulls; the *torus supraorbitalis* passes away imperceptibly in the frontal bone with a fluent, barely curved line." This also describes WLH 50. We believe it a matter of emphasis and taste whether the *fossa supraglabellaris* is described as absent or as weakly developed in these specimens.
20. Not to be confused with supraorbital thickness at the most lateral position (as in measurement 34 of Table 2, Kaifu et al. 2008), this position is not preserved on either side of the WLH 50 torus.
21. In this comparison and the comparisons following that express the difference from Ngandong in units of the standard deviation, the σ value used is the standard deviation of the Ngandong crania for the relevant measurement.
22. Only the Ng 11 cranial rear resembles this condition, and the downward dip at the midline is not as pronounced, nor was it obviously caused by an enlarged suprainiac fossa.
23. Key elements of the WLH 50 cranial base medial to the mastoid process were not preserved, but some of the nuchal plane does remain, as we describe. There is much variation in this area of the skull and we can never be certain about the missing portions of WLH 50. But the anatomy that best fits the lines and crests that remain WLH 50 is that of Ng 11, and we believe the best-supported hypothesis is that Ng 11 reflects the missing portions of WLH 50. None of the preserved anatomy disproves it.
24. There are no Ngandong zygomatic bones for comparison. Sangiran 17 has the largest of the earlier zygomatic bones from the region.
25. Westaway and Groves (2009) confuse this issue in their discussion of whether Ngandong traits can be validly identified in fossil and recent Australian samples. They argue that the claim of multiple ancestors for Australians that includes Ngandong Indonesians is impossible because it would necessitate the hybridization of two different species. This is an example of assuming their conclusions, since a different interpretation would be that successful interbreeding between populations from different geographic sources would be a demonstration that the populations were *in the same species.* In fact, what demonstration could be more convincing than successful interbreeding?
26. In Figure 20 we compared humans to *Pan*, the living primate sister species. One of us (Lee 2011) recorded 53 homologous observations for *Homo* (n=113) and *Pan* (n=44) crania at the Cleveland Museum of Natural History, and STET was calculated for all inter-species and

intra-species combinations. The intraspecific STET distributions for *Homo* and *Pan* are virtually identical, while the interspecific *Homo-Pan* STET distribution is almost completely outside the ranges of these two (see Table 17). For these closely related living taxa, STET describes the variability and unambiguously separates intra- and inter-species variation. Within sites such as Ngandong, Skhul-Qafzeh, Sterkfontein, and Swartkrans, STET values are lower than in the *Homo-Pan* comparisons (see Table 17).

27. But not limited to China or Indonesia. For instance, analyzing genome-wide SNP data, Pugach and colleagues (2013) report evidence of an ancient association between populations of Australia, New Guinea, and a Negrito group from the Philippines, as well as recent (4230 years BP) gene flow to Australia from India.
28. In the sense that the *order* of ancestry does not provide a test for the *pattern* of ancestry.
29. The date for the Sima de los Huesos hominids is most recently reported at approximately 430 kyr (Arsuaga et al. 2014). For the purposes of this discussion it is not important where the correct date lies, only that it is older than European Neandertals. Ultimately, however, this will be an important date assessment because it marks the first known appearance of mtDNA that shares a common ancestor with Denisovan rather than Neanderthal mtDNAs.
30. This is a quite different assessment than prior suggestions (Birdsell 1957 and others following) that there was an early ecological saturation of the continent with population numbers for most of Australian prehistory at or close to the levels present when Europeans first began to colonize.
31. For instance, we may speculate about the possibility of a magnitude of immigrants that are visible genetically but may have been too small to leave archaeological traces (e.g., Mulvaney and Kamminga 1999).
32. As we have noted, even neutral models indicate there was significant gene flow throughout the continent (Habgood and Franklin 2008), and worldwide Pleistocene gene flow is indicated by the fact that nDNA and mtDNA phylogenies differ.
33. We take this to mean that one of the ancestral lines leading to present-day indigenous Australians extended from the earliest humans to occupy the continent.

REFERENCES

Abbie, A.A. 1968. The homogeneity of Australian Aborigines. *Archeology and Physical Anthropology in Oceania* 3: 221–231.

Adcock, G.J., E.S Dennis, S. Easteal, G.A. Huttley, L. Jermiin, W.J. Peacock, and A. Thorne. 2001. Mitochondrial DNA sequences in ancient Australians: implications for modern human origins. *Proceedings of the National Academy of Sciences, USA* 98: 537–542.

Ahern, J.C.M., J.D. Hawks, and S-H. Lee. 2005. Neandertal taxonomy reconsidered...again: a response to Harvati. *Journal of Human Evolution* 48(6): 647–652.

Aiello, L.C., M. Collard, J.F. Thackeray, and B.A. Wood. 2000. Assessing exact randomization-based methods for determining the taxonomic significance of variability in the human fossil record. *South African Journal of Science* 96: 179-183.

Allen, J. and J.F. O'Connell. 2008. Getting from Sunda to Sahul. In (G. Clark, F. Leach, and S. O'Connor, eds.): *Islands of Inquiry: Colonization, Seafaring and the Archaeology of Maritime Landscapes*, pp. 31–46. *Terra Australis* 29. Canberra: Australian National University Press.

Antón, S.C. 2003. Natural history of *Homo erectus*. *Yearbook of Physical Anthropology* 46: 126–170.

Antón, S.C., F. Spoor, C.D. Fellmann, and C.C. Swisher III. 2007. Defining *Homo erectus*: size considered. In (W. Henke and I. Tattersall, eds.) *Handbook of Paleoanthropology*, pp. 1655–1693. New York: Springer.

Antón, S.C. and K.J. Weinstein. 1999. Australian cranial deformation and fossil Australians revisited. *Journal of Human Evolution* 36: 195–209.

Arsuaga, J.L., I. Martínez, L.J. Arnold, A. Aranburu, A. Gracia-Téllez, W.D. Sharp, R.M. Quam, 1C. Falguères, A. Pantoja-Pérez, J. Bischoff, E. Poza-Rey, J.M. Parés, J.M. Carretero, M. Demuro, C. Lorenzo, N. Sala, M. Martinón-Torres, N. García, A. Alcázar de Velasco, G. Cuenca-Bescós, A. Gómez-Olivencia, D. Moreno, A. Pablos, C-C. Shen, L. Rodríguez, A.I. Ortega, R. García, A. Bonmatí, J.M. Bermúdez de Castro, and E. Carbonell. 2014. Neandertal roots: Cranial and chronological evidence from Sima de los Huesos. *Science* 344: 1358–1363.

Arsuaga, J.L., I. Martínez, A. Gracia, and C. Lorenzo. 1997. The Sima de los Huesos crania (Sierra de Atapuerca, Spain). A comparative study. *Journal of Human Evolution* 33: 219–281.

Ballard, W.J.O. and M.C. Whitlock. 2004. The incomplete natural history of mitochondria. *Molecular Ecology* 13: 729–744.

Balme, J. 2013. Of boats and string: The maritime colonization of Australia. *Quaternary International* 285: 68–75.

Balzeau, A. 2006. Are thickened cranial bones and equal participation of the three structural bone layers autapomorphic traits of *Homo erectus*? *Bulletins et Mémoires de la Société d'Anthropologie de Paris* Numéro 18 (3–4): 145–163.

Balzeau, A. 2013. Thickened cranial vault and parasagittal keeling: Correlated traits and autapomorphies of *Homo erectus*? *Journal of Human Evolution* 64: 631–644.

Bednarik, R. 2003. The maritime dispersals of Pleistocene humans. *Cambridge Archaeological Journal* 13(1): 41–66.

Bellwood P. 1997. *Prehistory of the Indo-Malaysian archipelago*. Honolulu: University of Hawaii Press.

Bellwood, P., J.J. Fox, and D.T. Tryon. 1995. *The Austronesians: Historical and Comparative Perspectives*. Canberra: Australian National University Press.

Birdsell J.B. 1957. Some population problems involving Pleistocene man. *Cold Spring Harbor Symposia on Quantitative Biology* 22: 47–69.

Birdsell, J.B. 1967a. Preliminary data on the trihybrid origin of the Australian Aborigines. *Archaeology and Physical Anthropology in Oceania* 2: 100–155.

Birdsell, J.B. 1967b. The recalibration of a paradigm for the first peopling of Greater Australia. In (J. Allen, J. Golson, and R. Jones, eds.) *Sunda and Sahul*, pp. 113–168. London: Academic Press.

Birdsell, J.B. 1977. The recalibration of a paradigm for the peopling of Greater Australia. In (J. Allen, J. Golson, and R. Jones, eds.) *Sunda and Sahul: Prehistoric studies in Southeast Asia, Melanesia and Australia*, pp. 113–167. London: Academic Press.

Bowler, J.M., H. Johnston, J.M. Olley, J.R. Prescott, R.G. Roberts, W. Shawcross, and N.A. Spooner. 2003. New ages for human occupation and climatic change at Lake Mungo, Australia. *Nature* 421: 837–840.

Bräuer, G. 1989. The evolution of modern humans: a comparison of the African and non-African evidence. In (P. Mellars and C. Stringer, eds.) *The Human Revolution: Behavioural and Biological Perspectives on the Origins of Modern Humans*, pp. 123–154. Edinburgh: Edinburgh University Press.

Bräuer, G., M. Collard, and C. Stringer. 2004. On the reliability of recent tests of the Out of Africa hypothesis for modern human origins. *Anatomical Record* 279A: 701–707.

Brown, P. 1981. Artificial cranial deformation: a component in the variation in Pleistocene Australian Aboriginal crania. *Archaeology in Oceania* 16: 156–167.

Brown, P. 1987. Pleistocene homogeneity and Holocene size reduction: the Australian human skeletal evidence. *Archaeology in Oceania* 22: 41–67.

Brown, P. 1989. *Coobool Creek*. Terra Australis 13. Canberra: Department of Prehistory, Research School of Pacific Studies, Australian National University.

Brown, P. 1992. Recent human evolution in East Asia and Australasia. *Philosophical Transactions of the Royal Society B* 337: 235–242.

Brown, P. 2010. Nacurrie 1: mark of ancient Java, or a caring mother's hands, in terminal Pleistocene Australia? *Journal of Human Evolution* 59: 168–187.

Brown, P. 2013. Palaeoanthropology: Of humans, dogs and tiny tools. *Nature* 494: 316–317.

Brown, P. and T. Maeda. 2004. Post-Pleistocene diachronic change in East Asian facial skeletons: the size, shape and volume of the orbits. *Anthropological Science* 112: 29–40.

Buikstra, J.E. and D.H. Ubelaker. 1994. *Standards for Data Collection from Human Skeletal Remains*. Arkansas Archaeological Survey Research Series No.44. Indianapolis: Western Newspaper Company.

Bulbeck, D. 1982. A re-evaluation of possible evolutionary processes in Southeast Asia since the Late Pleistocene. *Bulletin of the Indo-Pacific Prehistory Association* 3: 1–20.

Bulbeck, D. 2001. Robust and gracile Australian Pleistocene crania: the tale of the Willandra Lakes. In (T. Simanjuntak, B. Prasetyo, and R. Handini, eds.) *Sangiran: Man, Culture, and Environment in Pleistocene Times.* Proceedings of the International Colloquium on Sangiran, pp. 60–106. Jakarta: Yayasan Obor Indonesia (The National Research Centre of Archaeology/Ecole Française d'Extrême-Orient).

Burkitt, A.N and J.I. Hunter. 1922. The description of a Neanderthaloid Australian skull, with remarks on the production of the facial characteristics of Australian skulls in general. *Journal of Anatomy* 57: 31–54.

Caddie, D., D. Hunter, P. Pomery, and H. Hall. 1987. The aging chemist - can electron spin resonance (ESR) help? In (W. Ambrose and J. Mummery, eds.) *Archaeometry: Further Australasian Studies*, pp. 156–166. Canberra: Department of Prehistory, Australian National University.

Cameron, D.W. and C.P. Groves. 2004. *Bones, Stones and Molecules*. California and London: Elsevier.

Caspari, R. 2005. The suprainiac fossa: the question of homology. *Anthropologie* (Brno) 43(2–3): 251–261.

Caspari, R. and M.H. Wolpoff. 1996. Weidenreich, Coon, and multiregional evolution. *Human Evolution* 11(3/4): 261–268.

Caspari, R. and M.H. Wolpoff. 2013. The process of modern human origins: the evolutionary and demographic changes giving rise to modern humans. In (F.H Smith and J. Ahern, eds.) *The Origins of Modern Humans: Biology Reconsidered*, pp. 355–390. New York, Wiley.

Clark, J.L., S.D. Dobson, S.C. Antón, J. Hawks, K.L. Hunley, and M.H. Wolpoff. 2007. Identifying artificially deformed crania. *International Journal of Osteoarchaeology* 17(6): 596–607.

Cochran, G. M. and H. Harpending. 2009. *The 10,000 Year Explosion: How Civilization Accelerated Human Evolution*. New York: Basic Books.

Collard, M. and N. Franchino. 2002. Pairwise difference analysis in modern human origins research. *Journal of Human Evolution* 43: 323–352.

Collier, S. 1989. The influence of economic behaviour and environment upon robusticity of the post-cranial skeleton: a comparison of Australian Aborigines and other populations. *Archaeology in Oceania* 24(1): 17–30.

Condemi, S. 1992. *Les Hommes Fossiles de Saccopastore et leurs Relations Phylogénétiques*. Paris: Cahiers de Paléoanthropologie, Centre National de la Recherche Scientifique.

Coon, C.S. 1962. *The Origin of Races*. New York: Knopf.

Cooper, A. and C.B. Stringer. 2013. Did the Denisovans cross Wallace's Line? *Science* 342: 321–323.

Cunningham, D.J. 1907. The head of an Aboriginal Australian. *Journal of the Royal Anthropological Institute of Great Britain and Ireland* 37: 47–57.

Curnoe, D. 2003. Problems with the use of cladistic analysis in palaeoanthropology. *Homo* 53(3): 225–234.

Curnoe, D. 2007. Modern human origins in Australasia: testing the predictions of competing models. *Homo* 58(2): 117–157.

Curnoe, D. 2009. Causes and significance of cranial robusticity among Pleistocene-Early Holocene Australians. *Journal of Archaeological Science* 36: 980–990.

Curnoe, D. 2011. A 150-year conundrum: cranial robusticity and its bearing on the origin of Aboriginal Australians. *International Journal of Evolutionary Biology*: doi: 10.4061/2011/632484.

Curnoe, D. and H. Green. 2013. Vault thickness in two Pleistocene Australian calvarii. *Journal of Archaeological Science* 40(2): 1310–1318.

Curnoe, D. and A. Thorne. 2003. Number of ancestral human species: a molecular perspective. *Homo* 53(3): 201–224.

Curnoe, D. and A. Thorne. 2006a. Human origins in Australia: the skeletal evidence. *Before Farming* 2006/1 article 5: 1–28.

Curnoe, D. and A. Thorne. 2006b. The question of cranial robusticity. *Before Farming* 2006/2 Article 2: 1–13.

Davidson, I. 2010. The colonization of Sunda and Sahul and its adjacent islands and the evolution of modern cognition. *Current Anthropology* 51(S1): S177–S189.

Dennell, R. and M. Porr, eds. 2014. *Southern Asia, Australia and the Search for Human Origins*. New York: Cambridge University Press

d'Errico, F. and C.B. Stringer. 2011. Evolution, revolution or saltation scenario for the emergence of modern cultures. *Philosophical Transactions of the Royal Society B* 366: 1060–1069.

Dubois, E. 1922. The proto-Australian fossil man of Wadjak, Java. *Koninklijke Akademie Wetenschappen te Amsterdam,* Series B, 23: 1013–1051.

Durband A.C. 2008. Artificial cranial deformation in Pleistocene Australia: The Coobool Creek sample. *Journal of Human Evolution* 54: 795–813.

Durband, A.C. 2009. Southeast Asian and Australian paleoanthropology: a review of the last century. *Journal of Archaeological Sciences* 87: 7–31.

Eyre-Walker, A. 2006. Size does not matter for mitochondrial DNA. *Science* 312: 537–538.

Flood, J. 2006. *The Original Australians: Story of the Aboriginal People*. Crows Nest NSW: Allen & Unwin.

Frayer, D.W., J. Jelínek, M. Oliva, and M.H. Wolpoff. 2006. Aurignacian Male Crania, Jaws, and Teeth from the Mladeč Caves, Moravia, Czech Republic. In (M. Teschler-Nicola, ed.) *Early Modern Humans at the Moravian Gate: The Mladeč Caves and their Remains*, pp. 185–272. Wien: Springer.

Freedman, L. and M. Lofgren. 1979. The Cossack Skull and a dihybrid origin of the Australian aborigines. *Nature* 282: 298–300.

Friedlaender, J.S., F.R. Friedlaender, J.A. Hodgson, M. Stolz, G. Koki, G. Horvat, S. Zhadanov, T.G. Schurr, and D.A. Merriwether. 2007. Melanesian mtDNA complexity. *PloS One* 2 (2), e248. doi:10.1371/journal.pone.0000248.

Fu, Q., M. Meyer, X. Gao, U. Stenzel, H.A. Burbano, J. Kelso, and S. Pääbo. 2013. DNA analysis of an early modern human from Tianyuan Cave, China. *Proceedings of the National Academy of Sciences USA* 110: 2223–2227.

Gordon, A.B. and B. Wood. 2013. Evaluating the use of pairwise dissimilarity metrics in paleoanthropology. *Journal of Human Evolution* 65: 465–477.

Grün, R., N. Spooner, J. Magee, A.G. Thorne, J. Simpson, Ge Yan, and G. Mortimer. 2011. Stratigraphy and chronology of the WLH 50 human remains, Willandra Lakes World Heritage Area, Australia. *Journal of Human Evolution* 60: 597–604.

Habgood, P.J. 1986. The origin of the Australians: a multivariate approach. *Archaeology in Oceania* 21: 130–137.

Habgood, P.J. and N.R. Franklin. 2008. The revolution that didn't arrive: A review of Pleistocene Sahul. *Journal of Human Evolution* 55: 187–222.

Hammer, M.F., A.E. Woerner, F.L. Mendez, J.C. Watkins, and J.D. Wall. 2011. Genetic evidence for archaic admixture in Africa. *Proceedings of the National Academy of Sciences USA* 108(37): 15123-15128.

Hawks, J. 2004. How much can cladistics tell us about early hominid relationships? *American Journal of Physical Anthropology* 125: 207–219.

Hawks, J. 2013. Significance of Neandertal and Denisovan genomes in human evolution. *Annual Review of Anthropology* 42: 433–449.

Hawks J. and G. Cochran. 2006. Dynamics of adaptive introgression from archaic to modern humans. *PaleoAnthropology* 2006: 101–115.

Hawks, J., S. Oh, K. Hunley, S. Dobson, G. Cabana, P. Dayalu, and M.H. Wolpoff. 2000. An Australasian test of the recent African origin theory using the WLH 50 calvarium. *Journal of Human Evolution* 39(1): 1–22.

Hawks , J., E.T. Wang , G.M. Cochran, H.C. Harpending, and R.K. Moyzis. 2007. Recent acceleration of human adaptive evolution. *Proceedings of the National Academy of Sciences USA* 104: 20753–20758.

Heim, J-L. 1976. *Les Hommes Fossiles de La Ferrassie*. Tome I. Le Gisement. Les Squelettes Adultes (Crâne et Squelette du Tronc). Paris: *Archives de l'Institut de Paléontologie Humaine, Mémoire 35*.

Hershkovitz, I., B. Latimer, O. Dutour, L.M. Jellema, S. Wish-Baratz, C. Rothschild, and B.M. Rothschild 1997. Why do we fail in aging the skull from the sagittal suture? *American Journal of Physical Anthropology 103*(3): 393–399.

Hill C, P. Soares, M. Mormina, V. Macaulay, D. Clarke, P.B. Blumbach, M. Vizuete-Forster, P. Forster, D. Bulbeck, S. Oppenheimer, and M. Richards. 2007. A mitochondrial stratigraphy for island southeast Asia. *American Journal of Human Genetics* 80: 29–43.

Hiscock, P. 2008. *Archaeology of Ancient Australia*. Oxford: Routledge.

Holliday, T.W. 2006. Neanderthals and modern humans: an example of a mammalian syngameon? In (K. Harvati and T. Harrison, eds.). *Neanderthals revisited: new approaches and perspectives*, pp. 281–298. Dordrecht: Springer.

Holloway, R.L. 1980. Indonesian 'Solo' (Ngandong) endocranial reconstruction: preliminary observations and comparison with Neanderthal and *Homo erectus* groups. *American Journal of Physical Anthropology* 53: 285–295.

Hooton, E.A. 1946. *Up from the Ape*, 2d edition. New York: Macmillan.

Howells, W.W. 1967. *Mankind in the Making*, revised edition. Garden City: Doubleday.

Howells, W.W. 1976. Metrical analysis in the problem of Australian origins. In (R.L. Kirk and A.G. Thorne, eds.) *The Origin of the Australians*, pp. 141–160. Canberra: Australian Institute of Aboriginal Studies.

Howells, W.W. 1977. Sources of human variation in Melanesia and Australia. In (J. Allen, J. Golson and R. Jones, eds.) *Sunda and Sahul: Prehistoric Studies in Southeast Asia, Melanesia, and Australia*, pp. 169–186. New York: Academic Press.

Huerta-Sánchez, E., Xin Jin, Asan, Zhuoma Bianba, B.M. P.N. Vinckenbosch, Yu Liang, Xin Yi, Mingze He, Mehmet Somel, Peixiang Ni, Bo Wang, Xiaohua Ou, Huasang, Jiangbai Luosang, Zha Xi Ping Cuo, Kui Li, Guoyi Gao, Ye Yin, Wei Wang, Xiuqing Zhang, Xun Xu, Huanming Yang, Yingrui Li, Jian Wang, Jun Wang,

and R. Nielsen. 2014. Altitude adaptation in Tibetans caused by introgression of Denisovan-like DNA. *Nature* 512: 194–197.

Huffman, O.F., J. deVos, A.W. Berkhout, and F. Aziz. 2010. Provenience reassessment of the 1931-1933 Ngandong *Homo erectus* (Java), Confirmation of the bone-bed origin reported by the discoverers. *PaleoAnthropology* 2010: 1–60.

Huopenen, K, T.G. Schurr, Y-S. Chen, and D. Wallace. 2001. Mitochondrial DNA variation in an Aboriginal Australian population: evidence for genetic isolation and regional differentiation. *Human Immunology* 62: 954–969.

Huxley, T.H. 1863. *Evidence as to Man's Place in Nature*. London: Williams & Norgate.

Indriati, E., C.C. Swisher, C. Lepre, C., R.L. Quinn, R.A. Suriyanto, A.T. Hascaryo, R. Grün, R., C.S. Feibel, B.L. Pobiner, M. Aubert, W. Lees, and S. Antón. 2011. The age of the 20 meter Solo River Terrace, Java, Indonesia and the survival of *Homo erectus* in Asia. *PLoS One* 6(6): e21562.

Jelínek, J. 1979. *Anthropology of the Rembrranga People: a contribution of the Czechoslovak Anthropos Expedition to Arnhem Land N.T. Australia*. Brno: Anthropos Institute, Moravian Museum.

Jiggins, C.D., R.E. Naisbit, R.L. Coe, and J. Mallet. 2001. Reproductive isolation caused by colour pattern mimicry. *Nature* 411: 302–305.

Jinam, T.A., L-C. Hong, M.E. Phipps, M. Stoneking, M. Ameen, J. Edo, HUGO Pan-Asian SNP Consortium, and N. Saitou. 2012. Evolutionary history of continental Southeast Asians: "Early Train" Hypothesis based on genetic analysis of mitochondrial and autosomal DNA data. *Molecular Biology and Evolution* 29(11): 3513–3527.

Jones, F.W. 1934. Contrasting types of Australian skulls. *Journal of Anatomy London* 68: 323–330.

Kaifu, Y., F. Aziz, E. Indriati, T. Jacob, I Kurniawan, and H. Baba. 2008. Cranial morphology of Javanese *Homo erectus*: new evidence for continuous evolution, specialization, and terminal extinction. *Journal of Human Evolution* 55: 551–580.

Kennedy, G.E. 1991. On the autapomorphic traits of *Homo erectus*. *Journal of Human Evolution* 20: 375–412.

Keith, A. 1936. *History from Caves: A New Theory of the Origin of Modern Races of Mankind*. London: British Speleological Association (publication of the First Speleological Conference).

Kimbel, W.H. and L.B. Martin (eds.). 1993. *Species, Species Concepts, and Primate Evolution*. New York: Plenum.

Kirk, R.L. and A.G. Thorne (eds.). 1976. *The Origin of the Australians*. Canberra: Australian Institute of Aboriginal Studies.

Klaatsch, H. 1908a. The skull of the Australian aboriginal. *Report from the Pathological Laboratory of the Lunacy Department, New South Wales* 1: 43–167.

Klaatsch, H. 1908b. Das Gesichtsskelet der Neandertalrasse und die Australier. Verhandlungen Anatomische Gesellschaft Erg.-H. *Anatomischer Anzeiger* 32: 223–271.

Klecka, W.R. 1980. *Discriminant Analysis*. Newbury Park (CA): Sage Publications, Inc.

Lee, S.H. 2011. How many variables are too few? Effect of sample size in STET, a method to test conspecificity for pairs of unknown species. *PaleoAnthropology* 2011: 260–267.

Lee, S-H. and M.H. Wolpoff. 2005. Habiline variation: a new approach using STET. *Theory in Biosciences* 124(1): 25–40.

Lieberman, D.E. 1995. Testing hypotheses about recent human evolution from skulls. Integrating morphology, function, development, and phylogeny. *Current Anthropology* 36(2): 159–197.

Lieberman, D.E. 2011. *The Evolution of the Human Head*. Cambridge (MA): The Belknap Press of Harvard University Press.

Lieberman, D.E., B.M. McBratney, and G. Krovitz. 2002. The evolution and development of cranial form in *Homo sapiens*. *Proceedings of the National Academy of Sciences*, USA 99(3): 1134–1139.

Lordkipanidze, D., M.S. Ponce de León, A. Margvelashvili, Y. Rak, G.P. Rightmire, A. Vekua, and C.P.E. Zollikofer. 2013. A complete skull from Dmanisi, Georgia, and the evolutionary biology of early *Homo*. *Science* 342: 326–331.

Lovejoy, C.O. 1979. Contemporary methodological approaches to individual primate fossil analysis. In (M.E. Morbeck, H. Preuschoft, and N. Gomberg, eds.) *Environment, Behavior, and Morphology: Dynamic Interactions in Primate,* pp. 229–243. New York: Gustav Fischer.

Macintosh, N.W.G. 1965. The physical aspect of man in Australia. In (R.M. Berndt and C.H. Berndt, eds.) *Aboriginal Man in Australia*: essays in honour of Emeritus Professor A. P. Elkin, pp. 29–70. Sidney: Angus & Robertson.

Macintosh, N.W.G. 1967. Fossil man in Australia. *Australian Journal of Science* 30: 86–98.

Macumber, P.G. 1977. The geology and palaeohydrology of the Kow Swamp fossil hominid site, Victoria, Australia. *Journal of the Geological Society of Australia* 24: 307–320.

Marsh, H.E. 2013. *Beyond thick versus thin: mapping cranial vault thickness patterns in recent Homo sapiens*. Iowa City: Anthropology dissertation, University of Iowa.

Martin, R. 1928. *Lehrbuch der Anthropologie. Volume 2: Kraniologie, Osteologie.* Jena: Gustav Fischer.

Martinón-Torres, M., J.M. Bermudez deCastro, A. Gomez-Robles, L. Prado-Simon, and J-L. Arsuaga. 2012. Morphological description and comparison of the dental remains from Atapuerca-Sima de los Huesos site (Spain). *Journal of Human Evolution* 62: 7–58.

Matsumura, H. 2006. The population history of Southeast Asia viewed from morphometric analyses of human skeletal and dental remains. In (M. Oxenham and N. Tayles, eds.) *Bioarchaeology of Southeast Asia*, pp. 33–58. Cambridge: Cambridge University Press.

Mayr, E. 1963. *Animal Species and Evolution*. Cambridge: Belknap Press of Harvard University Press.

McEvoy, B.P., J.M. Lind, E.T. Wang, R.K. Moyzis, P.M. Visscher, S.M. van Holst Pellekaan, and A.N. Wilton. 2010.

Whole-genome genetic diversity in a sample of Australians with deep Aboriginal ancestry. *American Journal of Human Genetics* 87: 297–305.

Meindl, R.S. and C.O. Lovejoy. 1985. Ectocranial suture closure: a revised method for the determination of skeletal age at death based on the lateral-anterior sutures. *American Journal of Physical Anthropology* 68: 57–66.

Mellars, P., K.C. Gori, M. Carr, P.A. Soares, and M.B. Richards. 2013. Genetic and archaeological perspectives on the initial modern human colonization of southern Asia. *Proceedings of the National Academy of Sciences USA* 110(26): 10699–10704.

Meyer, M., M. Kircher, M-T. Gansauge, Heng Li, F. Racimo, S. Mallick, J. G. Schraiber, F. Jay, K. Prüfer, C. de Filippo, P.H. Sudmant, C. Alkan, Qiaomei Fu, Ron Do, N. Rohland, A. Tandon, M. Siebauer, R.E. Green, K. Bryc, A.W. Briggs, U. Stenzel, J. Dabney, J. Shendure, J. Kitzman, M.F. Hammer, M.V. Shunkov, A.P. Derevianko, N. Patterson, A.M. Andrés, E.E. Eichler, M. Slatkin, D. Reich, J. Kelso, and S. Pääbo. 2012. A high-coverage genome sequence from an archaic Denisovan individual. *Science* 338: 222–226.

Meyer, M., Qiaomei Fu, A. Aximu-Petri, I. Glocke, B. Nickel, J-L. Arsuaga, I. Martínez, A. Gracia, J.M. Bermúdez de Castro, E. Carbonell & S. Pääbo. 2014. A mitochondrial genome sequence of a hominin from Sima de los Huesos. *Nature* 505: 403–406.

Milham, P. and P. Thompson. 1976. Relative antiquity of human occupation and extinct fauna at Madura Cave, southeastern Western Australia. *Mankind* 10: 175–180.

Miller, J.A. 1991. Cranial thickening in WLH 50: pathology or populational variation? (abstract). *American Journal of Physical Anthropology* Supplement 12: 131.

Morant, G.M. 1927. A study of the Australian and Tasmanian skulls based on previously published measurements. *Biometrika* 19(3/4): 417–440.

Mulvaney, J. and J. Kamminga. 1999. *Prehistory of Australia*. Washington: Smithsonian Institution Press.

O'Connell, J.F. and J. Allen. 2004. Dating the colonization of Sahul (Pleistocene Australia-New Guinea): a review of recent research. *Journal of Archaeological Science* 31: 835–853.

O'Connell, J.F. and J. Allen. 2008. Getting from Sunda to Sahul. In (G. Clark, B.F. Leach, and S. O'Connor, eds.) *Colonisation, Seafaring and the Archaeology of Maritime Landscapes*, pp. 31–46. Canberra: Australian National University Press.

O'Connell, J.F. and J. Allen. 2012. The restaurant at the end of the universe: modelling the colonisation of Sahul. *Australian Archaeology* 74: 5–31.

O'Connell, J.F., J. Allen, and K. Hawkes. 2010. Pleistocene Sahul and the origins of seafaring. In (A. Anderson, J. Barrett, andK. Boyle, eds.) *The Global Origins and Development of Seafaring*, pp. 57–68. Cambridge: McDonald Institute for Archaeological Research.

Oppenheimer, S. 2009. The great arc of dispersal of modern humans: Africa to Australia. *Quaternary International* 202: 2–13.

Pääbo, S. 2014. *Neanderthal Man: In Search of Lost Genomes*. New York: Basic Books.

Pardoe, C. 1991. Competing paradigms and ancient human remains: the state of the discipline. *Archaeology in Oceania* 26: 79–85.

Pardoe, C. 2006. Becoming Australian: evolutionary processes and biological variation from ancient to modern times. *Before Farming* (on-line version) 2006/1: Article 4.

Pennisi, E. 2013. More genomes from Denisova cave show mixing of early human groups. *Science* 340: 799.

Pietrusewsky, M. 1984. Metric and non-metric cranial variation in Australian Aboriginal populations compared with populations from the Pacific and Asia. *Occasional Papers in Human Biology* 3. Canberra Australian Institute of Aboriginal Studies.

Pietrusewsky, M. 1990. Craniofacial variation in Australasian and Pacific populations. *American Journal of Physical Anthropology* 82: 319–340.

Prüfer, K., F. Racimo, N. Patterson, F. Jay, S. Sankararaman, S. Sawyer, A. Heinze, G. Renaud, P.H. Sudmant, C. deFilippo, Heng Li, S. Mallick, M. Dannemann, Qiaomei Fu, M. Kircher, M. Kuhlwilm, M. Lachmann, M. Meyer, M. Ongyerth, M. Siebauer, C. Theunert, A. Tandon, P. Moorjani, J. Pickrell, J.C. Mullikin, S.H. Vohr, R.E. Green, I. Hellmann, P.L.F. Johnson, H. Blanche, H. Cann, J.O. Kitzman, J. Shendure, E.E. Eichler, E.S. Lein, T.E. Bakken, L.V. Golovanova, V.B. Doronichev, M.V. Shunkov, A.P. Derevianko, B. Viola, M. Slatkin, D. Reich, J. Kelso, and S. Pääbo. 2014. The complete genome sequence of a Neanderthal from the Altai Mountains. *Nature* 505: 43–49.

Pugach, I., F. Delfin, E. Gunnarsdóttir, M. Kayser, and M. Stoneking. 2013. Genome-wide data substantiate Holocene gene flow from India to Australia. *Proceedings of the National Academy of Sciences* USA 110(5): 1803–1808.

Rasmussen, M., X. Guo, Y. Wang, K.E. Lohmueller, S. Rasmussen, A. Albrechtsen, L. Skotte, S. Lindgreen, M. Metspalu, T. Jombart, T. Kivisild, W. Zhai, A. Eriksson, A. Manica, L. Orlando, F. De La Vega, S. Tridico, E. Metspalu, K. Nielsen, M.C. Ávila-Arcos, J.V. Moreno-Mayar, C. Muller, J. Dortch, M.T.P. Gilbert, O. Lund, A. Wesolowska, M. Karmin, L.A. Weinert, Bo Wang, Jun Li, S. Tai, Fei Xiao, T. Hanihara, G. van Driem, A.R. Jha, F-X. Ricaut, P. de Knijff, A.B Migliano, I. Gallego-Romero, K. Kristiansen, D.M. Lambert, S. Brunak, P. Forster, B. Brinkmann, O. Nehlich, M. Bunce, M. Richards, R. Gupta, C.D. Bustamante, A. Krogh, R.A. Foley, M.M. Lahr, F. Balloux, T. Sicheritz-Pontén, R. Villems, R. Nielsen, Jun Wang, and E. Willerslevand. 2011. An Aboriginal Australian genome reveals separate human dispersals into Asia. *Science* 334: 94–98.

Reich, D, R.E. Green, M. Kircher, J. Krause, N. Patterson, Y. Eric, B. Durand, B. Viola, A.W. Briggs, U. Stenzel, P.L.F. Johnson, T. Maricic, J.M. Good, T. Marques-Bonet, C. Alkan, Qiao-mei Fu, S. Mallick, Heng Li, M. Meyer, E.E. Eichler, M. Stoneking, M. Richards, S. Talamo, M.V. Shunkov, A.P. Derevianko, J-J. Hublin, J. Kelso, M. Slatkin, and S. Pääbo. 2010. Genetic history of an

archaic hominin group from Denisova Cave in Siberia. *Nature* 468: 1053–1060.

Reich, D., N. Patterson, M. Kircher, F. Delfin, M.R. Nandineni, I. Pugach, Ko AM-S, Y-C. Jinam, T.A. Phipps, M.E. Naruya Saitou, A. Wollstein, M. Kayser, S. Pääbo, and M. Stoneking. 2011. Denisova admixture and the first modern human dispersals into Southeast Asia and Oceania. *American Journal of Human Genetics* 89: 516–528.

Reyes-Centeno, H., S. Ghirotto, F. Détroit, D. Grimaud-Hervé, G. Barbujani, and K. Harvati. 2014. Genomic and cranial phenotype data support multiple modern human dispersals from Africa and a southern route into Asia. *Proceedings of the National Academy of Sciences USA* 111(20): 7248-7253.

Sergi, S. 1948. Il cranio del secondo paleanthropo de Saccopastore. *Paleontolographia Italica* 42: 25–164.

Shang Hong, Haowen Tong, Shuangquan Zhang, Fuyou Chen, and E. Trinkaus. 2007. An early modern human from Tianyuan Cave, Zhoukoudian, China. *Proceedings of the National Academy of Sciences USA* 104(16): 6573–6578.

Simpson, J.J. and R. Grün. 1998. Non-destructive gamma spectrometric U-series dating. *Quaternary Science Review* 18: 1009–1022.

Skoglund. P. and M. Jakobsson. 2011. Archaic human ancestry in East Asia. *Proceedings of the National Academy of Sciences USA* 108: 18301–18306.

Smith, F.H. and S.M. Ranyard. 1980. Evolution of the supraorbital region in Upper Pleistocene fossil hominids from south-central Europe. *American Journal of Physical Anthropology* 53: 589–609.

Smith, M.A., P.C. Tacon, D. Curnoe, and A.G. Thorne. 2007. Human dispersal into Australasia. *Science* 315: 597–598.

Smith, R.J. 1996. Biology and body size in human evolution. *Current Anthropology* 37(3): 451–481.

Smith, S.A. 1918. The fossil human skull found at Talgai, Queensland. *Transactions of the Royal Society of London,* Series B 208: 351–387.

Stone, T. and M.L. Cupper. 2003. Last glacial maximum ages for robust humans at Kow Swamp, southern Australia. *Journal of Human Evolution* 45: 99–111.

Stringer, C.B. 1998. A metrical study of WLH 50 calvaria. *Journal of Human Evolution* 34(3): 327–332.

Stringer, C.B. and P. Andrews. 1988. Genetic and fossil evidence for the origin of modern humans. *Science* 239: 1263–1268.

Stuart-McAdam, P. 1992. Cranial thickening and anemia: reply to Dr. Webb. *American Journal of Physical Anthropology* 88: 109–110.

Suzuki, H. 1970. The skull of the Amud man. (In H. Suzuki and F. Takai, eds.) *The Amud Man and his Cave Site*, pp. 123–206. Tokyo: University of Tokyo.

Templeton, A. 2005. Haplotype trees and modern human origins. *Yearbook of Physical Anthropology* 48: 33–59.

Templeton, A.R. 2007. Genetics and recent human evolution. *Evolution* 61: 1507–1519.

Thorne, A.G. 1976. Morphological contrasts in Pleistocene Australia. In (R.L. Kirk and A.G. Thorne, eds.) *The Origin of the Australians*, vol. 6: 95–112 of Human Biology Series. Canberra: Australian Institute of Aboriginal Studies.

Thorne, A.G. 1977. Separation or reconciliation: biological clues to the development of Australian society. In (J. Allen, J. Golson and R. Jones, eds.) *Sunda and Sahul: Prehistoric Studies in Southeast Asia, Melanesia, and Australia.* pp. 187–204. London: Academic Press.

Thorne, A.G. 1980. The longest link: human evolution in Southeast Asia and the settlement of Australia. In (J.J. Fox, R.G. Garnaut, P.T. McCawley, and J.A.C. Maukie, eds.) *Research Indonesia: Australian Perspectives,* pp. 35–43. Canberra: School of Pacific Studies.

Thorne, A.G. 1984. Australia's human origins - how many sources? (Abstract) *American Journal of Physical Anthropology* 63(2): 227.

Thorne, A.G. and D. Curnoe. 2000. The sex and significance of Lake Mungo 3: reply to Brown "Australian Pleistocene variation and the sex of Lake Mungo 3". *Journal of Human Evolution* 39: 587–600.

Thorne, A.G. and S.R. Wilson. 1977. Pleistocene and recent Australians: A multivariate comparison. *Journal of Human Evolution* 6(4): 393–402.

Thorne, A.G. and M.H. Wolpoff. 1981. Regional continuity in Australasian Pleistocene hominid evolution. *American Journal of Physical Anthropology* 55(3): 337–349.

Thorne, A.G. and M.H. Wolpoff. 2003. The multiregional evolution of humans (updated). *Scientific American*13(2), pp. 46–53, in M. Fischetti (ed.), *New Look at Human Evolution*)).

Trinkaus, E. 2004. Eyasi 1 and the suprainiac fossa. *American Journal of Physical Anthropology* 124(1): 28–32.

van Holst Pellekaan, S. 2012. Genetic evidence for the colonization of Australia. *Quaternary International* 285(8): 44–56.

van Holst Pellekaan, S. and R. Harding. 2006. Excavating the mitochondrial genome identifies major haplogroups in Aboriginal Australians. *Before Farming* 2006/1: Article 3: 1–26.

Webb, S.G. 1989. *The Willandra Lakes Hominids*. Canberra: Department of Prehistory, Research School of Pacific Studies Australian National University.

Webb, S.G. 1990. Cranial thickening in an Australian hominid as a possible palaeoepidemiological indicator. *American Journal of Physical Anthropology* 82(4): 403–411.

Webb, S.G. 1995. *Palaeopathology of Aboriginal Australians*. Cambridge (UK): Cambridge University Press.

Webb, S.G. 2006. *The First Boat People*. Cambridge (UK): Cambridge University Press.

Weidenreich, F. 1943. The skull of *Sinanthropus pekinensis*: a comparative study of a primitive hominid skull. *Palaeontologica Sinica* (New Series D) 10: 1–484.

Weidenreich, F. 1945. The Keilor skull. A Wadjak skull from southeast Australia. *American Journal of Physical Anthropology* 3: 21–33.

Weidenreich, F. 1946. *Apes, Giants, and Man*. Chicago: University of Chicago Press.

Weidenreich, F. 1951. Morphology of Solo man. *Anthropological Papers of the American Museum of Natural History* 43(3): 205–290.

Weiss, K.M. 1971. On the systematic bias in skeletal sexing. *American Journal of Physical Anthropology* 37: 239–250.

Westaway, M.C. 2006. The Pleistocene human remains collection from the Willandra Lakes World Heritage Area, Australia, and its role in understanding modern human origins. In (Y. Tomida, T. Kubodera, S. Akiyama, and T. Kitayama, eds.) *Proceedings of the Seventh and Eighth Collection Building and Natural History Studies in Asia and the Pacific Rim*, pp. 127–138. National Science Museum Monographs No. 34. Tokyo: National Science Museum.

Westaway, M.C. and C.P Groves. 2009. The mark of ancient Java is on none of them. *Archaeology in Oceania* 44: 84–95.

Westaway, M.C. and D. Lambert. 2014. First Australians: origins. In ([C. Shen and Z. Jacobs, eds.] Human Evolution: Theory and Progress section of C. Smith, ed.) *Encyclopedia of Global Archaeology*, pp. 2787–2800. New York: Springer Science and Business Media.

White, T.D., B. Asfaw, D. Degusta, H. Gilbert, G.D. Richards, G. Suwa, and F.C. Howell. 2003. Pleistocene *Homo sapiens* from Middle Awash, Ethiopia. *Nature* 423: 742–747.

Williams, A.N. 2013. A new population curve for prehistoric Australia. *Proceedings of the Royal Society B* 280: 20130486 (http://dx.doi.org/10.1098/rspb.2013.0486).

Wolpoff, M.H. 1980. *Paleoanthropology*, First Edition. New York: Knopf.

Wolpoff, M.H. 2009. How Neandertals inform human variation. *American Journal of Physical Anthropology* 139(1): 91-102.

Wolpoff, M.H. 2014. Who were the Denisovans? In (A.P. Derevianko and M.V. Shunkov, eds.) *Cultural Developments in the Eurasian Paleolithic and the Origin of Anatomically Modern Humans*, pp. 180-188. Proceedings of the International Symposium (July 1-7, 2014, Denisova Cave, Altai). Novosibirsk: Institute of Archaeology and Ethnography, Siberian Branch, Russian Academy of Sciences.

Wolpoff, M.H. and R. Caspari. 1997. *Race and Human Evolution*. New York: Simon & Schuster.

Wolpoff, M.H. and R. Caspari. 2013. Paleoanthropology and race. In (D. Begun, ed.) *A Companion to Paleoanthropology*, Chapter 17, pp. 321–338. Wiley-Blackwell, London.

Wolpoff, M.H., J.D. Hawks, D.W. Frayer, and K. Hunley. 2001. Modern human ancestry at the peripheries: a test of the replacement theory. *Science* 291: 293–297.

Wolpoff, M.H. and S-H. Lee. 2001. The Late Pleistocene human species of Israel. *Bulletins et Mémoires de la Société d'Anthropologie de Paris* 13(3-4): 291–310.

Wolpoff, M.H. and S-H. Lee. 2006. Variation in the habiline crania – must it be taxonomic? *Human Evolution* 21: 71–84.

Wolpoff, MH. and S-H. Lee. 2012. The African origin of recent humanity. In (S.C. Reynolds and A. Gallagher, eds.) *African Genesis: Perspectives on Hominin Evolution*, Chapter 18, pp. 347–364. Cambridge Studies in Biological and Evolutionary Anthropology. Cambridge (UK): Cambridge University Press.

Wolpoff, M.H., A.G. Thorne, J. Jelínek, and Yinyun Zhang. 1994. The case for sinking *Homo erectus*. 100 years of *Pithecanthropus* is enough! *Courier Forschungsinstitut Senckenberg* 171: 341–361.

Wright, R.V.S. 1976. Evolutionary process and semantics: Australian prehistoric tooth size as a local adjustment. In (R.L. Kirk and A.G. Thorne, eds.) *The Origin of the Australians*, pp. 265–276. Canberra: Australian Institute of Aboriginal Studies.

Wu Xinzhi. 1998. Continuity or replacement: viewed from the source of certain features of modern humans in China. In (K. Omoto and P. V. Tobias, eds.) *Origins and Past of Modern Humans: Towards Reconciliation*, pp. 139–144. Singapore: World Scientific.

Wu Xinzhi and S. Athreya. 2013. A description of the geological context, discrete traits, and linear morphometrics of the Middle Pleistocene hominin from Dali, Shaanxi Province, China. *American Journal of Physical Anthropology* 150: 141–157.

Wunderly, J. 1943. The Keilor fossil skull: anatomical description. *Memoirs of the National Museum of Melbourne* 13: 57–70.

Xu Shuhua, I. Pugach, M. Stoneking, M. Kayser, Li Jina, and HUGO Pan-Asian SNP Consortium. 2012. Genetic dating indicates that the Asian–Papuan admixture through Eastern Indonesia corresponds to the Austronesian expansion. *Proceedings of the National Academy of Sciences USA* 109: 4574–4579.

Zerjal, T., Yali Xue, G. Bertorelle, R.S. Wells, Weidong Bao, Suling Zhu, R. Qamar, Q. Ayub, A. Mohyuddin, Songbin Fu, Pu Li, N. Yuldasheva, R. Ruzibakiev, Jiujin Xu, Qunfang Shu, Ruofu Du, Huanming Yang, M.E. Hurles, E. Robinson, T. Gerelsaikhan, B. Dashnyam, S.Q. Mehdi, and C. Tyler-Smith. 2003. The genetic legacy of the Mongols. *American Journal of Human Genetics* 72(3): 717–721.